AN ABSTRACT OF THE THESIS OF

Katherine E. Jones for the degree of Master of Science in Geography presented on June 7, 2016.

Title: Spatio-Temporal Patterns of Tree Establishment in the M1 Meadow of the HJ Andrews Experimental Forest.

Abstract approved:

_____

Julia A. Jones

Montane meadows in the Cascade Range of Oregon have been declining due to tree establishment since records began. Montane meadow complexes in the H.J. Andrews Experimental Forest shrank by 60 to 75% from 1949 to 2005, but fine scale temporal and spatial processes of tree establishment in these meadows are unknown. In the 4.8-ha M1 meadow in the Andrews Forest, the species and diameter of all trees of any size were measured in seven 20x20 m plots and one 40x55 m plot in August 2015. A total of 1385 trees were sampled, including 1008 in the 40x55 m plot. In the 40x55m plot, all trees were mapped to the nearest 0.1 m and 252 were aged to the nearest +/- 2 years. Spatial patterns of tree locations were assessed using second order analysis (Ripley's K, pair correlation function [PCF], J-function). In the 40x55m plot, the oldest tree established in the 1870s, and tree establishment has accelerated since 1950, as invasion has progressed from the edges toward the center of the meadow. Nine conifer species occurred in the plots, but almost 84% of individuals were *Abies amabilis* (Pacific silver fir, ABAM) or *Abies grandis* (grand fir, ABGR), and 8% were *Pseudotsuga menziesii* (Douglas-fir, PSME). PSME and ABAM dominated the basal area, and >90% of ABAM and ABGR and 50% of PSME individuals were

<5 cm DBH. Some individuals with basal diameter <3 cm were up to 30 (ABGR) or 50 (ABAM) yrs of age. Trees were clustered at scales of <6 m (Ripley's K) or <3 m (PCF), clusters were dispersed at scales >6 m, and trees have become increasingly clustered over time (J-function). However, trees aged <30 yrs were only weakly clustered relative to trees aged >30 yrs, and evidence of facilitation was weak. Thus, all conifer species appear capable of establishing in the montane meadow, but in many cases trees established several decades before they began to grow rapidly. Based on current rates of tree establishment, the meadow will continue to shrink in the future. Because many trees are small, complete tree removal is an initial step toward meadow restoration in this and comparable sites. However, additional approaches will be necessary to counteract legacy effects of trees on soils. Future work should combine fine-scale analysis of tree spatial patterns with environmental (light, moisture and soil) data in order to reveal the local environmental drivers of tree establishment patterns in montane meadows.

# Spatio-temporal Patterns of Tree Establishment in the M1 Meadow of the HJ Andrews Experimental Forest

by
Katherine E. Jones

A THESIS

submitted to

Oregon State University

in partial fulfillment of
the requirements for the
degree of

Master of Science

Presented June 7, 2016
Commencement June 2017

Master of Science thesis of Katherine E. Jones presented on June 7, 2016

APPROVED:

---

Major Professor, representing Geography

---

Dean of the College of Earth, Ocean, and Atmospheric Sciences

---

Dean of the Graduate School

I understand that my thesis will become part of the permanent collection of Oregon State University libraries. My signature below authorizes release of my thesis to any reader upon request.

---

Katherine E. Jones, Author

# ACKNOWLEDGEMENTS

I am humbled by the many friends, colleagues, and mentors I have to thank. I would first like to acknowledge Dr. Julia Jones for the immense personal and professional support she provided me throughout my tenure at Oregon State. Her patience and perspective are inspiring. Without her influence, my development as an aspiring scientist, professional, and young person would be less enriched. In addition, I also acknowledge my committee members Dr. Mark Christensen, Dr. Mary Santelmann, and Dr. Mark Schulze for their time and improvements to this thesis.

This thesis would not have been completed without the countless hours of physical labor and companionship contributed by Jeff Traver. I cannot express the appreciation I have for his positive attitude, his work ethic, and his taste in potato chips. Thank you for the many weekends spent in the field. I am forever appreciative, and those weekends will not soon be forgotten.

The research guidance and equipment provided by Dr. John Bailey's Laboratory for Tree-Ring Research were invaluable. Special thanks to Andrew Merschel for his advice, availability, and willingness to help. Many thanks to Dr. Steve Voelker, Pat MacMeekin, Brett Murphy, and Michael Hafer for borrowed supplies, power tools, and troubleshooting.

The team of researchers, staff, and sense of place at the H.J. Andrews Experimental Forest fosters an environment that is near impossible to leave. Thank you to those who make it such a wonderful place to work and enjoy. This study was supported by funding from the NSF Long-term Ecological Research (LTER) program (NSF 1440409, NSF 0823380) at the H.J. Andrews Experimental Forest and the grant 1261550 (D. Tullos and J.A. Jones, co-PIs). To the 2015 Ecosystem Informatics Summer Institute students: Marissa Childs, Brian Draeger, Ben Freiberg, Erin Howard, Nate Sadowsky, Ashley Sanders, Carson Smith, Levi Stovall, Emelie

Traub, and Anna Young, thank you for an excellent summer. The hours spent discussing field sampling designs and your help implementing plots are appreciated.

Lastly, with love and heartfelt sincerity, I would like to thank my parents, Bob and Beth Jones, for their selfless, unshakeable foundation of love and support. Thank you for instilling in me the desire to be a lifelong learner and the curiosity to keep exploring. While we are physically separated, know that you are the origin of, and continue to be, the core of my successes.

# TABLE OF CONTENTS

Page

# LIST OF FIGURES

# LIST OF TABLES

# LIST OF APPENDIX FIGURES

Figure Page

# LIST OF APPENDIX TABLES

## 1. Introduction

Loss of grasslands and meadows elicits global concern (Scholes and Archer 1997). Tree establishment, "encroachment," or "invasion" of montane meadows, the cause of decreasing meadow area, has been documented in many parts of the Oregon Cascades over the past half-century (Dailey 2007; Halpern et al. 2010; Haugo and Halpern 2007; Haugo and Halpern 2010; Miller and Halpern 1998). The extent and connectivity of montane meadows can be viewed from the perspective of island biogeography theory. Meadows function as islands within a predominantly forested landscape. As meadows lose area, biodiversity is inevitably lost (Brooks et al. 2003; Fahrig, L. 2003). Tree invasion of meadows is of concern because it may influence ecological networks dependent on meadow habitat. Plant-pollinator networks depend on the presence of meadow habitat patches within a forested landscape (Pfeiffer 2012; Rathcke and Jules, E. 1993; Steffan-Dewenter, I. 2003). Plant-pollinator networks may be resilient to meadow loss because generalist plant and pollinator species often represent a large fraction of the interactions in these networks (Fontaine et al. 2005; Helderop 2015; Potts, S G. et al. 2010). Nevertheless, decreasing meadow habitat may have adverse effects, especially on rare plant-pollinator species relationships. Thus, it is important to improve our understanding of the process of tree establishment in montane meadows.

Various factors are believed to influence the timing and location of tree invasion of meadows. Livestock grazing and burning of montane meadows are thought to have historically maintained montane meadow habitat (Miller and Halpern 1998). The process of meadow encroachment varies by meadow habitat. The interactions of landscape-scale processes (cessation of anthropogenic influences and changing climate regimes) and topographic characteristics (aspect, elevation, and slope) yield a variety of temporal and spatial patterns of meadow encroachment (Miller and Halpern 1998; Zald et al. 2012).

Existing trees may also influence the process of tree invasion of meadows. Tree establishment in meadows may involve spatial clustering or dispersal, which link to the ecological relationships of

facilitation and repulsion, respectively. At Bunchgrass Ridge in the High Cascades of Oregon, young individuals of *Abies grandis (*grand fir, ABGR), a shade tolerant species, were clustered near older individuals of *Pinus contorta* (lodgepole pine, PICOM), a pioneer species which facilitates the establishment of *Abies*. This facilitation produces an increasingly clustered pattern of tree establishment over time (Rice et al. 2012).

Montane meadows in the western Cascades of Oregon provide an opportunity to study the process of tree invasion. Meadow complexes (collections of fragmented meadows) within the H.J. Andrews Experimental Forest have declined by as much as 60 to 75 % from 1949 to 2005 (Figure 1 (a) and (b)).The Carpenter meadow complex decreased from ~100 acres in 1949 to ~30 acres in 2005 (Figure 1(a)) (Rice et al. 2009). However, little is known about the timing or spatial pattern of tree invasion in these meadows. This study was designed to address the fine-scale spatial patterns of tree invasion in the M1 Meadow of the H.J. Andrews Experimental Forest.

This study addresses the following research questions:

1) What is the temporal and spatial pattern of individual trees in Plot F?

2) How do interactions among tree species and tree ages influence the spatial pattern of invasion in Plot F?

3) What aspects of invasion in Plot F occur throughout the forest edge in a large (4.8-ha) montane meadow?

(a)

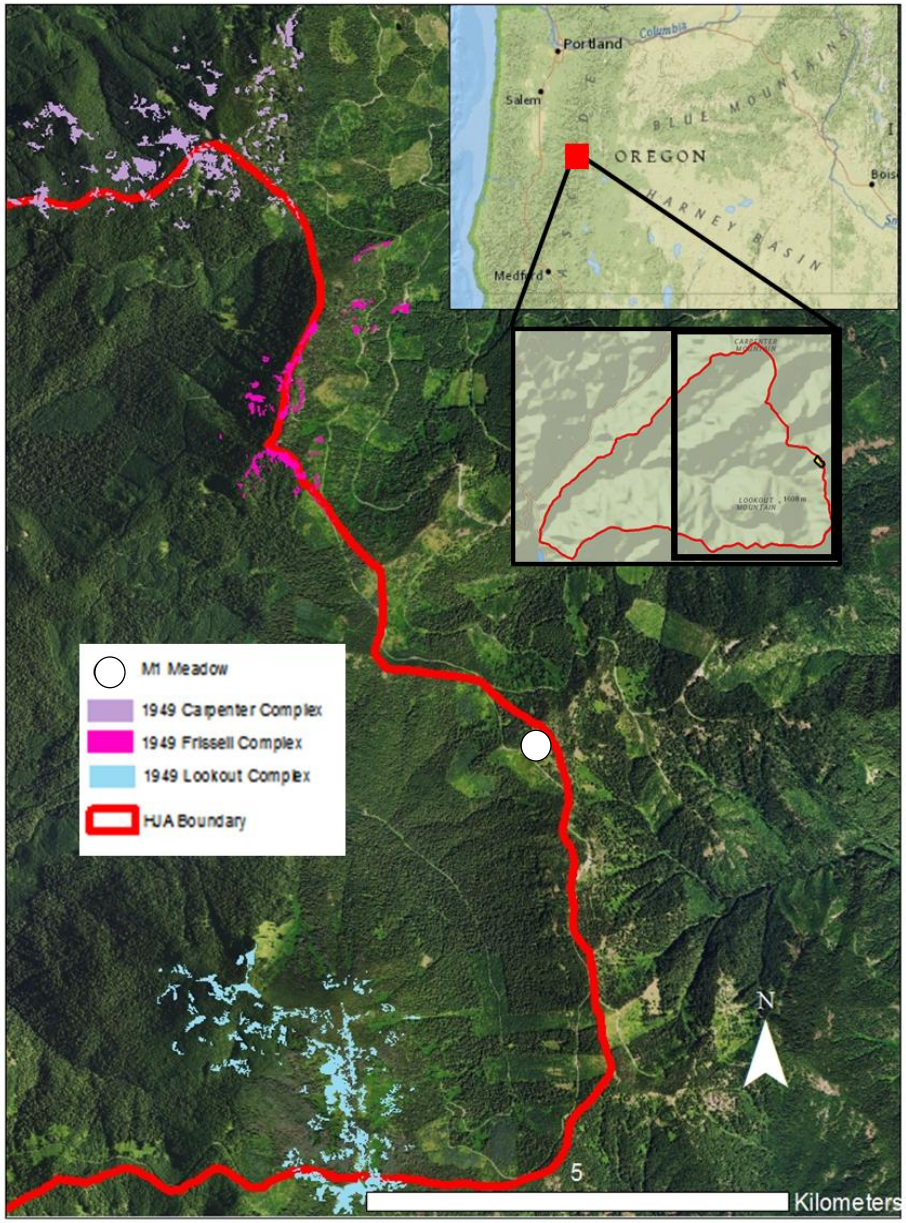
Portland
Columbia
Salem
OREGON
BLUE MOUNTAINS
HARNEY BASIN
Medford
M1 Meadow
1949 Carpenter Complex
1949 Frissell Complex
1949 Lookout Complex
HJA Boundary
N
5
Kilometers

(b)

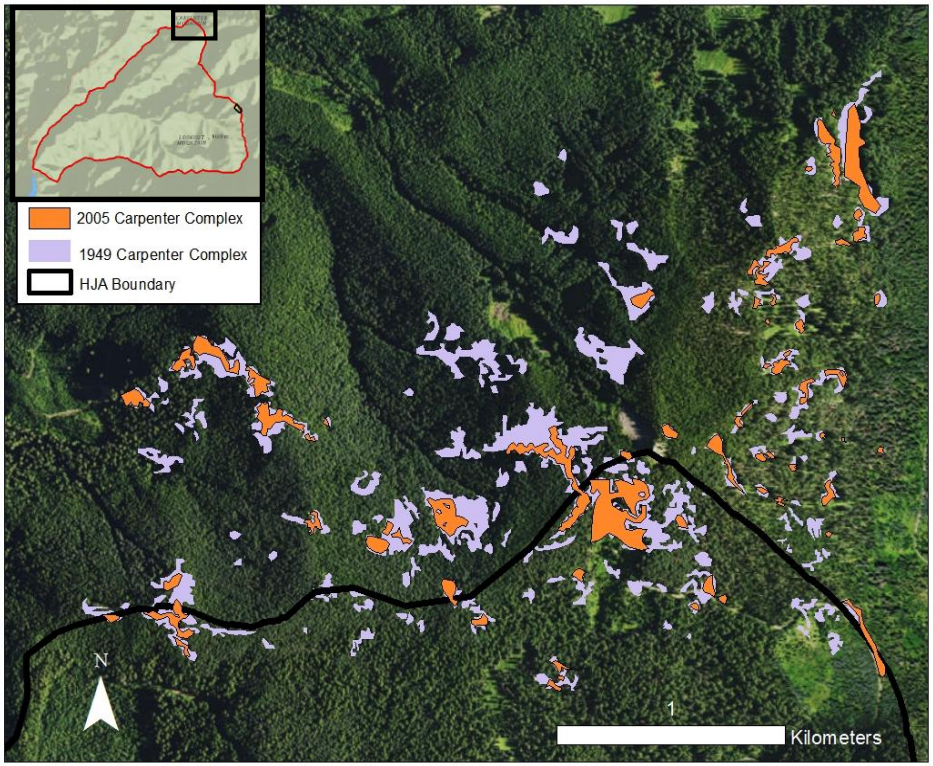
2005 Carpenter Complex
1949 Carpenter Complex
HJA Boundary
N
1
Kilometers

(c)

(d)

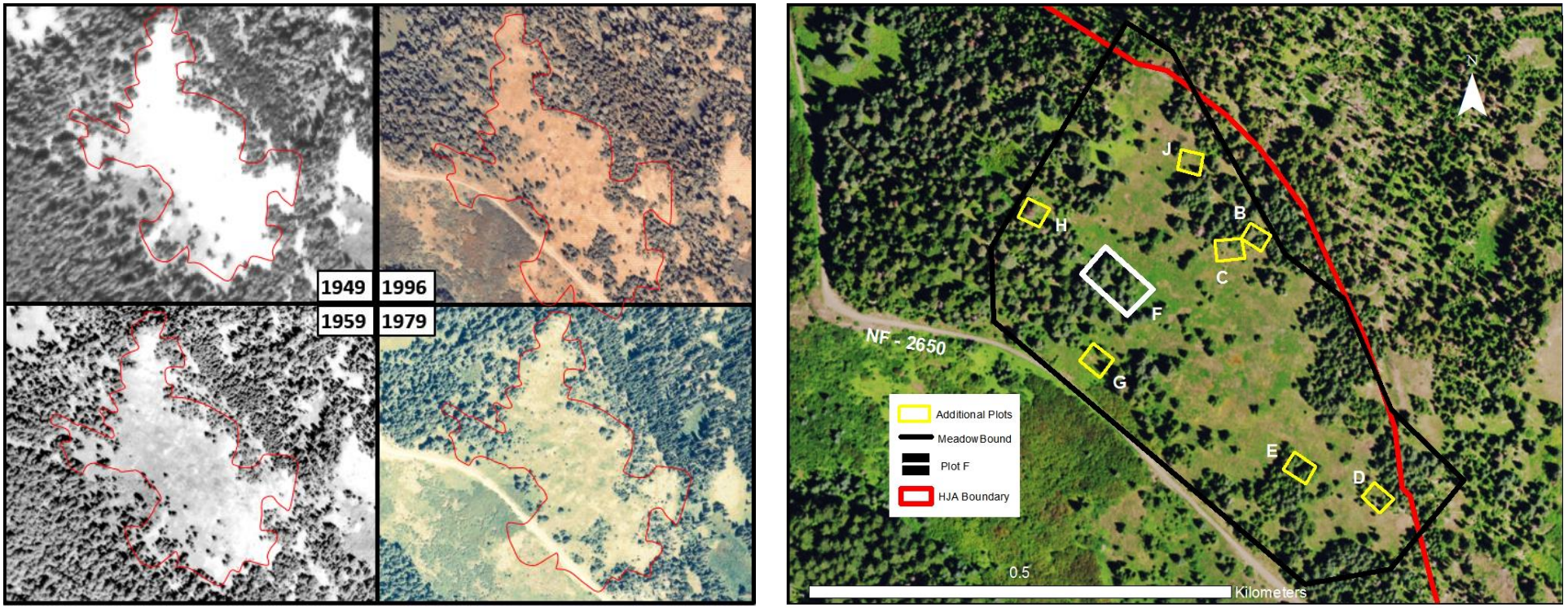


*Figure 1.* (a) The study site, meadow M1 (white dot) is located among three meadow complexes within the HJ Andrews Experimental Forest in western Oregon (2014 aerial photograph). (b) change in meadow area in Carpenter complex from 1949 to 2005. (c) change in meadow area of M1 from 1949 to 1996 (red polygon approximates 1959 meadow perimeter). (d) location of M1 meadow plot A (black polygon) and eight subplots.

## 2. Study site

The study site is a 4.8-ha montane meadow located in the HJ Andrews Experimental Forest (62-$km^2$), located approximately 80 km east of Eugene, OR, near the town of Blue River, OR (Figure 1 (a)). The Andrews Forest has an elevation range of 420 to 1615 meters. Andesitic lava flows underlie mostly loamy soils that have a high percentage of macrospace and porosity, contributing to water retention. The climate is marine temperate, characterized by winter precipitation and warm, dry summers. Less than 20% of total precipitation falls between May and October. Seasonal snowpack occurs above approximately 1000m and may persist into early summer (Swanson and Jones 2001). Mean January temperature was 1.67 ° C and mean July temperature was 19.44° C based on 2000 to 2014 at the of the United States Historical Climatology Network McKenzie Bridge station (elev. 450.5 meters, Lat. 44.1781, Long. -122.1156), (http://cdiac.ornl.gov/epubs/ndp/ushcn/access.html).

The ecoregion encompassing the Andrews Forest is temperate coniferous forest. Dominant tree species include *Pseudotsuga menziesii* (Douglas-fir) (PSME), *Tsuga heterophylla* (western hemlock) (TSHE), *Thuja plicata* (western red cedar) (THPL), *Abies amabalis* (Pacific silver fir) (ABAM), *Abies grandis* (grand fir) (ABGR), and *Tsuga mertensiana* (mountain hemlock) (TSME). The majority of the landscape is mature (150 yr old) and old growth (500-yr old) forests, and approximately one quarter of the landscape is forest plantations in clearcuts created from 1948 to the early 1980s.

Less than 5% of the Andrews Forest consists of montane meadows (Highland, Miller, and Jones 2013). Meadows include woody shrub communities, conifer saplings, and a variety of herb species occupying hydric to xeric meadows (Takaoka and Swanson 2008). Within the Andrews Forest, three meadow complexes, each containing multiple meadows, occur along the ridges of Carpenter Mountain, Frissell Mountain, and Lookout Mountain (Figure 1 (a)). Within and among meadows there is much variability in aspect, slope, and soils, which range from rock or talus slopes to deep soils (Dailey 2007; Highland, Miller, and Jones 2013; Pfeiffer 2012; Rice et al. 2012).

The study was located in the M1 meadow (Figure 1 (c) and (d)), located along the eastern bounding ridge of the HJ Andrews Forest, along the crest of the western Cascades. The meadow covers 4.8-ha and elevation ranges from 1445 to 1540 m. The study site was selected from the montane meadows in the Andrews Forest (Figure 1 (a)) because it is relatively large, with good road access, and aerial photograph evidence documents historical tree encroachment on the site.

The M1 meadow (Figure 1 (c)) is southwest facing with slopes ranges from 35 to 50%. It is bounded by the following coordinates:

44°14'8.24"N, 122° 6'44.93"W

44°14'19.38"N, 122° 6'37.51"W

44°14'0.26"N, 122° 6'27.65"W

44°14'10.34"N, 122° 6'20.37"W

Vegetation in the M1 meadow is dominated by *Ligusticum grayii, Achillea millefolium, Cirsium callilepis, Carex sp.,* and other flowering species, with very little woody shrub cover. The dominant overstory tree species surrounding the meadow are *Abies amabilis* (Pacific silver fir) (ABAM) with frequent *Pseudotsuga menziesii* (Douglas-fir) (PSME) and *Abies grandis* (grand fir) (ABGR). Aerial imagery from 1949, 1959, 1979, 1996 (Figure 1 (c)), and 2014 (Figure 1 (d)), shows an increase in edge complexity with changing locations and densities of trees entering the M1 meadow.

## 3. Methods

### *3.1. Site Selection*

Along the meadow margins of M1 (plot A), seven 20 by 20 m plots and one 40 by 55 m plot were established (Figure 1 (d)) using stratified random sampling. A 20 x 20 m grid coordinate system was superimposed over plot A and random coordinates were generated. Points that fell in grid cells which contained both forest and meadow were selected for plot locations. GPS locations of the corners of all plots were recorded.

One large plot (plot F, 40 x 55m, Figure 1 (d)) spanning the forest-meadow boundary was selected for high spatial resolution sampling of recent invasion. Based on historical aerial photographs (Figure 1 (c)), plot F had experienced tree invasion, but it still maintained vestiges of meadow species, and it contained a high density of seedlings as well as understory and overstory trees.

### *3.2. Field methods*

All trees in the eight plots were sampled (n = 1385). The following data were determined for each tree in plots B, C, D, E, F, G, H, and J: species, DBH (diameter at breast height, 1.4 meters) or DBA (diameter at tree base, for trees without DBH). Age data were collected from plot F either by increment borer or basal cross section. Ease of access for coring and the shape of the base of the tree determined whether a tree was cored or whether a basal section was obtained. Cored trees ranged from 2 to 79 cm DBH, while trees with basal diameters ranged from 0.1 to 4 cm DBA."

Within plot F, the spatial coordinates of each tree (n=1008) were obtained. A 5 x 5m grid was established, and the x,y coordinates of each tree were obtained to the nearest 0.1m resolution. All stems in plot F were surveyed irrespective of height. A total of 885 trees were measured for DBA, and 123 trees were measured for DBH. Of the 885 trees measured for DBA, basal sections were obtained for 571. The remaining tree seedlings with a basal diameter <0.25 cm were too small for basal cross sections and too

small to age, and were extracted entirely (including root structures) from the ground (n=314) to begin a meadow restoration experiment. Of the 123 trees measured for DBH, 60 were cored, and basal sections were obtained for 63 (

*Table S 1*).

When possible, basal cross sections were preferred over tree cores for ease of sample processing. Basal cross sections were cut on site using a small handsaw. Tree cores were extracted with either a 12" or 20" (5.15mm) increment borer. Basal cross sections were taken as close to the ground as possible, while cores were extracted with enough distance, respective to borer size, to turn the arm of the borer (Grissino-Mayer 2003). If hillslope or tree shape inhibited tree coring near the ground, the height at which the tree core was taken was recorded. If the core encountered rot, another core was attempted; if the second attempt also failed due to rot, no sample was obtained from that tree. Cases in which the pith was not reached or rot prevented coring the tree were recorded. Each tree core, basal section, and extracted seedling was given a unique identifier, wrapped, and transported to the dendrochronology lab at Oregon State University for analysis.

### *3.3. Laboratory methods*

Tree cores and basal cross sections were prepared for age analysis in the lab following standard dendrochronology processing techniques. Samples were visually assessed to determine whether they could be aged accurately. Very small size (basal diameter <0.25 cm) and natural deformities precluded aging for 314 samples (

*Table S 1*). The remaining basal section samples (n = 634, Table S 1) were grouped by species (ABAM, ABGR, and PSME) and size classes (

*Table S 1*). Within each of these basal size distributions, samples were randomly selected for aging. A total of 252 samples were aged from plot F, and an additional 18 samples from other plots were aged (Table S 2).

Samples that were too large or did not have a smooth face for sanding were trimmed using a miter saw (Figure 2. Then all basal cross sections were prepared for analysis using a belt sander (Figure 2 (b)) and three different belt grits (100, 180, 240). Tree cores were mounted in 3/8" x 3/8" mounts, glued, and dried overnight. Mounted tree cores were sanded with a 240 grit belt and polished with fine (~400) grit finishing paper (Figure 2 (c)).

All samples were then aged using an ACU GAGE SYSTEMS microscope with 0.001mm resolution. Each year was based on the presence of lighter, early wood and darker, late wood (Figure 2 (c)). For tree cores that did not reach the pith, standard dendrochronology ring templates were used to

estimate missing years. The difficulty of dscriminating rings near the the pith of very small trees suggests that, for ~10% of the samples, the uncertainty of the measured age is +- 2 years.



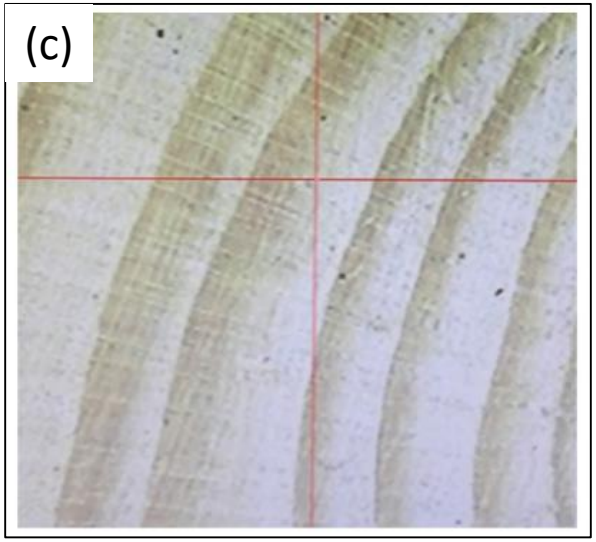


*Figure 2.*

(a) Miter saw used to trim smaller samples before sanding. (b) Belt sander used to polish the basal edge of the samples. Samples were initially sanded with the coarsest grit, then progressing to the finest grits for highest resolution. (c) A prepared basal cross section under the laboratory microscope.

## *3.4. Statistical Methods*

### 3.4.1. Spatial statistics

Spatial statistical analyses were conducted to quantify the spatial pattern of trees and examine relationships among species and age (time of establishment) of trees. The analyses used second-order point pattern analyses using Ripley's K, Cross-K, J-function, and PCF, following methods in Rice et al (2012).

Univariate Ripley's K and PCF analysis were conducted for all stems in Plot F (n=1008) and for individual species (PSME: n=63, ABAM: n=534, and ABGR: n=397) (

*Table S 1*). Bivariate Ripley's K and PCF analyses were conducted for pairs of species (ABAM and ABGR) and by age class (young and old). Young and old age classes were designated to represent an appropriate sample n for each sample class and to capture tree ages and sizes that could exert influence on one another. Age class thresholds were independently selected for each species by assessing apparent divisions in the age to diameter relationships and using prior knowledge regarding species' life history characteristics.

The J-function was calculated for trees established in three time periods: before 1990, 1990 to 2000, and after 2000. Size was used as a proxy for age to differentiate all stems without exact age data. For stems that were not aged, age was estimated from regression relationships calculated for that species from data obtained that related diameter and age.

### 3.4.2. Regression Models

Spatial analyses required an age for each tree, but there was insufficient time to age all the trees, so tree ages were estimated using diameter to age relationships fitted using linear regression. Linear regressions predicted age as a function of diameter for (generally very small) trees measured using DBA, and for (larger) trees measured using DBH.

Linear regression models were fitted to predict age (dependent variable) as a function of size (DBA, DBH, dependent variables) for each of three dominant tree species: ABAM, ABGR, and PSME (n values in Table S 2). The DBH and age data were log-transformed to meet the linear regression requirements for normally distributed data.

### 3.3.1. Ripley's K Method

Ripley's K is a cumulative distribution function that uses all pairwise distances between points to detect patterns of association (clustering) or repulsion (dispersal) in a sample area (A) (Ripley 1977). Ripley's K is defined as (Wiegand and Moloney 2004):

$$\mathbf{K(t) = A\sum^{n}_{i=1} \sum^{n}_{j=1} w_{ij} I_{t(i,j)} / n^2}$$

where $n_1$ and $n_2$ are the number of points within sample sets, $I_r$ is a counter variable, $d_{ij}$ represents the distance between each set of pairwise points, and $w_{ij}$ is a weighted edge correction term. The weight assigned to a point within a circle of a given radius is determined by how much of the circle is contained within the sample area (A). Edge correction is necessary to reduce the influence of points close to the sample boundary, which may have neighbors beyond the sample boundary that are not represented in the sample.

The K-function compares the cumulative distribution of pairwise distances to a cumulative distribution of an equivalent number of points distributed at random. These random points represent complete spatial randomness (CSR), which is simulated by drawing point locations from a Poisson distribution and computing the expected number of pairwise distances. A confidence interval around the

random distribution is generated through a chosen number of Monte Carlo permutations of the data. For example, 99 permutations are used to generate a 99% confidence interval. If the observed K function curve falls above the confidence interval around the random curve, this indicates there are more pairs of inter-point distances occurring within that distance than can be attributed to CSR, indicating clustering or association. If the observed K-function curve falls below the confidence interval, it indicates there are fewer pairs of inter-point distances occurring within that distance, indicating dispersal.

The Ripley's K functions (*kest, kinhom, and kross.inhom*) within the 'spatstat' package in R were used for this analysis (Baddeley and Turner 2013). The "Ripley's" edge correction was used for the correction argument due to the rectangular shape of the sample area. All other arguments of the function were executed using standard parameters.

The univariate Ripley's K method was used for the sample data of all stems in plot F (n=1008), all PSME stems (n=63), all ABAM stems (n=534), and all ABGR stems (n=397) (Table S 3).

The bivariate Ripley's K method was used for the sample data of old (n=130) and young (n=864) stems and to compare pattern between species. The bivariate Ripley's K also was used to compare all old stems (n=130) to young stems of ABGR (n=370) and young stems of ABAM (n=463); and to compare old ABGR (n = 26) to young ABGR and young ABAM; and to compare old ABAM (n=72) to young ABGR and young ABAM (Table S 4).

### 3.4.3. Pair Correlation Function

The Pair Correlation Function (PCF) is a distribution of pairwise distances in successive distance lags, rather than cumulative pairwise distances as in Ripley's K. The PCF eliminates bias in the cumulative pairwise distance method (Ripley's K), which is strongly affected by the pairwise distances at short lags. PCF is related to Ripley's K as the function g(r) is related to K(r). The PCF is defined as (Stoyan, D. and Stoyan, H. 1996):

$$g(r) = \frac{d}{dr} K(r) \ / 2\pi r \ for \ r \geq 0$$

where d represents probability density as a function of r (radius), while K(r) is the result of the K-function at a given distance r. A g(r) function representing CSR of a Poisson process would have probability values equal to 1 within all rings of different radii. If the value of g(r) is greater than 1 for a given ring, this indicates there are more pairwise distances in that concentric ring than expected with CSR, implying clustering. If the value of g(r) is between 0 and 1, this indicates there are fewer pairwise distances than expected with CSR, implying dispersal. Typically, smaller values for g(r) are associated with rings of larger radii. G(r) can only take one value per scale and can also equal 0, meaning there is no probability of pairwise distances at this distance. Hard-core distances generated through the g(r) function indicate the minimum sampling distance but are not relevant in this analysis because the minimum sampling distance was 0.05 to 0.1 m.

The bivariate form of PCF is (Stoyan, D. and Stoyan, H. 1996):

$$\hat{g}_{12}(r) = \frac{1}{2\pi r} \frac{A^2}{n_1 n_2} \sum_{i=1}^{n_1} \sum_{j=1}^{n_2} w_{ij}^{-1} k_h(r - | x_i - y_i | )$$

where A is the sample area, $n_1$ and $n_2$ represent the number of type 1 and type 2 points, $w_{ij}$ is the edge correction factor, and $x_i$ and $y_i$ represent the locations of type 1 and type 2 points, respectively.

The PCF functions (*pcf, pcfinhom, and pcfcross.inhom*) within the 'spatstat' package in R were used for this analysis (Baddeley and Turner 2013).

### 3.4.4. J-Function

The J-function was used to assess the spatial pattern of trees over time. The J-function is a ratio of the G-function to the F-function. The G-function calculates the cumulative distribution of nearest neighbor distances within a given radius normalized by the number of points in the point pattern. The F-

function, referenced as the 'empty space function', represents the cumulative distribution of the distances from random, fixed points in space to the nearest occurrence of a point 'x' in the point pattern. For univariate, unmarked point patterns, the J-function is (Lieshout 2006):

$$\boldsymbol{J(t) = \frac{1 - G(t)}{1 - F(t)}}$$

Both the G-function and the F-function are compared to CSR by plotting the expected values generated by Monte Carlo simulations against observed values. The G-function identifies clustering when the nearest neighbor distances are closer than the expected nearest neighbor distances calculated from a random point pattern. The G-function identifies dispersal when nearest neighbor distances are greater than the expected distances calculated from a random point pattern. The F-function identifies clustering when the gaps between fixed, random points and the nearest occurrence 'x' in the point pattern are greater than the expected distances calculated from random pattern. The F-function identifies dispersal when the gaps between fixed, random points and the nearest occurrence 'x' in the point pattern are less than the expected distances calculated from random pattern. When J(t) is greater than 1, this indicates that G(t) < F(t) and that the distribution of nearest neighbor distances is less than the distribution of the gaps measured from fixed points, implying clustering at a given scale. When J(t) is less than 1, G(t) > F(t), indicating that the distribution of nearest neighbor distances is greater than the distribution of measured gaps in the pattern, implying dispersal.

The J-functions (*Jest)* within the 'spatstat' package in R was used for this analysis (Baddeley and Turner 2013).

## 4. Results

A total of 1385 trees was sampled in the M1 meadow. Of these, 1008 were in plot F, and 377 were in the seven 20m x 20m plots. Nine tree species occurred in the meadow (

Table *S 5*, Figure 3). Pacific silver fir and grand fir together represented 84% of trees sampled, and Douglas-fir represented an additional 8% (Table 1). One or more Pacific silver fir, Douglas-fir and noble fir exceeded 100 years of age and one individual of Pacific silver fir exceeded 1 cm in diameter (Table 1). Small trees overwhelmingly dominated the sample. Trees < 5 cm in diameter represented >90% of Pacific silver fir and grand fir (Table 1).

Plots varied in numbers of trees and abundance of small trees (Figure 4). Four plots (B, C, E, G) had relatively few trees (< 30 stems) and lacked Pacific silver fir, but grand fir and Douglas-fir were present (Figure 4). Plot B had the highest tree species diversity (Figure 4). Three plots (D, H, and J) had many trees, and most individuals were small and predominantly Pacific silver fir and grand fir. Plot H contained the two largest noble firs observed in the meadow, a very large Pacific silver fir, and a very large grand fir (Figure 4).

Douglas-fir dominated the basal area in five plots and Pacific silver fir dominated in three plots (including plot F) (Table 2). Douglas-fir dominated the basal area of trees with diameter <10 cm in 4 plots (including plot F) (Table 2).

Plot F contained 800 trees ranging from 0.5 to 2 cm in basal diameter, which were overwhelmingly Pacific silver fir and grand fir (Figure 4). Plot F contained more than 109 stems/ha of Pacific silver fir > 20 cm DBH, whereas only 18 stems/ha of Pacific silver fir >20 cm DBH occurred in all the other plots combined (Figure 4).

The earliest tree in plot F established in the 1870s. Rates of tree establishment have accelerated since about 1950, and roughly three individuals of Pacific silver fir, and one or more individuals of Douglas-fir and grand fir, have established in plot F each year since the mid-1980s (Figure 5).

Small trees were quite variable in age. Ages of Pacific silver fir with basal diameter of 3 cm ranged from 10 to 50 years, and ages of 1-cm DBA individuals of ABGR ranged from 7 to 20 years, but ages of small Douglas-fir individuals were much less variable (Figure 6). Ages of trees that were tall enough to

be measured by DBH were closely related to size, with little difference in size:age relationships among the three species (Pacific silver fir, grand fir, and Douglas-fir) (Figure 6).

*Table 1.* Number and percent of trees by species, age of oldest tree, diameter of largest tree, and percent of stems < 5 cm DBH.

| | No. of individuals | Percent of individuals | Age of oldest tree | Diameter of largest tree | Percent of stems <5 cm DBH |
|---|---|---|---|---|---|
| ABAM | 622 | 44.9 | 138 | 119 | 92 |
| ABGR | 538 | 38.8 | 79 | 71 | 90 |
| PSME | 116 | 8.4 | 107 | 76 | 50 |
| TSME | 34 | 2.5 | 52 | 11 | 79 |
| ABLA | 33 | 2.4 | | 37.50 | 72 |
| ABPR | 24 | 1.7 | 126 | 83 | 50 |
| TSHE | 13 | 0.9 | 18 | 17.59 | 100 |
| PIMO | 4 | 0.3 | 15 | 15 | 75 |
| TABR2 | 1 | 0.01 | | | 100 |
| Total | 1385 | 100 | | | |

*Table 2.* Basal area (m2/ha) of trees in meadow M1 by species and size.

| Plot | DBH | ABAM | ABGR | ABLA | ABPR | PIMO | PSME | TSHE | TSME | TOTAL |
|---|---|---|---|---|---|---|---|---|---|---|
| B | All | 0 | 0 | 3.5 | 0.5 | 0 | 6.0 | 0 | 0.5 | 10.5 |
| | < 10 cm | 0 | 0 | 0.3 | 0.5 | 0 | 0.1 | 0 | 0.2 | 1.1 |
| C | All | 0 | 0.2 | 0 | 0 | 0 | 0.3 | 0 | 0 | 0.5 |
| | < 10 cm | 0 | 0.2 | 0 | 0 | 0 | 0.3 | 0 | 0 | 0.5 |
| D | All | 0.5 | 5.2 | 0.8 | 0.8 | 0 | 7.8 | 0 | 0.7 | 15.8 |
| | < 10 cm | 0.3 | 1.2 | 0.6 | 0.1 | 0 | 2.8 | 0 | 0.1 | 5.1 |
| E | All | 0 | 25.6 | 0.7 | 0 | 0 | 45.4 | 0 | 0 | 71.7 |
| | < 10 cm | 0 | 0.2 | 0 | 0 | 0 | 0 | 0 | 0 | 0.2 |
| F | All | 18.6 | 4.7 | 0 | 0 | 0 | 11.6 | 0 | 0 | 34.9 |
| | < 10 cm | 0.1 | 0.1 | 0 | 0 | 0 | 0.2 | 0 | 0 | 0.4 |
| G | All | 0 | 3.9 | 0 | 0 | 0 | 0.7 | 0 | 0 | 4.6 |
| | < 10 cm | 0 | 0.1 | 0 | 0 | 0 | 0.4 | 0 | 0 | 0.5 |
| H | All | 18.0 | 12.8 | 0 | 22.6 | 0 | 0.2 | 0 | 0.1 | 53.7 |
| | < 10 cm | 0.4 | 0.6 | 0 | 0.1 | 0 | 0.2 | 0 | 0.1 | 1.4 |
| J | All | 4.9 | 4.9 | 0 | 0.1 | 0.4 | 0 | 0 | 0.1 | 10.4 |
| | < 10 cm | 0.7 | 0.1 | 0 | 0.1 | 0 | 0 | 0 | 0.1 | 1.0 |
| | Average | 5.3 | 7.2 | 0.6 | 3.0 | 0.1 | 9.0 | 0.0 | 0.2 | 25.3 |
| | Stdev | 8.2 | 8.4 | 1.2 | 7.9 | 0.1 | 15.3 | 0.0 | 0.3 | 25.7 |
| | Max | 18.6 | 25.6 | 3.5 | 22.6 | 0.4 | 45.4 | 0.0 | 0.7 | |
| | Min | 0.0 | 0.0 | 0.0 | 0.0 | 0.0 | 0.0 | 0.0 | 0.0 | |

*Table 3.* Scales of significant spatial pattern (m) for various combinations of species and age classes in plot F, meadow M1. C = clustered, R = random, D = dispersed, -- indicates no pattern of this type was found. Grey shading indicates this test was not performed. "X<25" and "X>25" refer to subsets of the 40 by 50 m plot. Corresponding analyses are shown in figures (Figure S 1 – Figure S 38).

| | Ripley's K | | | Pair correlation function | | | J function | | |
|---|---|---|---|---|---|---|---|---|---|
| | C | R | D | C | R | D | C | R | D |
| All | <6 | -- | >6 | <3 | | >3 | <3 | -- | -- |
| PSME | -- | -- | all | <1 | | 1 to 8 | | | |
| ABAM | <6 | -- | >6 | <3 | | >3 | <3 | -- | -- |
| ABGR | <6 | -- | >6 | <3 | | >3 | <4 | -- | -- |
| ABAM, ABGR | <4 | -- | >4 | <2 | | >2 | | | |
| PSME, ABGR | <7 | -- | >7 | | | | | | |
| ABAM, PSME | <6 | -- | >6 | | | | | | |
| Old, Young | 1 to 3 | <1 | >3 | | | | | | |
| Old, Young ABGR | | <3 | >3 | | | | | | |
| Old, Young ABAM | 1 to 4 | <1 | >4 | | | | | | |
| Old ABAM, Young ABAM | 1 to 4 | <1 | >4 | <2 | | >2 | | | |
| Old ABAM Young ABGR | -- | -- | -- | <0.5 | 0.5 to 2 | >2 | | | |
| X < 25 m | <2 | -- | >2 | | | | | | |
| X > 25 m | <7 | -- | >7 | | | | | | |
| Old and Young, X < 25 | -- | <2 | >2 | | | | | | |
| Old and Young, X > 25 | -- | <2 | >2 | | | | | | |
| Old and Young ABAM, X < 25 | -- | <2 | >2 | | | | | | |
| Old and Young ABAM, X > 25 | <4 | -- | >4 | | | | | | |
| Old ABAM and Young ABAM, X < 25 | -- | -- | all | | | | | | |
| Old ABAM and Young ABGR, X > 25 | <5, >6 | 5 to 6 | -- | <0.5 | | >2 | | | |
| Old ABGR and Young ABGR, X > 25 | >2 | <2 | -- | | | | | | |
| Old ABAM and Young ABAM, X > 25 | all | -- | -- | <3 | | 3 to 5 | | | |
| Old ABGR and Young ABAM, X > 25 | all | -- | -- | <0.5 | | | | | |

Trees in plot F were clustered, with one long narrow dense cluster in the northern (left) part of the plot, and a more diffuse cluster in the southern (right) part of the plot (Figure 7). Overall, trees are significantly clustered at scales of <6 m (Ripley's K, Figure 8 (a)) or < 3 m (pair correlation function, Figure 8 (b)), but clusters are significantly dispersed at distances above 6 m (Ripley's K, Figure 8 (a))., Trees have become increasingly clustered over time (J-function) (Figure 9). Dominant scales of clustering were smaller in the northern compared to the southern portion of the plot (Figure S 1 – Figure S 38).

Bivariate spatial patterns of old vs. young trees show little or no clustering (Figure 10). Other bivariate spatial patterns (e.g., by species and/or age) do not reveal any differences in scales of clustering relative to the sample of all trees. (Table 3, Figure S 1 – Figure S 38).

(a)

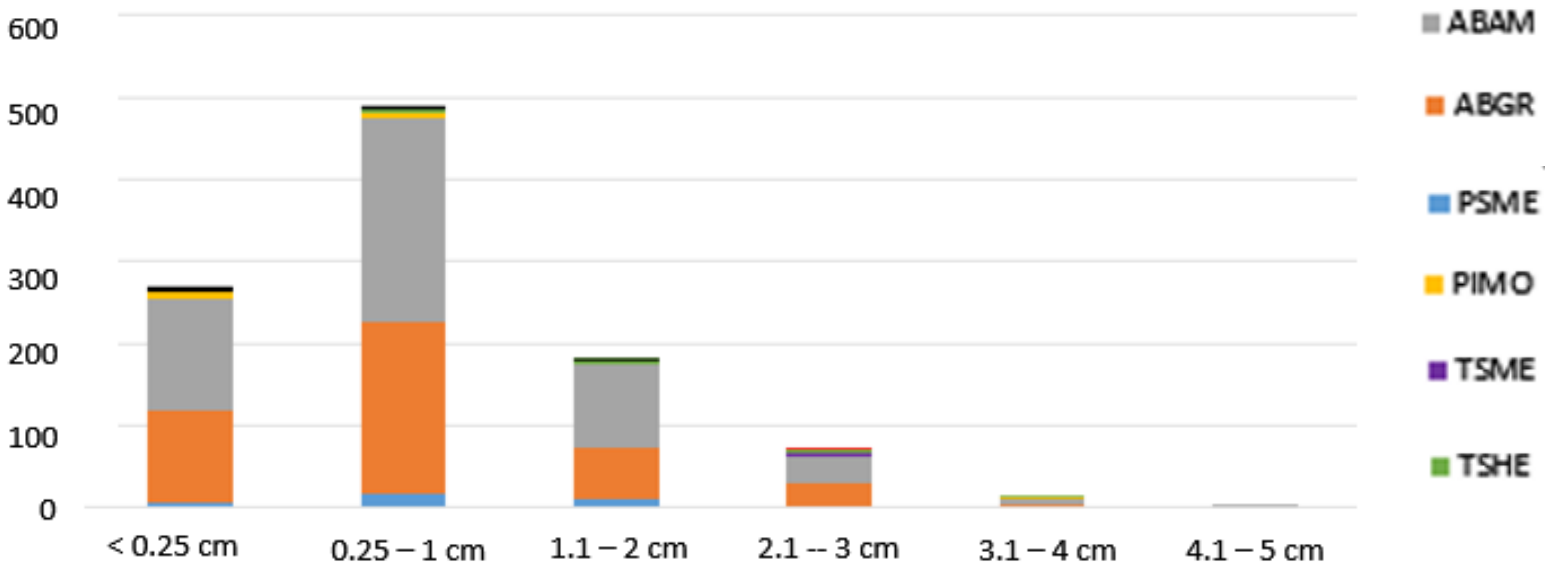
600
500
400
300
200
100
0
< 0.25 cm
0.25 – 1 cm
1.1 – 2 cm
2.1 -- 3 cm
3.1 – 4 cm
4.1 – 5 cm
ABAM
ABGR
PSME
PIMO
TSME
TSHE

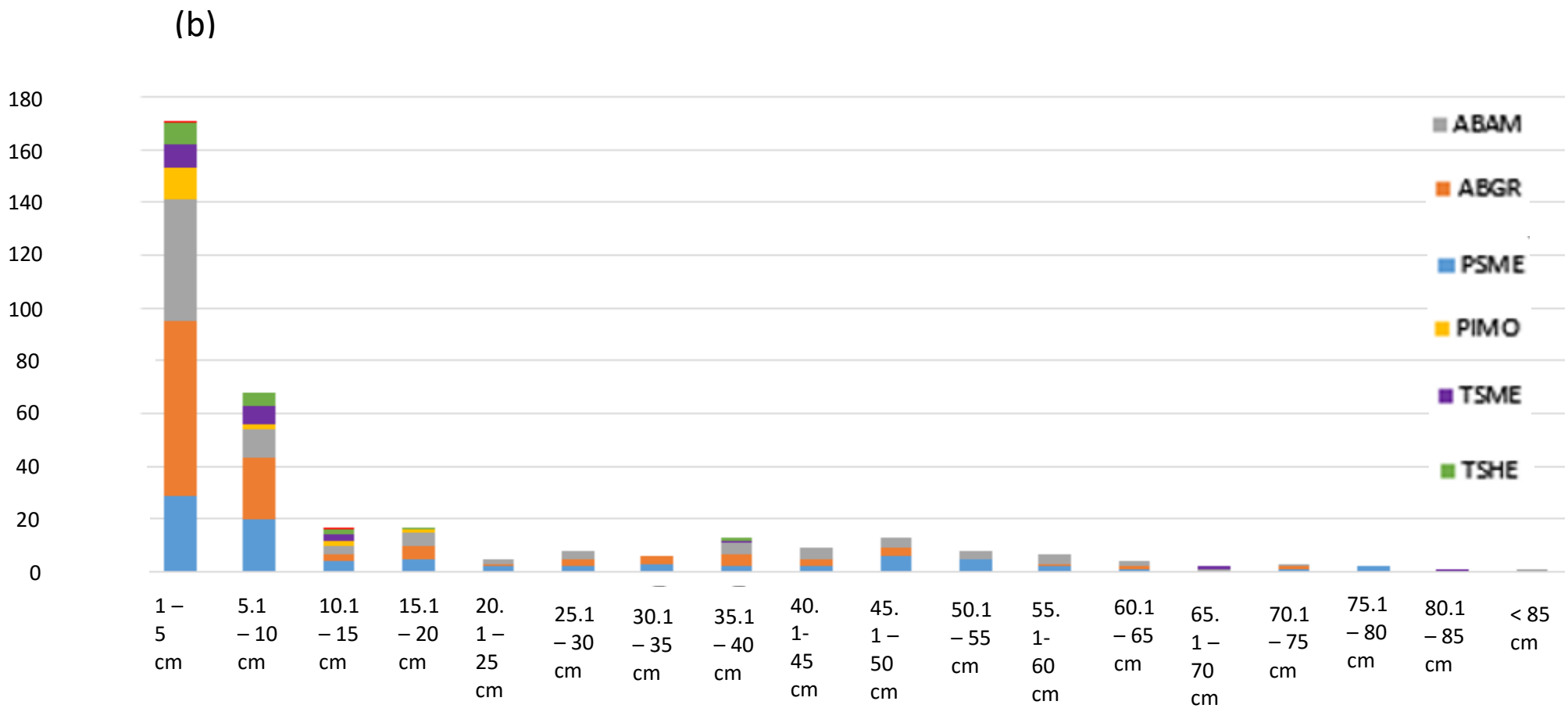


*Figure 3.* Number of trees by species and diameter class in all plots in meadow M1 (n = 1385) (a) < 5 cm diameter at base (DBA) (n = 1030) (b) >1 cm diameter at breast height (DBH) (n = 355).

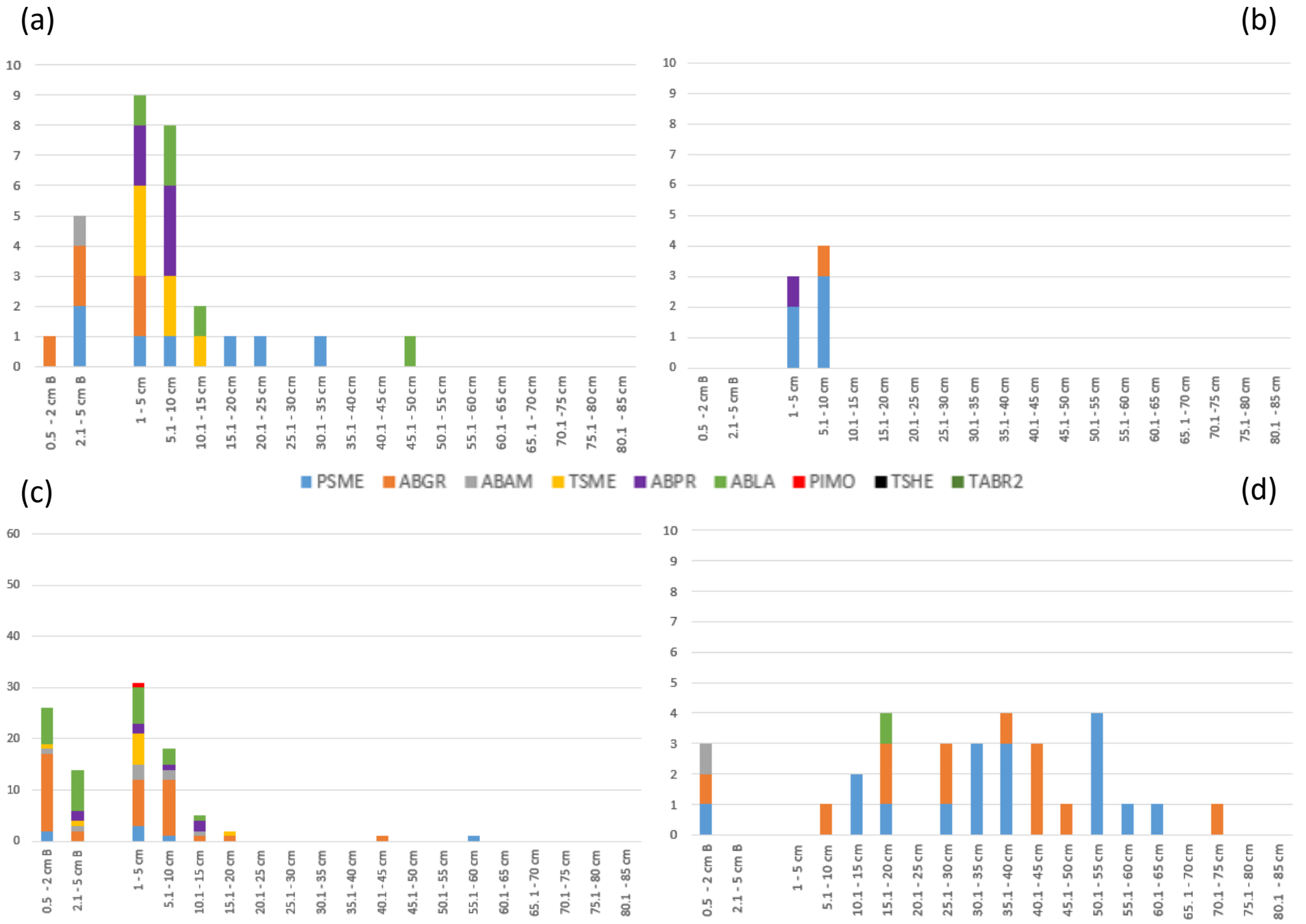
(a)
(b)
(c)
(d)
PSME
ABGR
ABAM
TSME
ABPR
ABLA
PIMO
TSHE
TABR2
0.5 - 2 cm B
2.1 - 5 cm B
1 - 5 cm
5.1 - 10 cm
10.1 - 15 cm
15.1 - 20 cm
20.1 - 25 cm
25.1 - 30 cm
30.1 - 35 cm
35.1 - 40 cm
40.1 - 45 cm
45.1 - 50 cm
50.1 - 55 cm
55.1 - 60 cm
60.1 - 65 cm
65. 1 - 70 cm
70.1 -75 cm
75.1 - 80 cm
80.1 - 85 cm

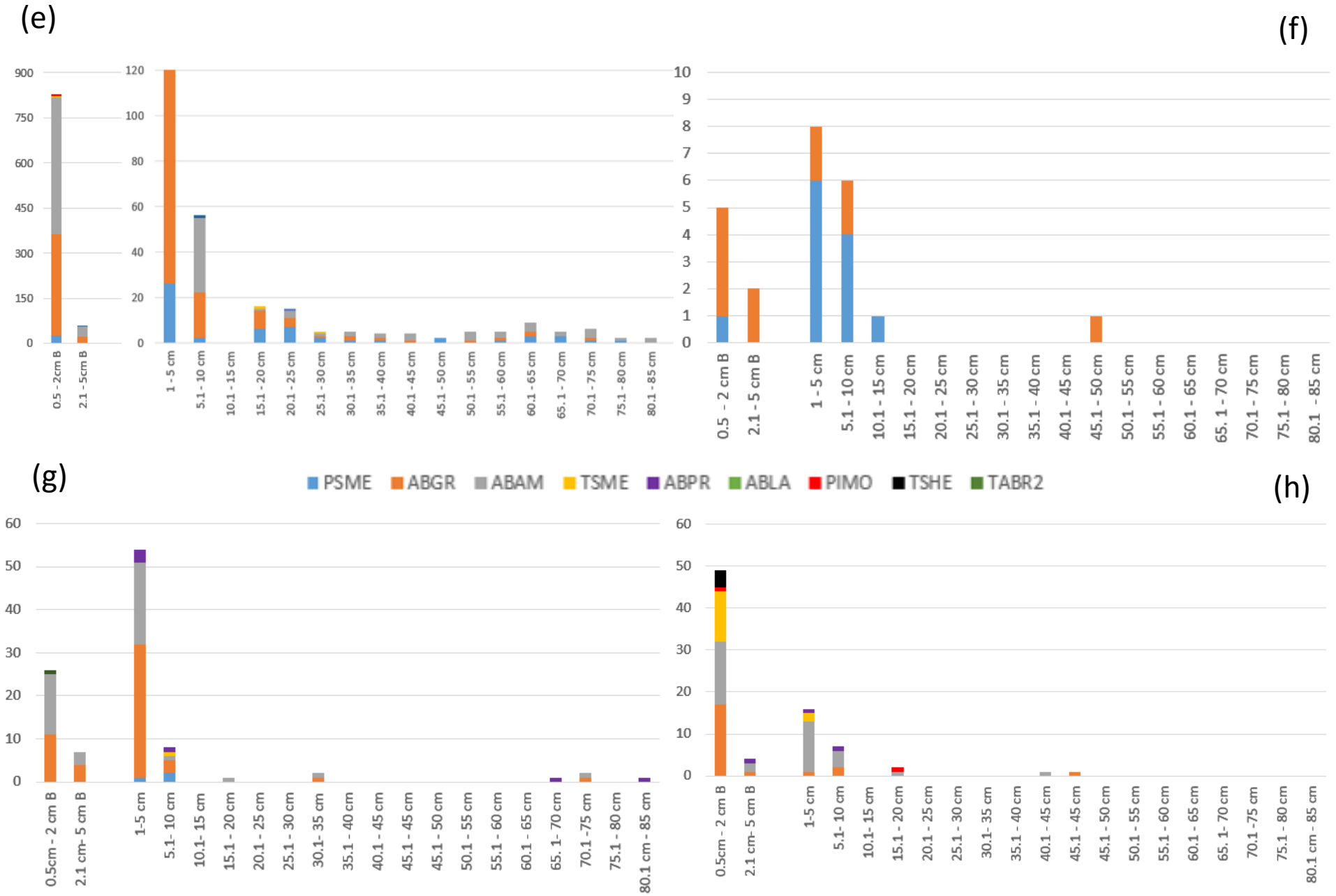


*Figure 4.* Numbers of trees by species and diameter class by plot in meadow M1. (a) Plot B, (b) Plot C, (c) Plot D, (d) Plot E, (e) Plot F (f) Plot G, (g) Plot H, (h) Plot J. Plots B, C, D, E, G, H, and J were 20 x 20 m. Plot F was 40 x 50 m. Note different Y-axis scales.

(a)

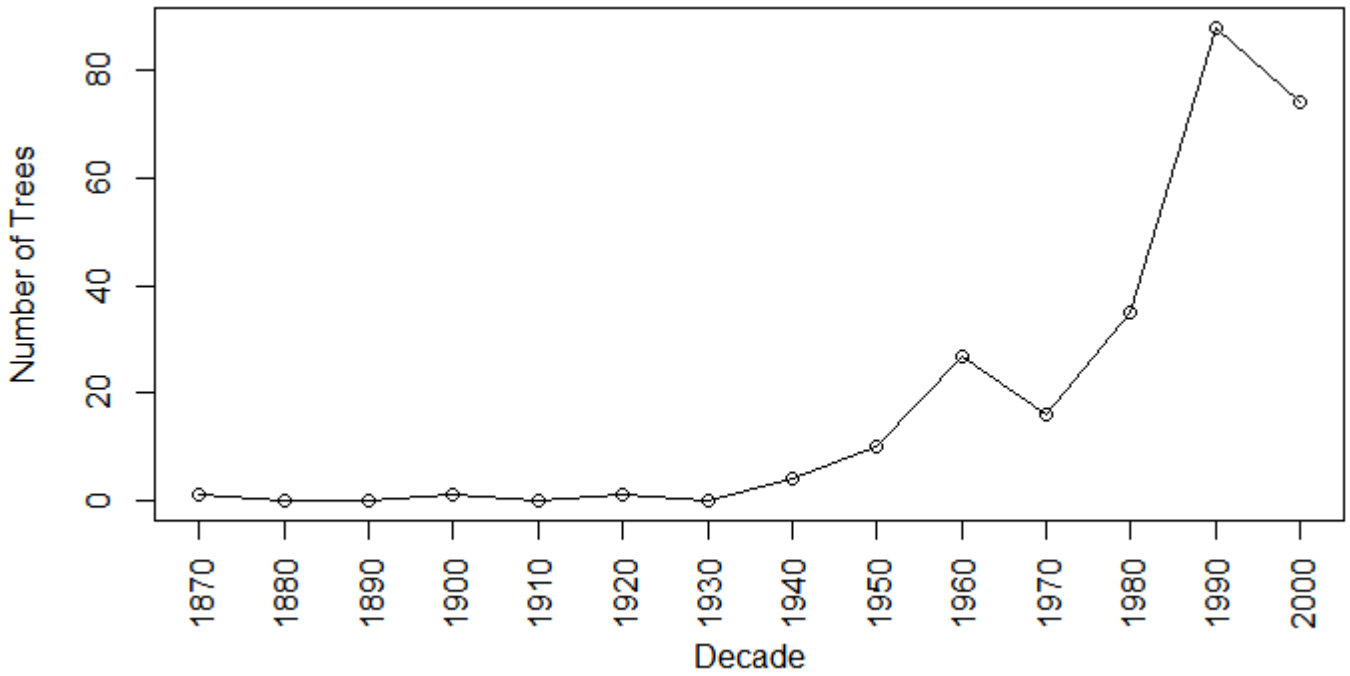
Number of Trees
0
20
40
60
80
1870
1880
1890
1900
1910
1920
1930
1940
1950
1960
1970
1980
1990
2000
Decade

(b)

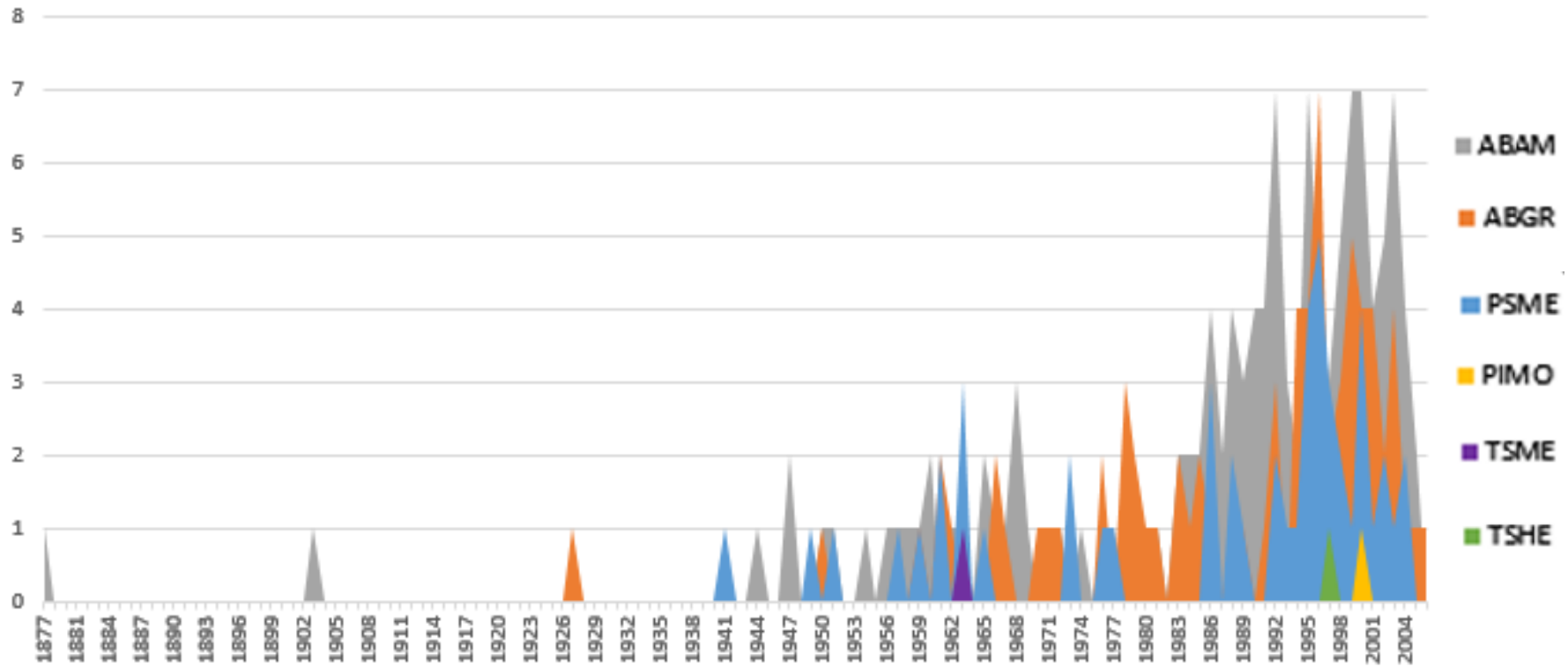


*Figure 5.* Number of trees by age, plot F, M1 meadow (n=252) (a) by decade, all species. (b) by year and species.

(a)

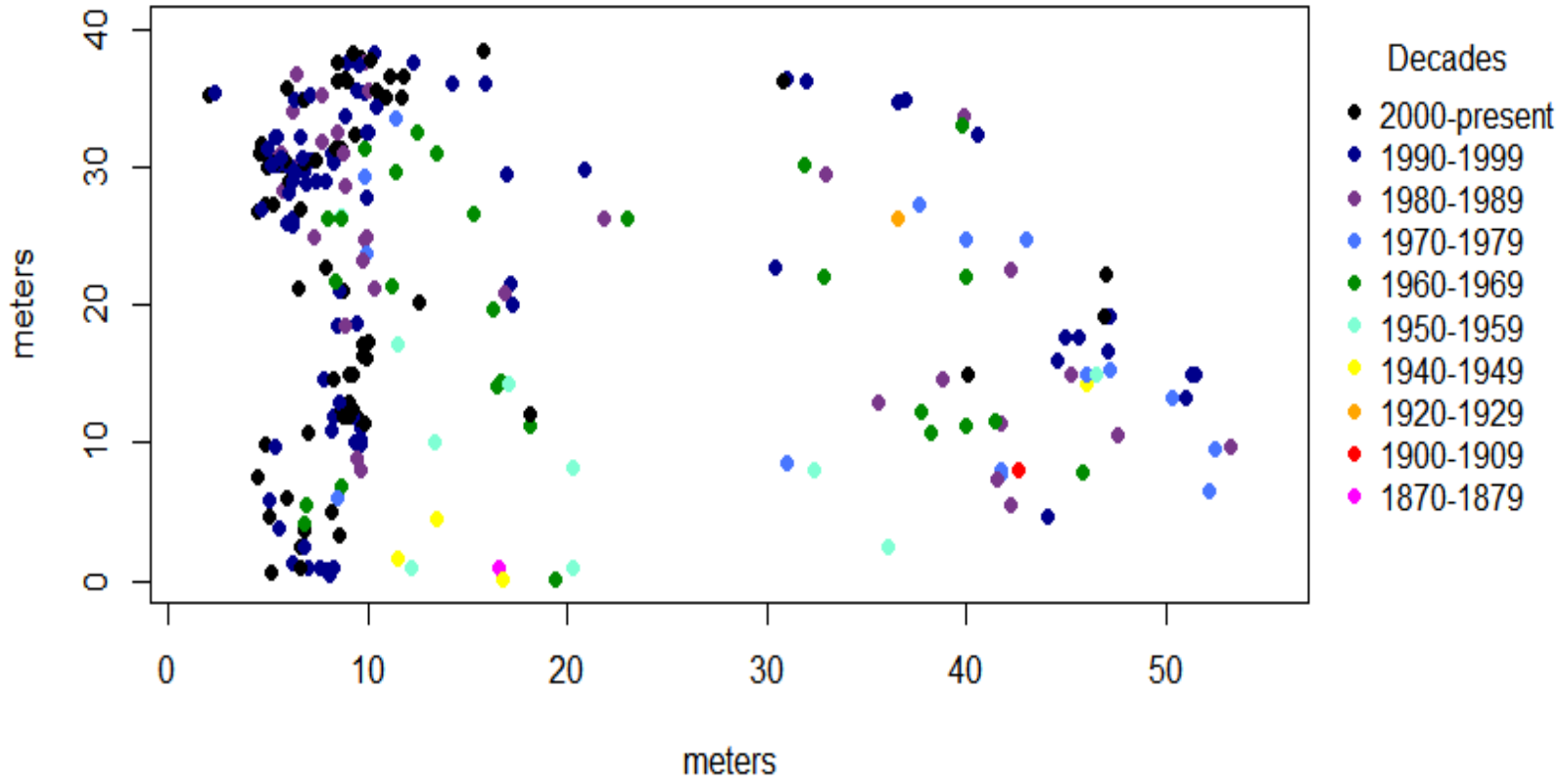
meters
0
10
20
30
40
0
10
20
30
40
50
meters
Decades
2000-present
1990-1999
1980-1989
1970-1979
1960-1969
1950-1959
1940-1949
1920-1929
1900-1909
1870-1879

(b)

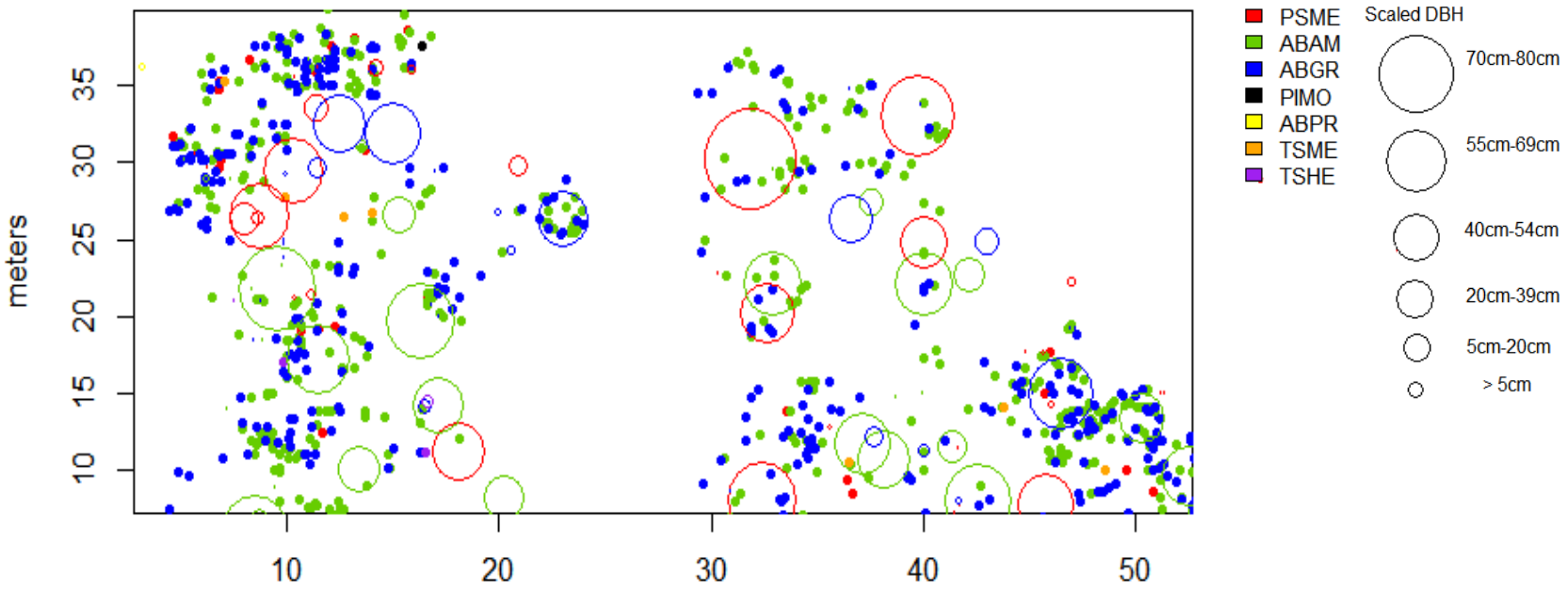


*Figure 6.* Spatial locations of trees in 2015, plot F, M1 meadow (n = 1008) (a) by decade (b) by diameter and species. In (b), open circles are scaled by DBH, closed dots trees with DBA measurements.

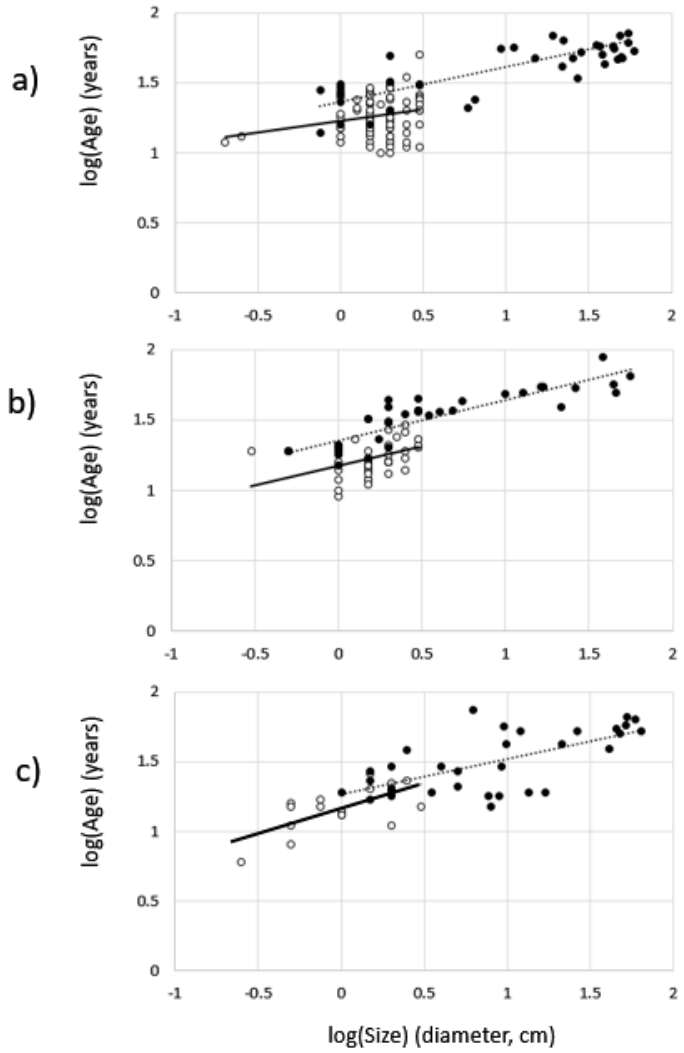


*Figure 7.* Size (diameter, cm) (x-axis) versus age (yrs) (y-axis). (a) ABAM: (DBA) y= 1.23+ 0.16x, r2= 0.05 (n=82); (DBH) y=1.37+ 0.25x, r2= 0.63 (n=50). (b) ABGR: (DBA) y= 1.17+ 0.28x, r2 = 0.14 (n=41); (DBH) y= 1.36 + 0.29x, r2 = 0.77 (n=44). (c) PSME: (DBA) y= y = 1.17+ 0.37x, r2 = 0.48 (n=19). (DBH) y= 1.27+ 0.25x, r2 = 0.42 (n=40).

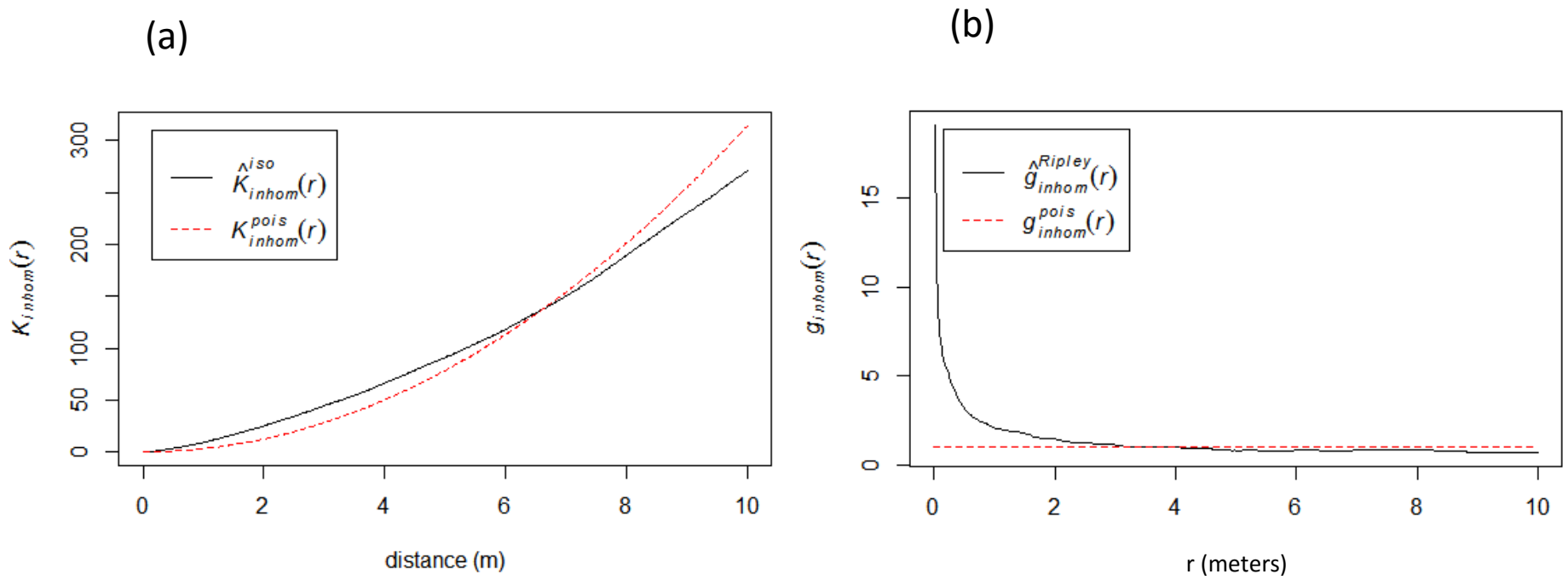


*Figure 8.* Second-order point pattern analysis of trees in plot F, meadow M1, 2015 (n=1008) (a) Univariate Ripley's K. (b) Univariate pair correlation function. Black curve = observed points, red dashed curve = random spatial pattern, grey shading = 95% confidence interval around random pattern.

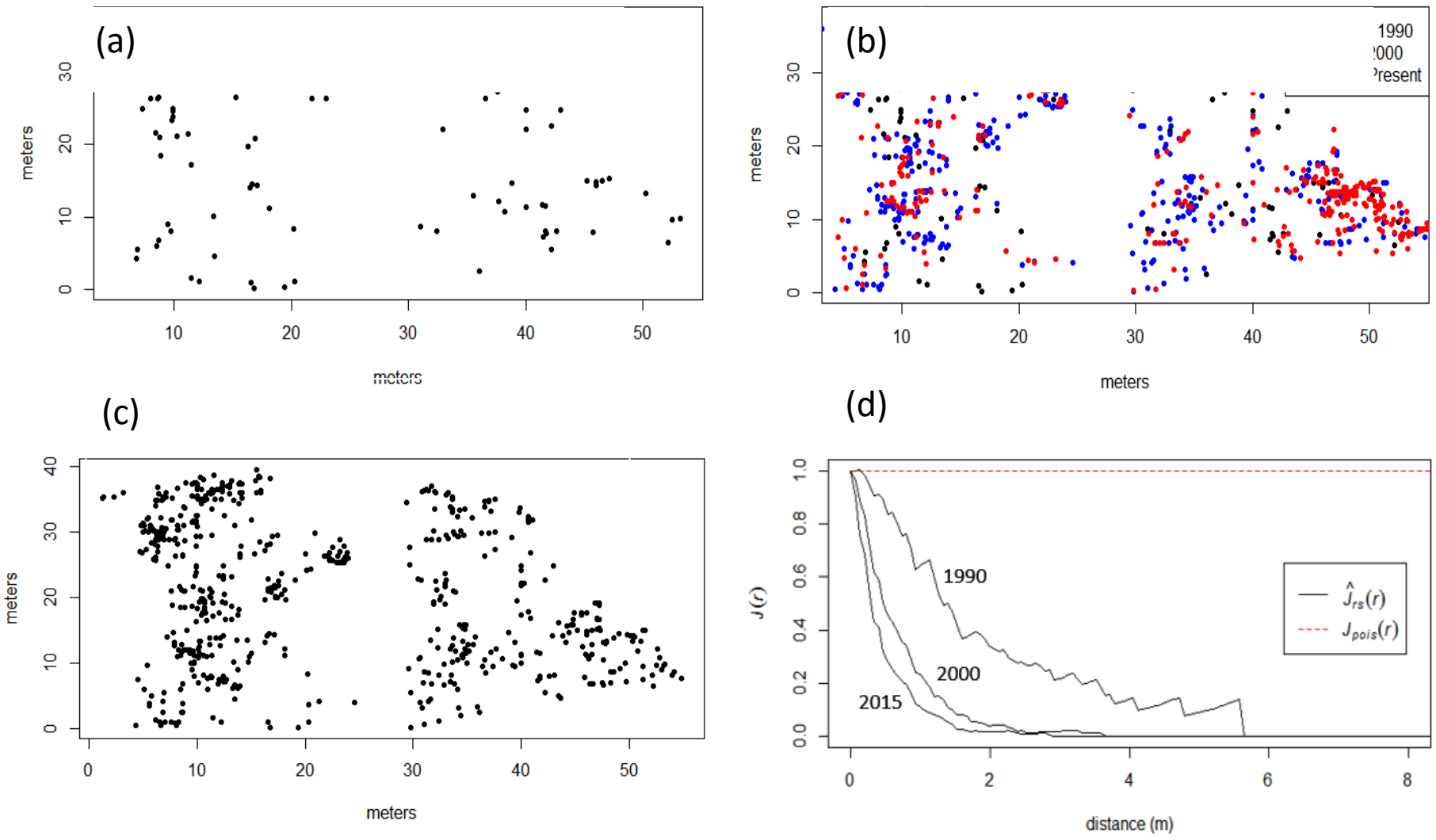


*Figure 9.* Spatial location of stems in plot F, established (a) through 1990 (n=95), (b) through 2000 (n=594), and (c) through 2015 (n=996), (d) J-Function for stems established before 1990 (n=95), in 2000 or before (n=601), and as of 2015 (n=996). The 996 stems include all of the stems for the species of interest in plot F (n=994), and two stems of other species that were aged in plot F.

(a)

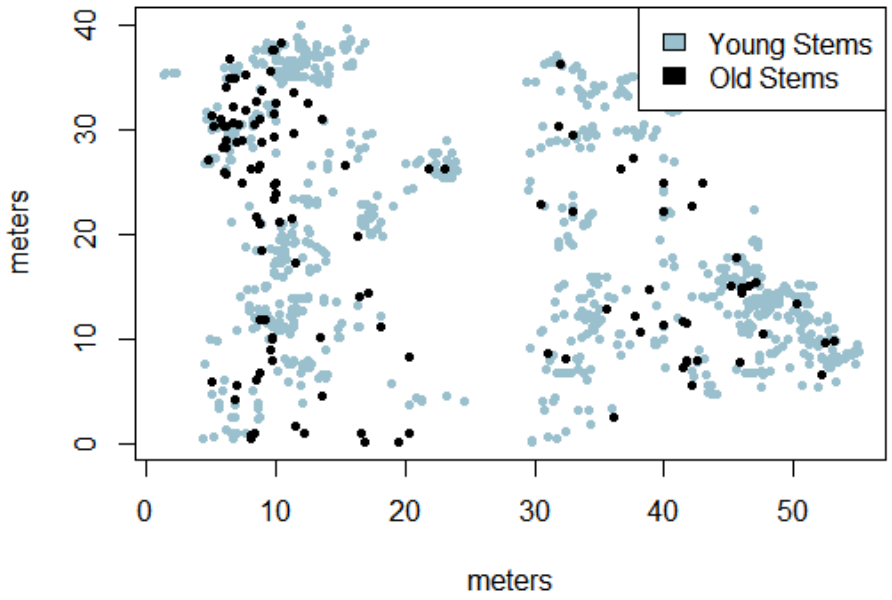


(b)

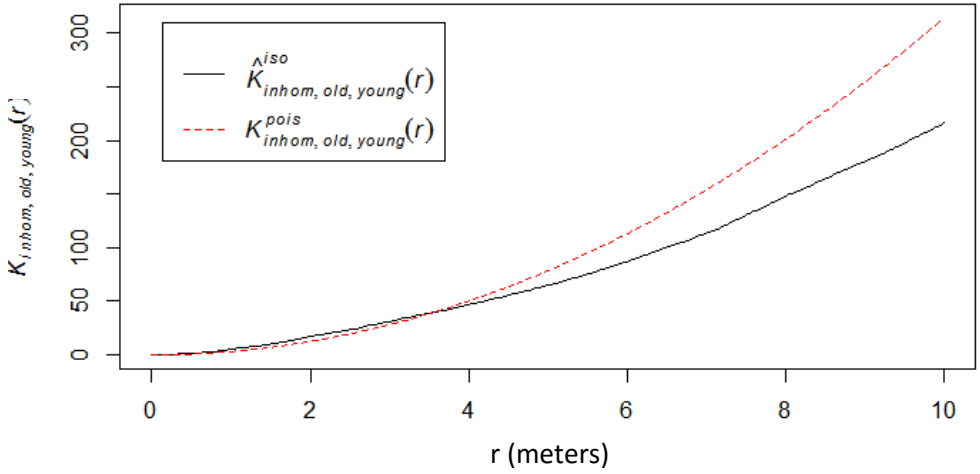


*Figure 10.* (a) spatial pattern of trees by age in plot F. Stems of ABGR greater than 30 years of age were designated as old, while those less than 30 years were designated as young. Stems of ABAM and PSME greater than 20 years of age were designated as old, while those less than 20 years of age were designated as young. Black circles = old (n=130). Grey circles = young (n=864). (b) Bivariate Ripley's K for old (n=130) and young (n=864) stems. The total number of stems is 994, instead of 1008, because only ABAM, ABGR, and PSME stems were included in this analysis.

## 5. Discussion

### *5. 1 Spatio-temporal pattern of invasion*

Over the past 150 years, tree establishment in the M1 meadow has progressed from the edges toward the center of the meadow. Forest structure and composition is quite variable along the meadow edge. Some locations have high tree species diversity, some locations have a few, early established trees with relatively few or no small, younger trees, whereas other locations have clusters of small, younger trees.

In the intensively studied plot, tree establishment has occurred in the form of dispersed clusters. Some of these clusters consist of a single older tree surrounded by small, mostly younger trees, while other clusters consist of only small, relatively trees. However, there are also individual large, old trees which lack any small, younger trees underneath or near them, and there are multiple patches which lack any trees.

### *5. 2 Biotic interactions*

This study found little evidence of biotic interactions among tree species and age classes as a factor structuring the spatial and temporal patterns of tree establishment. Trees <30 years of age did not appear to be more likely to be located near trees >30 years old. Trees that established early were no more likely to be shade intolerant (e.g., Douglas-fir) than shade tolerant (e.g., grand fir). Trees with shade-tolerant life history strategies (e.g., grand fir) were no more likely to occur under the canopy of an older tree than they were to occur in the open. In contrast, Halpern et al (2010) and Rice et al (2012) noted that biotic interactions among tree species strongly structured tree establishment in the Bunchgrass meadow, to the east of this study site. However, this analysis may have been limited because only 252 of the trees were aged, and ages of the remaining 742 trees in the analysis were estimated by size:age relationships, which were relatively weak for small trees.

The proportion of total stems and the spatial arrangement of PSME differed from that of ABAM and ABGR, consistent with known differences in species ecological traits. PSME stems may have a dispersed spatial pattern (Hermann, R. and Lavender, D. 1990). In contrast, the highly clustered spatial patterns of ABAM and ABGR may indicate that these species differ relatively little in their life history traits. Both species are known to successfully function as shade-tolerant understory species with the potential to assume the role of dominant overstory species in later successional stages (Crawford, P. and Oliver, Chadwick D. 1990; Foiles, M., Graham, R., and Olson, D. 1990). It is apparent that some trees spend decades in the seedling stage before they begin to grow in height, indicated by the lack of a relationship between diameter and age for stems < 3 cm in diameter. ABAM can also assume the role of a shade-intolerant, pioneer species; this is evident from the establishment of ABAM trees relatively early in the invasion process, in open locations (Crawford, P. and Oliver, Chadwick D. 1990; Foiles, M., Graham, R., and Olson, D. 1990).

### *5. 3 Environmental factors*

Environmental factors such as topography and resource availability may account for the observed patterns of tree establishment. Environmental and site-specific variables such as sunlight, moisture, disturbance by wildlife, soil depth, and soil chemistry may influence tree establishment. Although these factors varied among the study plots, there were no consistent differences in stand structure or composition based on edge orientation. The excavation and tunneling processes of gophers influenced biotic communities of the surface and subsurface in a meadow at Bunchgrass Ridge in the High Cascades (Case, Halpern, and Levin 2013), but no evidence of dens for ground-dwelling animals, such as gophers, was detected in plot F.

Soil characteristics, along with biogeochemical processes, may influence tree establishment. Soil chemistry differs significantly between meadow and forest sites (Griffiths, Madritch, and Swanson 2005). Once trees become established, soils transition rapidly to more forest-like chemistry, making the environment less hospitable for meadow species (Haugo and Halpern 2007). Forest litter speeds the

transition of soil chemistry from meadow to forest-like conditions in boundary transition zones (Griffiths, Madritch, and Swanson 2005). The main components of soil chemistry known to influence tree establishment are the concentrations of nitrogen and β-Glucosidase, governing the ability of trees to mineralize N and the concentration of microorganisms, respectively (Griffiths, Madritch, and Swanson 2005). Following tree establishment, when the slower cycling of N associated with forest species is superimposed over the already high concentrations of N found in meadow soils, this creates an opportune environment for accelerated tree establishment. The portion of plot F experiencing accelerated invasion had greater than 75% cover of forest litter, including areas that were not directly adjacent to trees. Forest litter-dominated ground cover gradually transitions to more meadow species-dominated ground cover for x >15 m in plot F. The intersection of accelerated invasion and the occurrence of forest litter suggests established stems may be sequestering nutrients and depositing forest litter, aiding in a shift to soil chemistry conditions that are favorable for tree establishment.

A well-developed mycorrhizal mat in the soil also may promote tree invasion in non-forested sites (Perry, Molina, and Amaranthus 1987). Tree seedling success in montane grassland environments was higher in sites within 4 m of pioneer trees and intact mycorrhizal networks preserved in forest soil, compared to sites in soils of open meadows or post-disturbance environments that lacked well-developed mycorrhizal networks (Amaranthus and Perry 1987), regardless of the species of the pioneer tree. This could be a possible explanation for the scales of facilitation (mostly < 4 m) found in this study.

### *5. 4 Meadow Restoration Prescription*

A variety of meadow restoration techniques have been employed in the montane meadows of the Cascade mountains (Lang and Halpern 2007; Halpern, Antos, and Beckman 2014; Kremer, Halpern, and Antos 2014; Halpern et al. 2016). The absence of previous meadow restoration within the Andrews Forest offers the opportunity to implement experimental meadow restoration methods. A restoration plan for the M1 meadow in the H.J. Andrews Experimental Forest must consider the environmental and ecological

factors influencing montane meadow health and the feasibility of implementing large-scale, restoration in meadows that have experienced more than 50 years of invasion.

For this study, all stems <10 cm DBH were removed from plot F (with the exception of 9 stems with a DBH less than 10 cm that were cored), mimicking a disturbance that selectively affects young, small trees, such as animal grazing or a low intensity burn. Because the type and date of disturbance (tree removal, October 2015) are known, this provides an opportunity to observe successional dynamics and the effectiveness of removing small trees for restoration. Old trees are still present in plot F, and the soils still retain forest litter, allowing forest soil chemistry to persist. Thus, the mechanical removal of small trees is not expected to be sufficient to promote recolonization by meadow species in plot F, necessitating other meadow restoration actions.

Meadow restoration is easiest and most effective during the early stages of tree encroachment, because less stem removal is required and future seed sources are eliminated. Burning for these purposes may not be desirable, as species such as *Carex spp.*, a common constituent of montane meadows, often disproportionately dominates seed banks and can dominate post-burn meadow communities, reducing biodiversity (Halpern et al. 2012; Halpern et al. 2016). Encroachment in plot F is not early onset and perhaps not ideal for restoration efforts. Yet, a previous study of meadow restoration displays no relationship between forest age and the success of restoration, indicating meadow restoration can succeed on sites similar to that of plot F (Halpern et al. 2016).

## 6. Conclusions and Future Work

This study in the M1 meadow of the H.J. Andrews Experimental Forest, along with previous work at Bunchgrass Ridge and other meadow locations in the Oregon Cascades, indicates that tree establishment in montane meadows is not a uniform process across the landscape. Although tree establishment is influenced by a number of factors, this study focused on the dynamics of individual invading trees and their species' life histories. Various tree species and densities of invasion were

observed along the > 1.7 km edge of this 4.8-ha meadow. Small individuals of ABAM and ABGR are present throughout the meadow edge, but PSME, ABGR, and ABAM dominate among large (> 10 cm DBH) individuals along the meadow edge.

A variety of meadow habitats occur in the H.J. Andrews Experimental Forest. This study in the M1 meadow may be only partly representative of tree invasion in other meadows in the H.J. Andrews Forest. Declining meadow habitat within the H.J. Andrews Forest raises concern for plant-pollinator networks and wildlife that rely on these patches in the landscape and prompts discussions about how to restore meadow habitat. The rapid rate of meadow decline in the past half century and the accelerated invasion evident in this study suggest that tree establishment in meadows will continue in the near future. Thus, active meadow restoration may be the only option to maintain meadow habitat.

## BIBLIOGRAPHY


Amaranthus, M.P., and D.A. Perry. 1987. “Effect of Soil Transfer on Ectomycorrhiza Formation and the Sruvival and Growth of Conifer Seedlings on Old, Nonreforested Clear-Cuts.” *Canadian Journal of Forest Research* 17: 944–950.

Baddeley, Adrian, and Rolf Turner. 2013. “Spatstat: Spatial Point Pattern Analysis, Model-Fitting, Simulation, Tests.” *R Foundation for Statistical Computing, Vienna, Austria*.

Brooks, J. R., F. C. Meinzer, J. M. Warren, J.C. Domec, and R. Coulumbe. 2003. “Seasonal Patterns and Vertical Profile of Soil Water Uptake and Utilization by Young and Old Douglas-Fir and Ponderosa Pine Forests.” presented at the North American Forest Ecology Workshop, Corvallis, OR.

Case, Madelon F., Charles B. Halpern, and Simon A. Levin. 2013. “Contributions of Gopher Mound and Casting Disturbances to Plant Community Structure in a Cascade Range Meadow Complex.” *Botany* 91 (8): 555–561. doi:10.1139/cjb-2013-0023.

Crawford, Peggy D., and Oliver, Chadwick Dearing. 1990. “Pacific Silver Fir.” In *Silvics of North America: 1. Conifers,* 2:5–25. Agriculture Handbook 654. Washington, D.C.: United States Department of Agriculture.

Dailey, Michele Meadows. 2007. “Meadow Classification in the Willamette National Forest and Conifer Encroachment Patterns in the Chucksney-Grasshopper Meadow Complex, Western Cascade Range, Oregon.” http://ir.library.oregonstate.edu/xmlui/handle/1957/7520.

Fahrig, Lenore. 2003. “Effects of Habitat Fragmentation on Biodiversity.” *Annual Review Ecology, Evolution, and Systematics* 34: 487–515.

Foiles, Marvin W., Graham, Russel T., and Olson, David F. 1990. “Grand Fir.” In *Silvics of North America: 1. Conifers,* 2:80–97. Agriculture Handbook 654. Washington, D.C.: United States Department of Agriculture.

Fontaine, Colin, Isabelle Dajoz, Jacques Meriguet, and Michel Loreau. 2005. “Functional Diversity of Plant–Pollinator Interaction Webs Enhances the Persistence of Plant Communities.” Edited by Nick Waser. *PLoS Biology* 4 (1): e1. doi:10.1371/journal.pbio.0040001.

Griffiths, Robert, Michael Madritch, and Alan Swanson. 2005. “Conifer Invasion of Forest Meadows Transforms Soil Characteristics in the Pacific Northwest.” *Forest Ecology and Management* 208 (1-3): 347–58. doi:10.1016/j.foreco.2005.01.015.

Grissino-Mayer, Henri D. 2003. “A Manual and Tutorial for the Proper Use of an Increment Borer.” *Tree-Ring Research* 59 (2): 63–79.

Halpern, Charles B., Joseph A. Antos, and Liam M. Beckman. 2014. “Vegetation Recovery in Slash-Pile Scars Following Conifer Removal in a Grassland-Restoration Experiment: Burn-Scar Recovery in Mountain Grasslands.” *Restoration Ecology* 22 (6): 731–740. doi:10.1111/rec.12130.

Halpern, Charles B., Joseph A. Antos, Donald McKenzie, and Annette M. Olson. 2016. “Past Tree Influence and Prescribed Fire Mediate Biotic Interactions and Community Reassembly in a Grassland-Restoration Experiment.” Edited by Lara Souza. *Journal of Applied Ecology* 53 (1): 264–73. doi:10.1111/1365-2664.12570.

Halpern, Charles B., Joseph A. Antos, Janine M. Rice, Ryan D. Haugo, and Nicole L. Lang. 2010. “Tree Invasion of a Montane Meadow Complex: Temporal Trends, Spatial Patterns, and Biotic Interactions.” *Journal of Vegetation Science* 21 (4): 717–732. doi:10.1111/j.1654-1103.2010.01183.x.

Halpern, Charles B., Ryan D. Haugo, Joseph A. Antos, Sheena S. Kaas, and Allyssa L. Kilanowski. 2012. “Grassland Restoration with and without Fire: Evidence from a Tree-Removal Experiment.” *Ecological Applications* 22 (2): 425–441.

Haugo, Ryan D., and Charles B. Halpern. 2007. “Vegetation Respones to Conifer Encroachment in a Western Cascade Meadow: A Chronosequence Approach.” *Canadian Journal of Botany* 85: 285–298.

Haugo, Ryan D., and Charles B. Halpern. 2010. “Tree Age and Tree Species Shape Positive and Negative Interactions in a Montane Meadow.” *Botany* 88 (5): 488–499.

Helderop, Edward. 2015. “Diversity, Generalization, and Specialization in Plant-Pollinator Networks of Montane Meadows, Western Cascades, Oregon.” https://ir.library.oregonstate.edu/xmlui/handle/1957/56285.

Hermann, Richard K., and Lavender, Denis P. 1990. “Douglas-Fir.” In *Silvics of North America: 1. Conifers*, 2:1080–1109. Agriculture Handbook 654. Washington, D.C.: United States Department of Agriculture.

Highland, Steven A., Jeffrey C. Miller, and Julia A. Jones. 2013. “Determinants of Moth Diversity and Community in a Temperate Mountain Landscape: Vegetation, Topography, and Seasonality.” *Ecosphere* 4 (10): art129. doi:10.1890/ES12-00384.1.

Kremer, Nicolas J., Charles B. Halpern, and Joseph A. Antos. 2014. “Conifer Reinvasion of Montane Meadows Following Experimental Tree Removal and Prescribed Burning.” *Forest Ecology and Management* 319: 128–137. doi:http://dx.doi.org/10.1016/j.foreco.2014.02.002.

Lang, Nicole L., and Charles B. Halpern. 2007. “The Soil Seed Bank of a Montane Meadow: Consequences of Conifer Encroachment and Implications for Restoration.” *Canadian Journal of Botany* 85: 557–569.

Lieshout, M. N. M. van. 2006. “A J-Function for Marked Point Patterns.” *Annals of the Institute of Statistical Mathematics* 58 (2): 235–259. doi:10.1007/s10463-005-0015-7.

Miller, Eric A., and Charles B. Halpern. 1998. “Effects of Environment and Grazing Disturbance on Tree Establishment in Meadows of the Central Cascade Range, Oregon, USA.” *Journal of Vegetation Science* 9 (2): 265–282.

Perry, D.A., R. Molina, and M.P. Amaranthus. 1987. “Mycorrhizae, Mycorrhizospheres, and Reforestation: Current Knowledge and Research Needs.” *Canadian Journal of Forest Research* 17: 929–940.

Pfeiffer, Vera W. 2012. “Influence of Spatial and Temporal Factors on Plants, Pollinators and Plant-Pollinator Interactions in Montane Meadows of the Western Cascades Range.” http://ir.library.oregonstate.edu/xmlui/handle/1957/30826.

Potts, Simon G., Biesmeijer, Jacobus C., Kremen, Claire, Neumann, Peter, Schweiger, Oliver, and Kunin, William E. 2010. “Global Pollinator Declines: Trends, Impacts and Drivers.” *Trends in Ecology and Evolution* 25 (6): 345–353.

Rathcke, B., and Jules, E. 1993. “Habitat Fragmentation and Plan-Pollinator Interactions.” *Current Science* 65: 273–277.

Rice, JanineM., CharlesB. Halpern, JosephA. Antos, and JuliaA. Jones. 2012. “Spatio-Temporal Patterns of Tree Establishment Are Indicative of Biotic Interactions during Early Invasion of a Montane Meadow.” *Plant Ecology* 213 (4): 555–568. doi:10.1007/s11258-012-0021-9.

Rice, Janine, and others. 2009. “Forest-Meadow Dynamics in the Central Western Oregon Cascades: Topographic, Biotic, and Environmental Change Effects.” http://ir.library.oregonstate.edu/jspui/handle/1957/13781.

Ripley, Brian D. 1977. “Modelling Spatial Patterns.” *Journal of the Royal Statistical Society. Series B (Methodological)*, 172–212.

Scholes, R. J., and S. R. Archer. 1997. “Tree-Grass Interactions in Savannas.” *Annual Review of Ecology and Systematics*, 517–544.

Steffan-Dewenter, Inolf. 2003. “Importance of Habitat Area and Landscape Context for Species Richness of Bees and Wasps in Fragmented Orchard Meadows.” *Conservation Biology* 17 (4): 1036–1044.

Stoyan, D., and Stoyan, H. 1996. “Estimating Pair Correlation Functions of Planar Cluster Processes.” *Biometrical Journal* 38 (3): 259–271.

Swanson, Frederick, and Julia Jones. 2001. “Geomorphology and Hydrology of the H.J. Andrews Experimental Forest, Blue River, Oregon.”

Takaoka, Sadao, and Frederick J. Swanson. 2008. “Change in Extent of Meadows and Shrub Fields in the Central Western Cascade Range, Oregon∗.” *The Professional Geographer* 60 (4): 527–540. doi:10.1080/00330120802212099.

Wiegand, Thorsten, and Kirk A. Moloney. 2004. “Rings, Circles, and Null-Models for Point Pattern Analysis in Ecology.” *Oikos* 104 (2): 209–229. doi:10.1111/j.0030-1299.2004.12497.x.

Zald, Harold S. J., Thomas A. Spies, Manuela Huso, and Demetrios Gatziolis. 2012. “Climatic, Landform, Microtopographic, and Overstory Canopy Controls of Tree Invasion in a Subalpine Meadow Landscape, Oregon Cascades, USA.” *Landscape Ecology* 27 (8): 1197–1212. doi:10.1007/s10980-012-9774-8.

# APPENDIX

*Table S 1.* Numbers of trees by species, type of size measurement, and tree aging method in plot F.

| | Species | | | | | |
|---|---|---|---|---|---|---|
| | **ABAM** | **ABGR** | **PSME** | **other** | **unknown** | **Total** |
| **Tree diameter obtained** | | | | | | |
| Measured by DBH (DBH > 1 cm) | 45 | 39 | 36 | 3 | | 123 |
| Measured by DBA (DBA < 5 cm) | 489 | 358 | 27 | 11 | | 885 |
| **Total** | 534 | 397 | 63 | 14 | | 1008 |
| | | | | | | |
| **Tree age sample obtained** | | | | | | |
| Tree core obtained for tree measured by DBH | 28 | 13 | 18 | 1 | | 60 |
| Basal section obtained for tree measured by DBH | 17 | 25 | 16 | 5 | | 63 |
| **of which** | | | | | | |
| 1 to 2cm | 14 | 16 | 8 | 0 | | |
| 2.1 to 3cm | 1 | 5 | 2 | 0 | | |
| 3.1 to 4 cm | 0 | 2 | 2 | 0 | | |
| 4.1 to 5cm | 0 | 0 | 4 | 0 | | |
| > 5cm | 2 | 2 | 0 | 0 | | |
| | | | | | | |
| **Basal section obtained for tree measured by DBA** | 319 | 226 | 20 | 6 | | 571 |
| **of which** | | | | | | |
| 0 to 0.25 cm | 2 | 0 | 1 | | | |
| 0.3 to 0.5 cm | 92 | 69 | 5 | | | |
| 0.51 to 1 cm | 100 | 88 | 5 | | | |
| 1 to 1.5 cm | 62 | 31 | 2 | | | |
| 1.5 to 2 cm | 30 | 18 | 5 | | | |
| 2.1 to 2.5 cm | 12 | 10 | 1 | | | |
| 2.51 to 3cm | 15 | 8 | 1 | | | |
| 3.51 to 3.5cm | 3 | 1 | 0 | | | |
| 3.51 to 4 cm | 3 | 1 | 0 | | | |
| **Extracted, no age determined (DBA < 0.25 cm)** | 170 | 132 | 7 | 5 | **Total** | 314 |
| | | | | | | 1008 |
| | | | | | | |
| **Additional tree age samples obtained from plots B, C, D, E, G, H, J** | | | | | | |
| DBA | 0 | 0 | 0 | 0 | | 0 |
| DBH | 5 | 4 | 6 | 3 | | 18 |
| **Total aged: other plots** | | | | | | 18 |

*Table S 2.* Numbers of samples aged from plot F. Of the 60 tree cores obtained (Table 1), 4 could not be aged due to rot or deformities. Of the 63 trees whose DBH was measured and a basal section was obtained (Table 1), 9 could not be aged to within +/- 2 years, due to rot or deformities. Of the 885 trees whose DBA was obtained using basal sections (Table 1), only 142 were aged and the remaining (~ 570) could have been aged but there was inadequate time to complete this, or they were too small (<0.25 cm DBA) to be aged within ± 2 yrs.

| | Species | | | | | |
|---|---|---|---|---|---|---|
| | **ABAM** | **ABGR** | **PSME** | **other** | **unknown** | **Total** |
| **Tree cores aged** | 26 | 11 | 18 | 1 | | 56 |
| **Basal sections aged w/ DBH** | 16 | 23 | 15 | 0 | | 54 |
| **of which** | | | | | | |
| 1 to 2cm | 13 | 16 | 8 | | | |
| 2.1 to 3cm | 1 | 5 | 2 | | | |
| 3.1 to 4 cm | 0 | 2 | 1 | | | |
| 4.1 to 5cm | 0 | 0 | 4 | | | |
| >5cm | 2 | 0 | 0 | | | |
| | | | | | | |
| **Basal sections aged w/ DBA** | 82 | 41 | 19 | | | 142 |
| **of which** | | | | | | |
| 0 to 0.25 cm | 2 | 0 | 1 | | | |
| 0.3 to 0.5 cm | 0 | 1 | 4 | | | |
| 0.51 to 1 cm | 9 | 5 | 5 | | | |
| 1 to 1.5 cm | 28 | 15 | 2 | | | |
| 1.5 to 2 cm | 26 | 11 | 5 | | | |
| 2.1 to 2.5 cm | 7 | 6 | 1 | | | |
| 2.51 to 3cm | 10 | 3 | 1 | | | |
| 3.51 to 3.5cm | 0 | 0 | 0 | | | |
| 3.51 to 4 cm | 0 | 0 | 0 | | | |
| **Total aged: plot F** | | | | | | 252 |
| | | | | | | |
| **Total aged: other plots** | | | | | | 18 |
| **Grand total aged** | | | | | | 270 |
| | | | | | | |
| **Aged from Plot F** | | | | | | |
| Total Samples Aged | | | | | | 252 |
| Of which, Basal Cross Sections | | | | | | 196 |
| Of which, Cores | | | | | | 56 |

*Table S 3.* Numbers of trees from Plot F used in point pattern analyses. In the J-function analysis, the sample included 2 trees (TSME and TSHE) with exact ages. Totals sum to less than the 1008 trees, because 12 samples of tree species other than ABAM, ABGR, or PSME could not be aged, nor could their ages be estimated, because too few samples from these species existed to create an estimated age based on diameter. Two samples of tree species other than ABAM, ABGR, or PSME were large basal cross sections that were aged and were included in the J-function analysis.

| | **ABAM** | **ABGR** | **PSME** | **other** | **All** |
|---|---|---|---|---|---|
| **Bivariate Ripley's K and PCF** | | | | | |
| Old | 72 | 26 | 32 | 0 | 130 |
| Young | 462 | 371 | 31 | 0 | 864 |
| **Total** | 534 | 397 | 63 | 0 | 994 |
| | | | | | |
| **J-function** | | | | | |
| before 1990 | 45 | 28 | 21 | 1 | 95 |
| 1990-2000 | 261 | 205 | 32 | 1 | 499 |
| after 2000 | 228 | 164 | 10 | 0 | 402 |
| **Total** | 534 | 397 | 63 | 2 | 996 |

*Table S 4*. Numbers of trees used for cross-Ripley's K comparisons of old trees (>30 years) (columns) vs. young trees (≤ 30 years) (rows).

| | **Old ABAM** | **Old ABGR** | **Old Stems** |
|---|---|---|---|
| **Young ABAM** | 534 | 488 | 592 |
| **Young ABGR** | 443 | 397 | 501 |

*Table S 5.* Number of stems per species by plot in the M1 meadow.

| Plot | Species | | | | | | | | | Total |
|---|---|---|---|---|---|---|---|---|---|---|
| | **ABAM** | **ABGR** | **PSME** | **ABPR** | **ABLA** | **TSME** | **PIMO** | **TSHE** | **TABR2** | |
| **B** | 1 | 5 | 6 | 5 | 5 | 6 | 0 | 0 | 0 | 28 |
| **C** | 0 | 1 | 5 | 1 | 0 | 0 | 0 | 0 | 0 | 7 |
| **D** | 8 | 40 | 7 | 7 | 27 | 9 | 1 | 0 | 0 | 99 |
| **E** | 1 | 12 | 15 | 0 | 1 | 0 | 0 | 0 | 0 | 29 |
| **F** | 534 | 397 | 63 | 1 | 0 | 4 | 1 | 8 | 0 | 1008 |
| **G** | 0 | 9 | 10 | 0 | 0 | 0 | 0 | 0 | 0 | 19 |
| **H** | 40 | 51 | 3 | 6 | 0 | 1 | 0 | 0 | 1 | 102 |
| **J** | 35 | 22 | 0 | 3 | 0 | 14 | 2 | 4 | 0 | 80 |
| **Total** | 619 | 537 | 109 | 23 | 33 | 34 | 4 | 12 | 1 | |

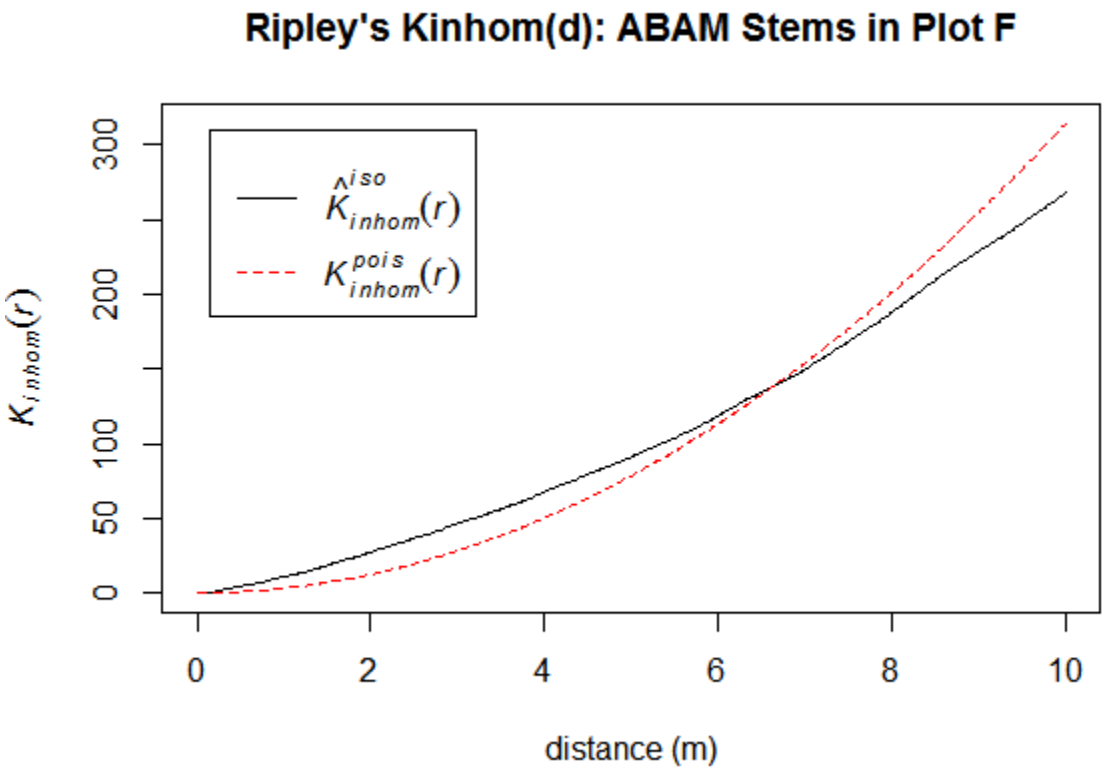


*Figure S 1*. Univariate Ripley's K for all ABAM stems in plot F (n=534). Indicates clustering between 0 to 7 meters, then transitioning to regular pattern at greater scales. This plot strongly resembles that of the Kinhom function for all stems in plot F, perhaps indicating that spatial pattern is dominated by ABAM that comprises just over half of all stems in plot F. This plot is corrected for inhomogeneity and isotropy given that the spatial pattern is not consistent throughout the extent of the rectangular plot F.

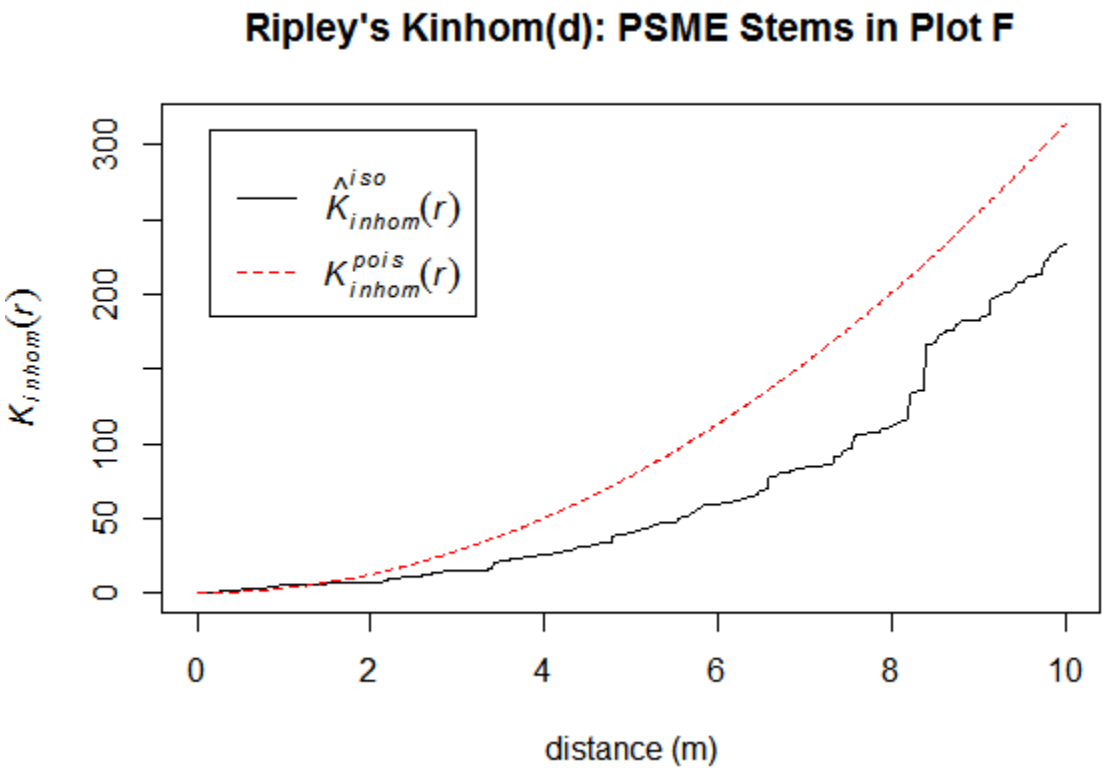


*Figure S 2*. Ripley's K for all PSME stems in plot F (n=63). Indicates slight clustering between 0 to 1 meters, then transitioning to regular pattern at greater scales. Sample n is low for this plot. This plot is corrected for inhomogeneity and isotropy given that the spatial pattern is not consistent throughout the extent of the rectangular plot F.

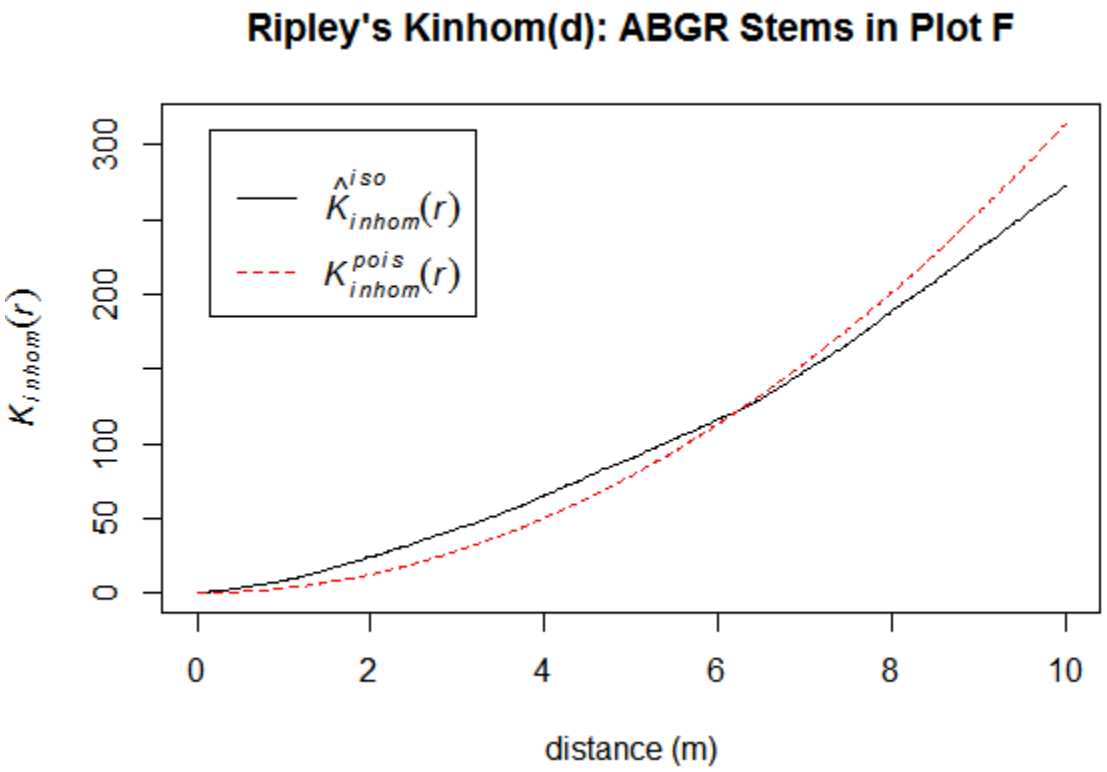


*Figure S 3.* Ripley's K for all ABGR stems in plot F (n=397). Indicates clustering between 0 to 6 meters, then transitioning to regular pattern at greater scales. The clustering of ABGR only deviates from that of ABAM by shifting the transition point from 7 to 6 meters. This plot is corrected for inhomogeneity and isotropy given that the spatial pattern is not consistent throughout the extent of the rectangular plot F.

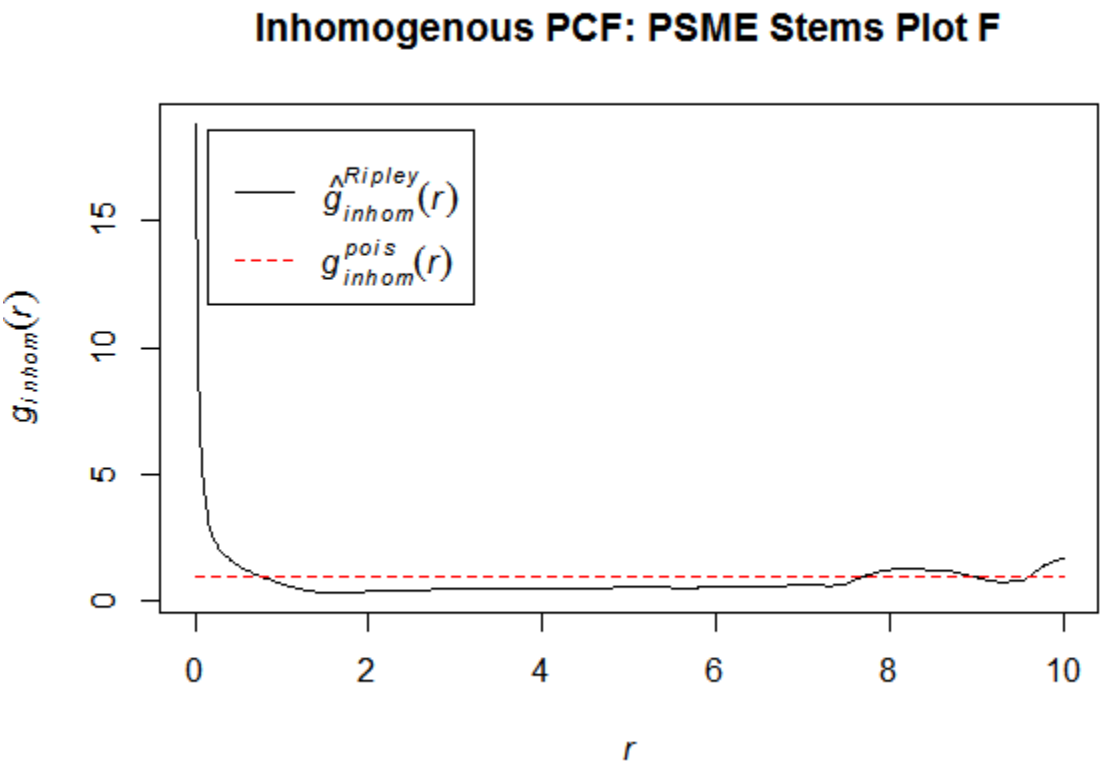


*Figure S 4.* Univariate PCF indicates a hard core distance of 0 meters for PSME stems (n=63). PSME stems are dispersed at all scales, likely due to small sample size. This plot is corrected for inhomogeneity and isotropy given that the spatial pattern is not consistent throughout the extent of the rectangular plot F.

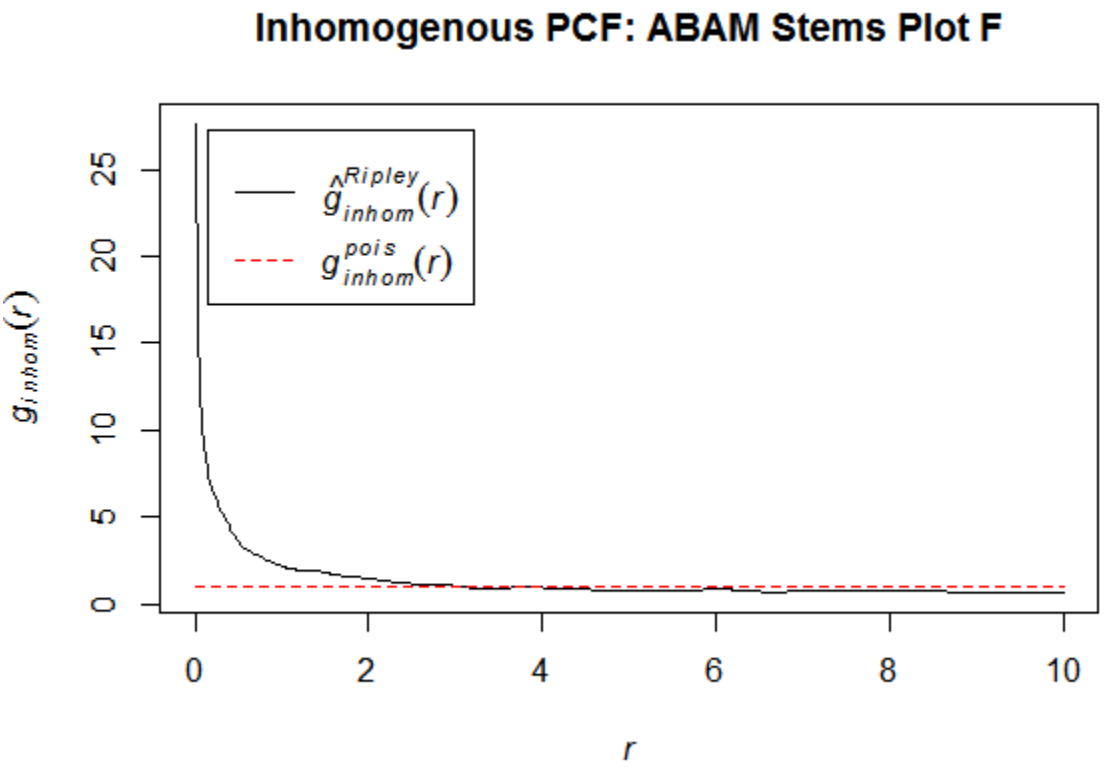


*Figure S 5.* Univariate Pair Correlation Function (PCF) for all ABAM stems in plot F (n=534). With number of stems on the y-axis and radius from the focal point on the x-axis. PCF returns a different result than Ripley's K in that clustering occurs at scales smaller than 3 meters, with a transition to regular pattern at greater scales. This plot is corrected for inhomogeneity and isotropy given that the spatial pattern is not consistent throughout the extent of the rectangular plot F.

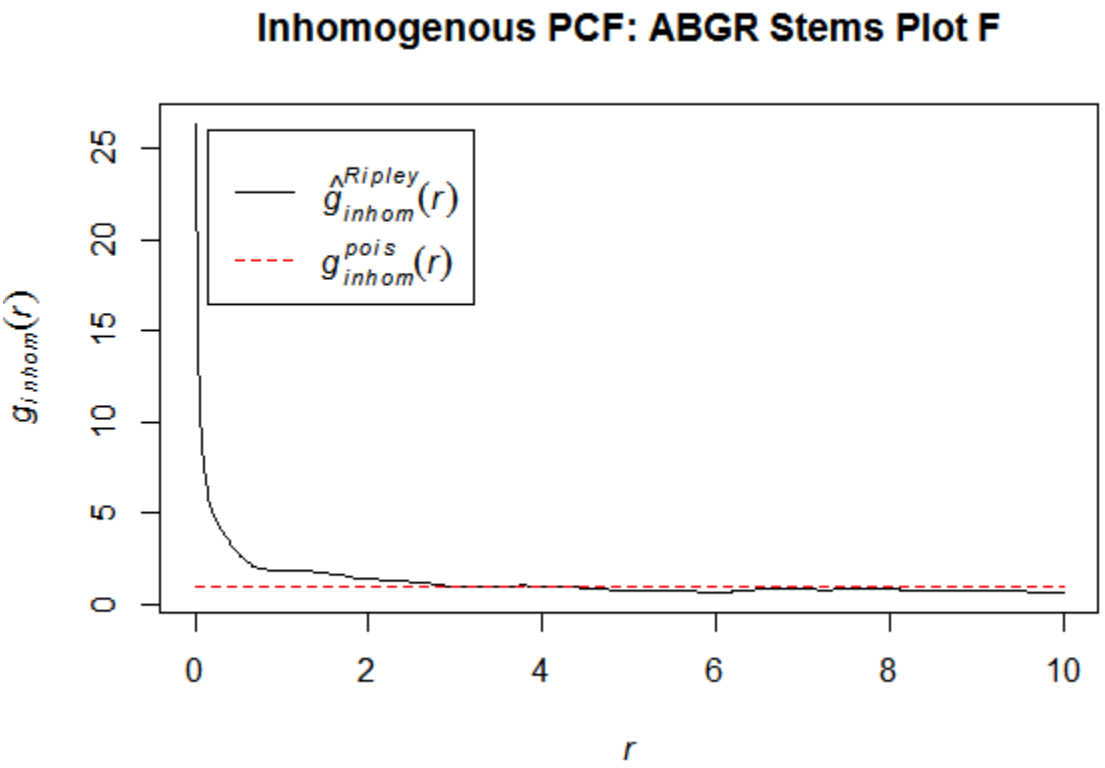


*Figure S 6.* Univariate Pair Correlation Function (PCF) for all ABGR stems in plot F (n= 397). With number of stems on the y-axis and radius from the focal point on the x-axis. PCF returns a different result than Ripley's K in that clustering occurs at scales smaller than 3 meters, with a transition to regular pattern at greater scales. This plot is corrected for inhomogeneity and isotropy given that the spatial pattern is not consistent throughout the extent of the rectangular plot F.

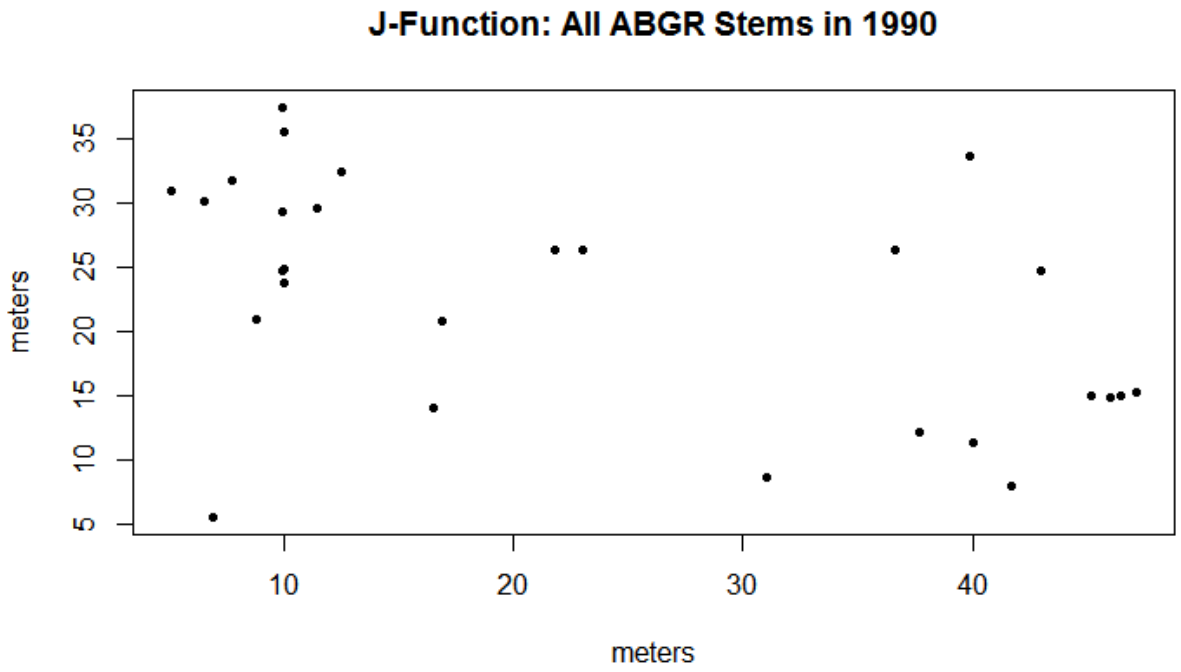


*Figure S 7.* ABGR stems in plot F, established 1990 and before (n=28).

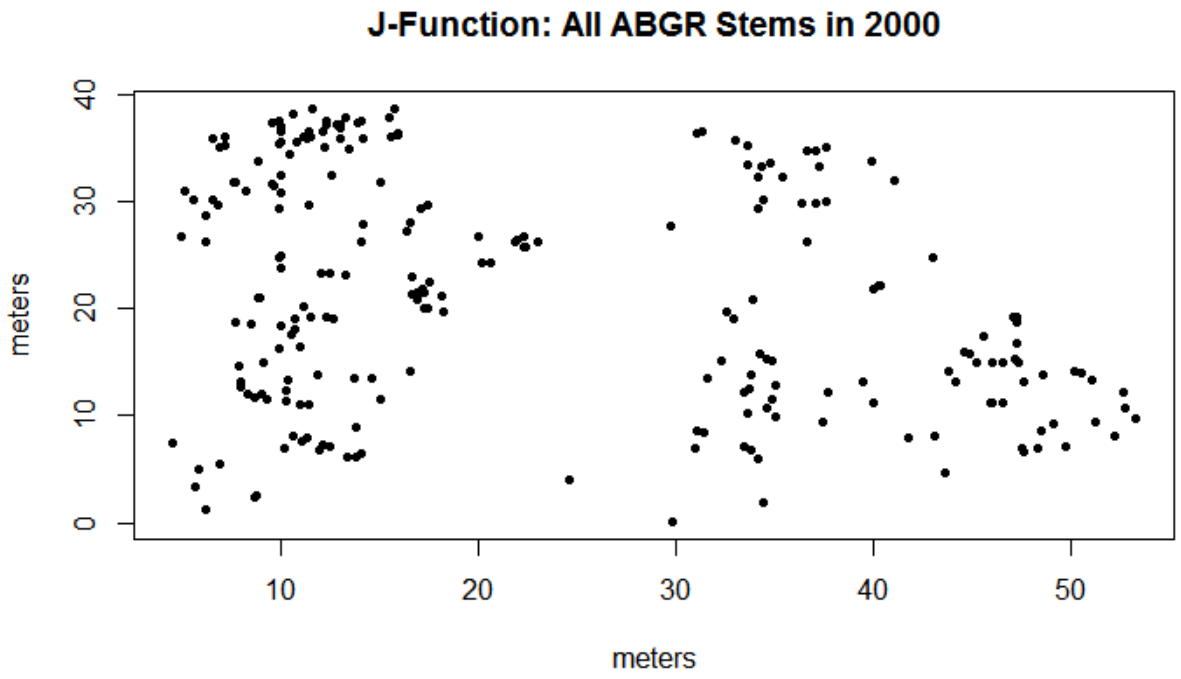


*Figure S 8.* ABGR stems in plot F, established 2000 and before (n=232).

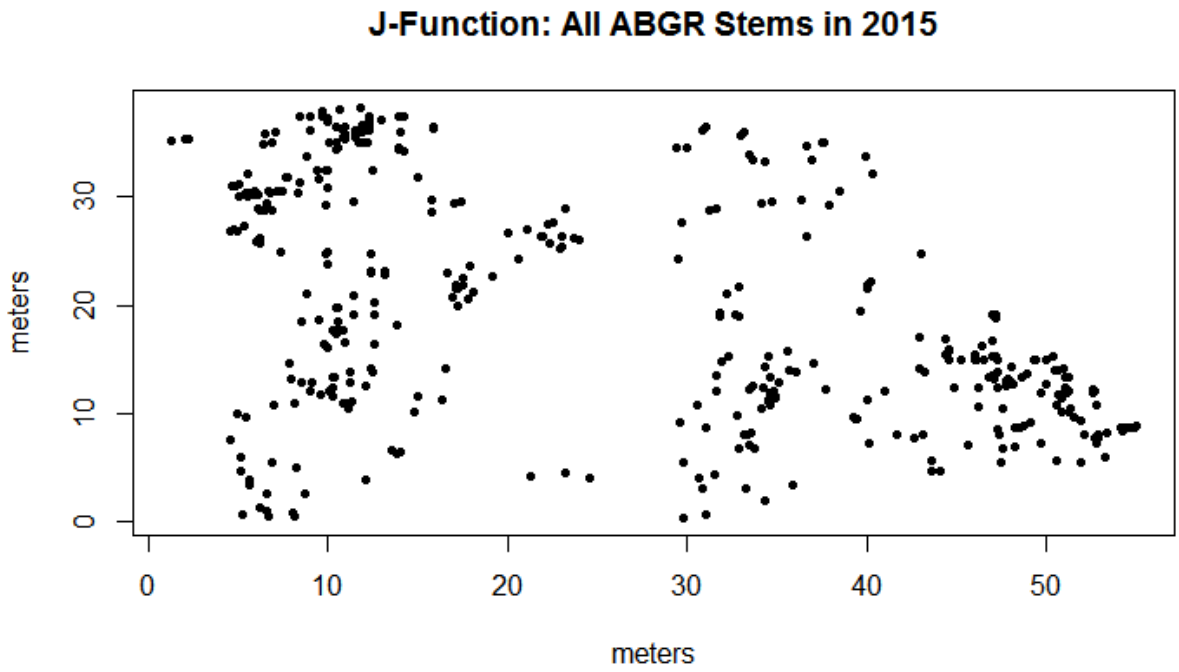


*Figure S 9.* ABGR stems in plot F, established as of 2015 (n=397).

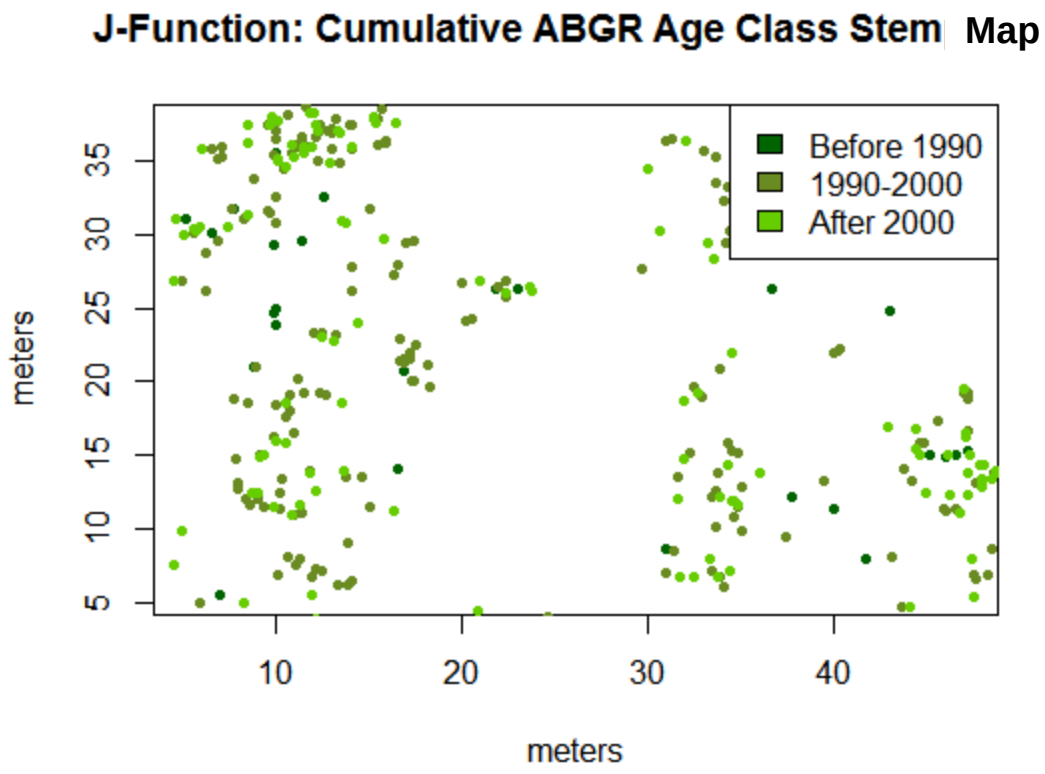


*Figure S 10.* Classes of ABGR stem encroachment from 1990-before (n=28), 1990-2000 (n=232), and 2000-present (n=395) used for J-function analysis.

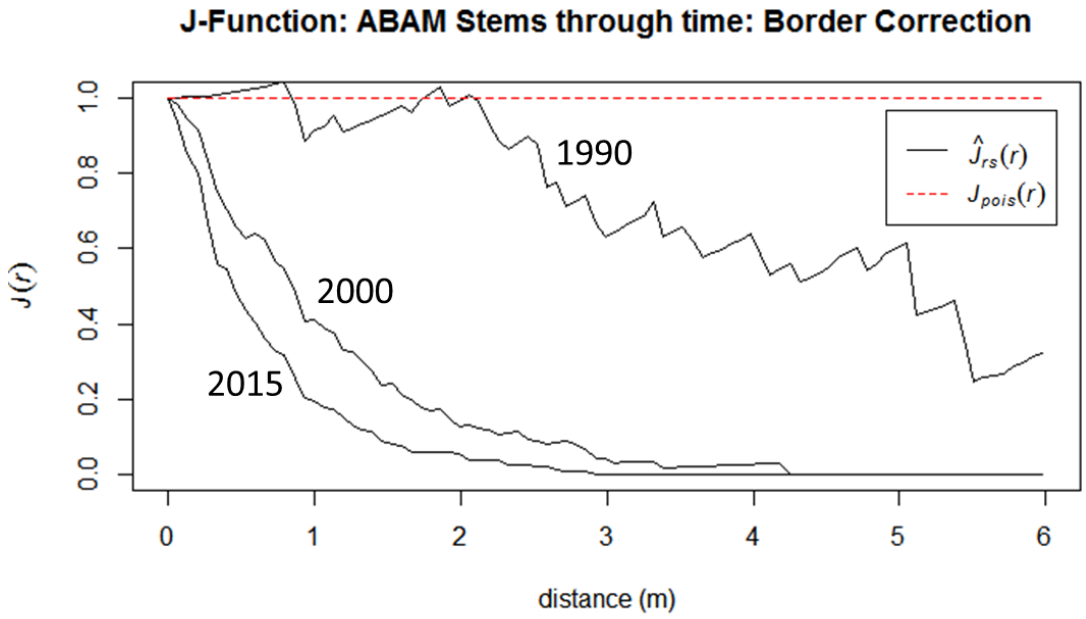


*Figure S 11*. Cumulative stems of ABAM become clustered through time. Stems established 1990 or before indicate dispersal at scales less than 1 meter, dispersal at 2 meters, and then weak clustering at greater scales. This plot is modified with border correction ($J_{rs}$) to address the influence of stems beyond the plot boundary. Stems established 1990- before (n=65), stems established 2000- before (n=256), and stems established in 2015 (n=276).

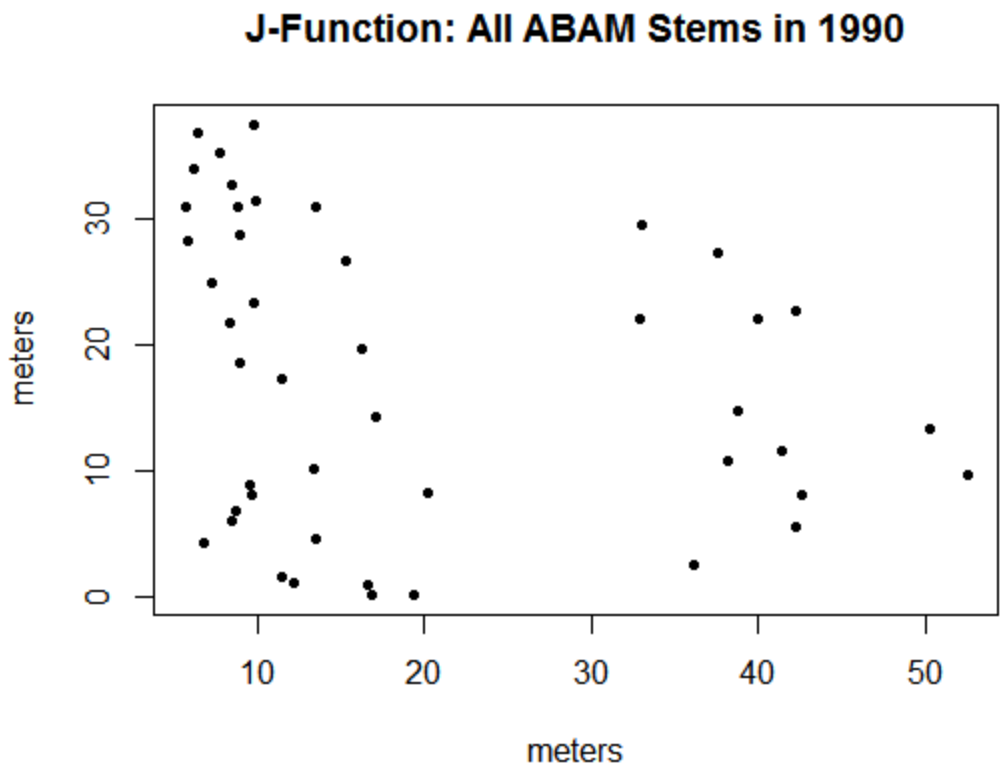


*Figure S 12.*. ABAM stems in plot F, established 1990 and before (n=45).

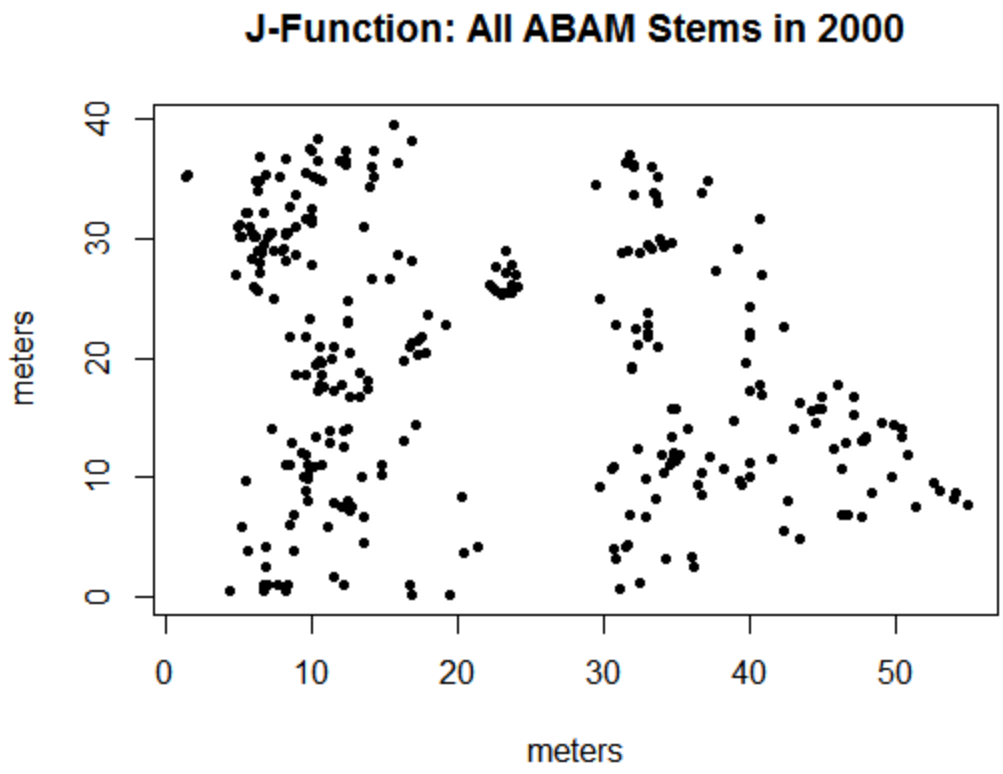


*Figure S 13.* ABAM stems in plot F, established 2000 and before (n=308).

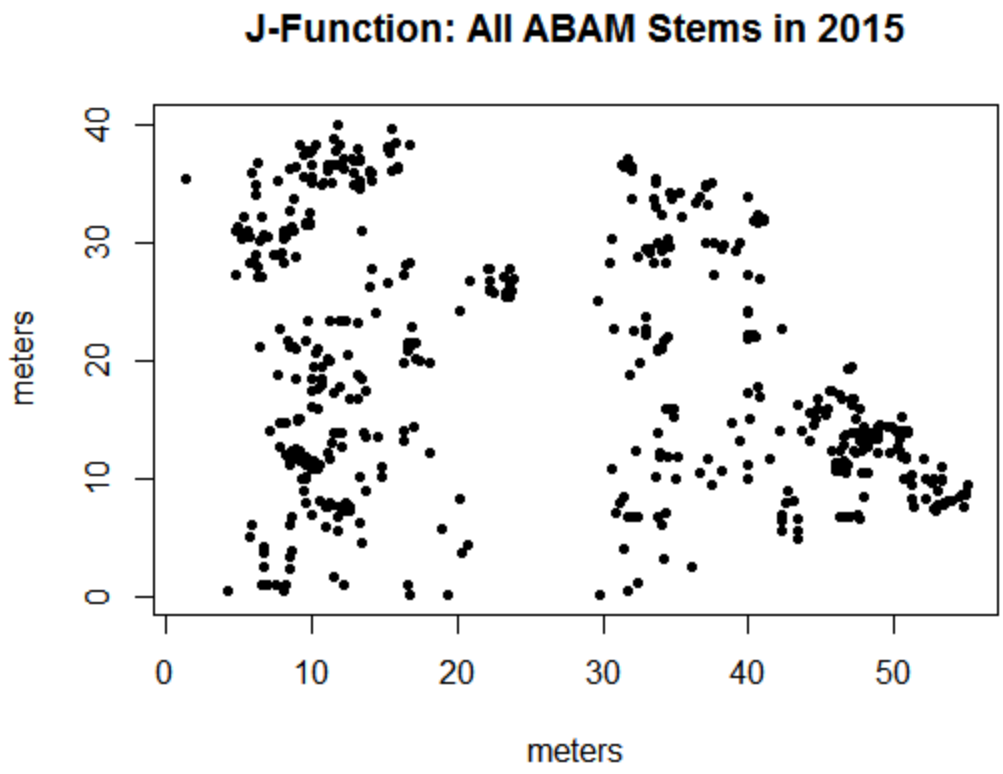


*Figure S 14.* ABAM stems in plot F, established as of 2015 (n=534).

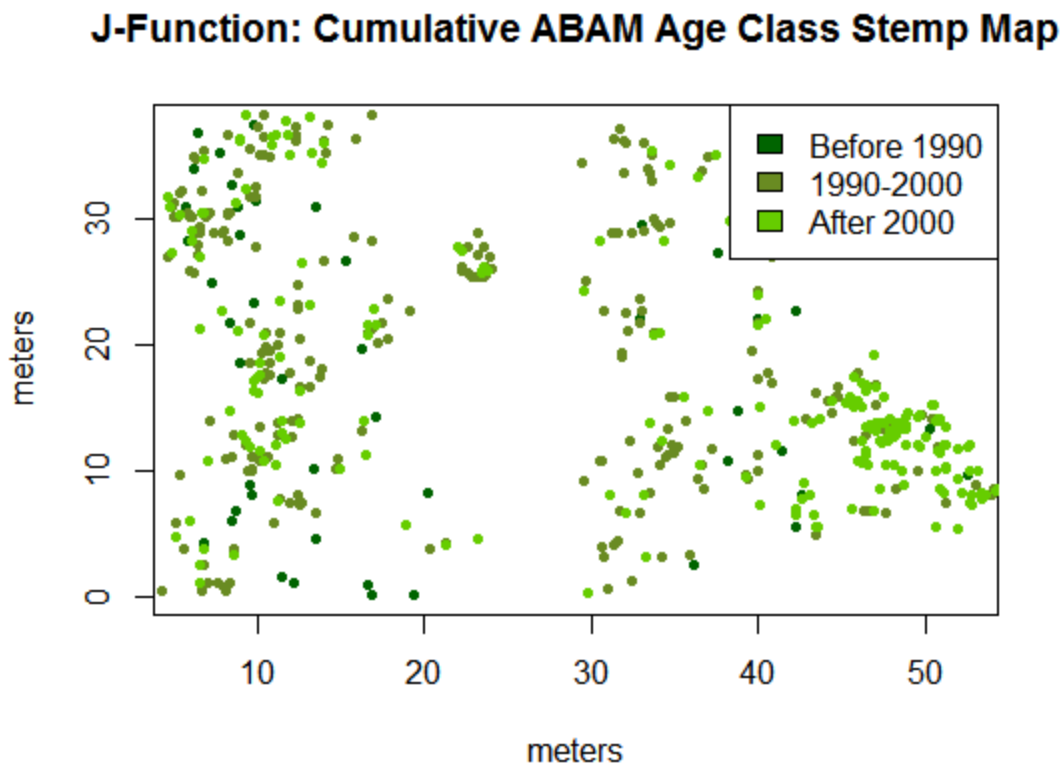


*Figure S 15.* Classes of ABAM stem encroachment from 1990-before (n=45), 1990-2000 (n=308), and 2000-present (n=536) used for J-function analysis.

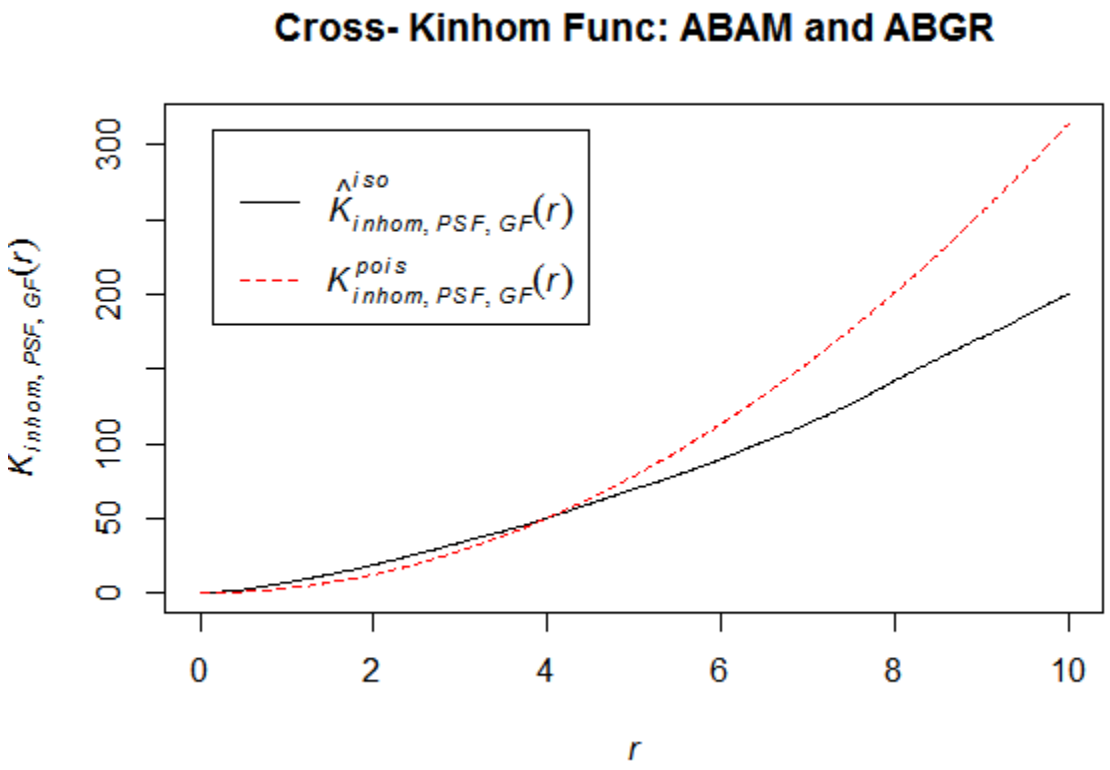


*Figure S 16.* Bivariate Ripley's K indicates weak clustering of ABAM (n=534) and ABGR (n=397) at scales smaller than 4 meters, then transitioning to regular spatial pattern at greater scales. This plot is corrected for inhomogeneity and isotropy given that the spatial pattern is not consistent throughout the extent of the rectangular plot F.

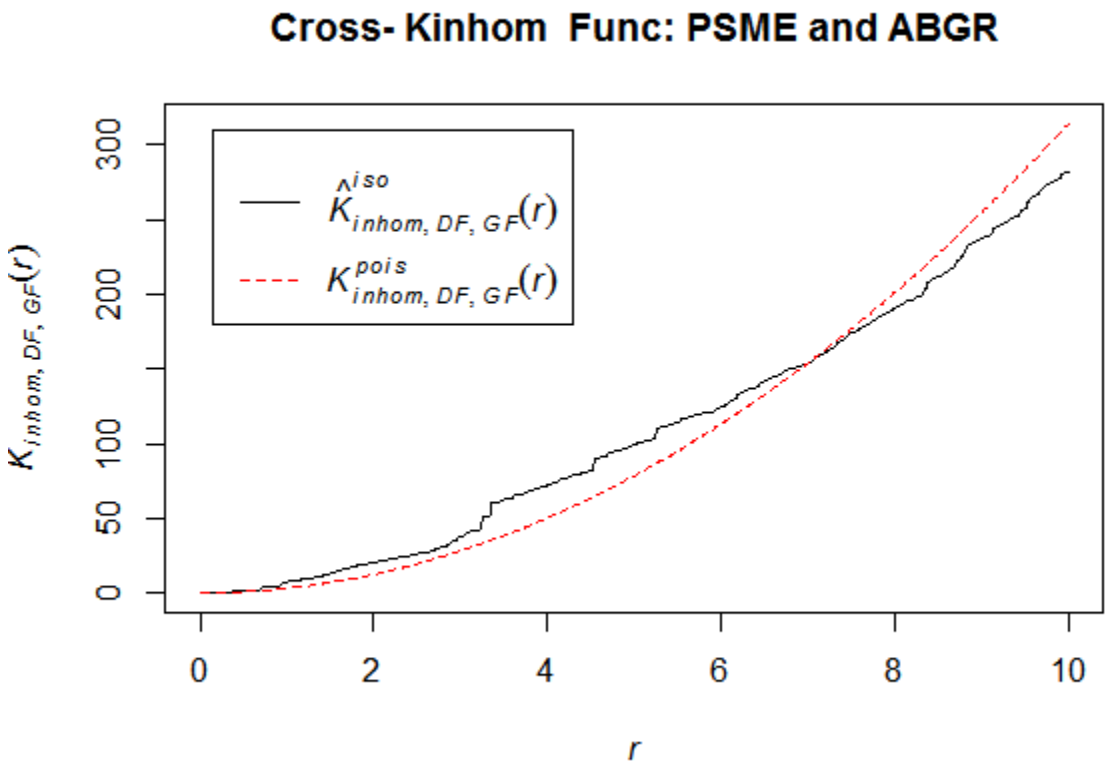


*Figure S 17.* Bivariate Ripley's K indicates weak clustering of PSME (n=63) and ABGR (n=397) at scales less than 7 meters, then transitioning to regular spatial pattern at greater scales. This plot is corrected for inhomogeneity and isotropy given that the spatial pattern is not consistent throughout the extent of the rectangular plot F.

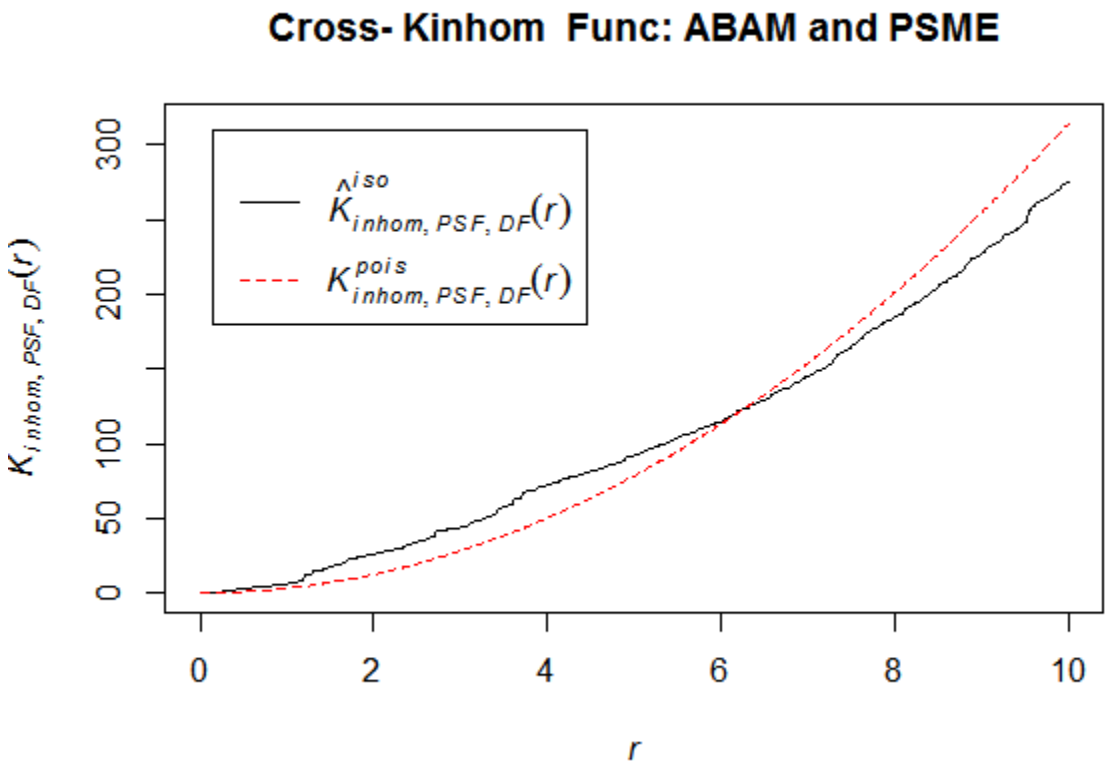


*Figure S 18.* Bivariate Ripley's K indicates weak clustering of ABAM (n=534) and PSME(n=63) at scales less than 6 meters, then transitioning to regular spatial pattern at greater scales. This plot is corrected for inhomogeneity and isotropy given that the spatial pattern is not consistent throughout the extent of the rectangular plot F.

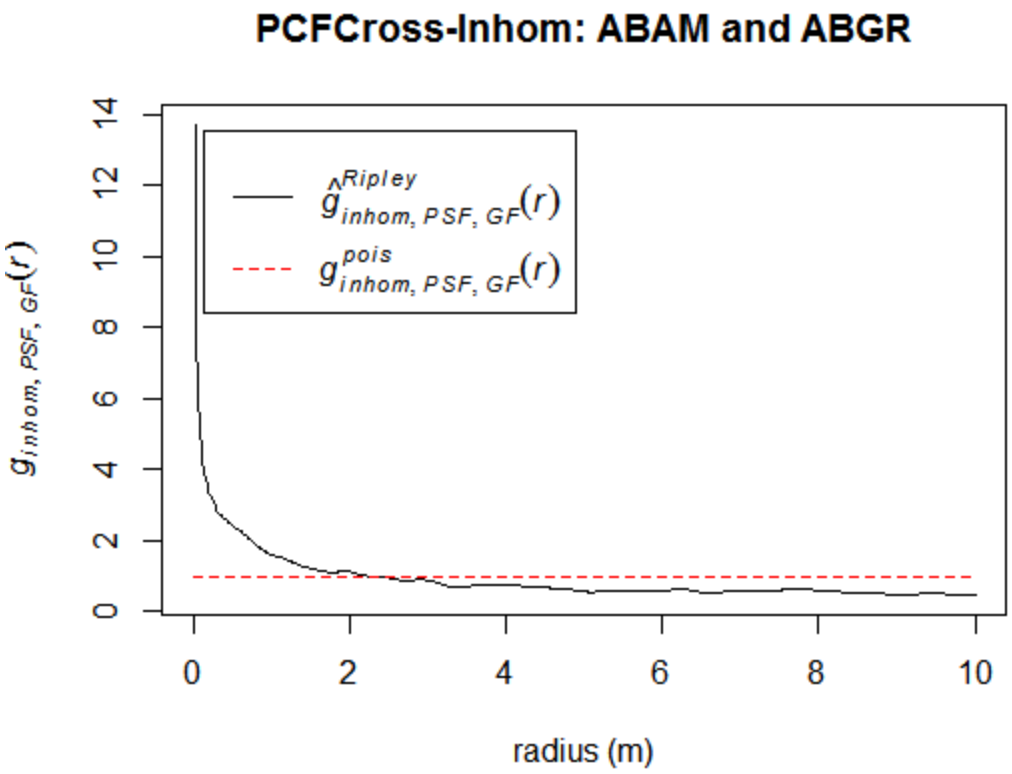


*Figure S 19.* Bivariate Ripley's K describes decreasing, fine scale clustering between ABAM and PSME between 2 to 3 meters, then transitioning to regular spatial pattern.

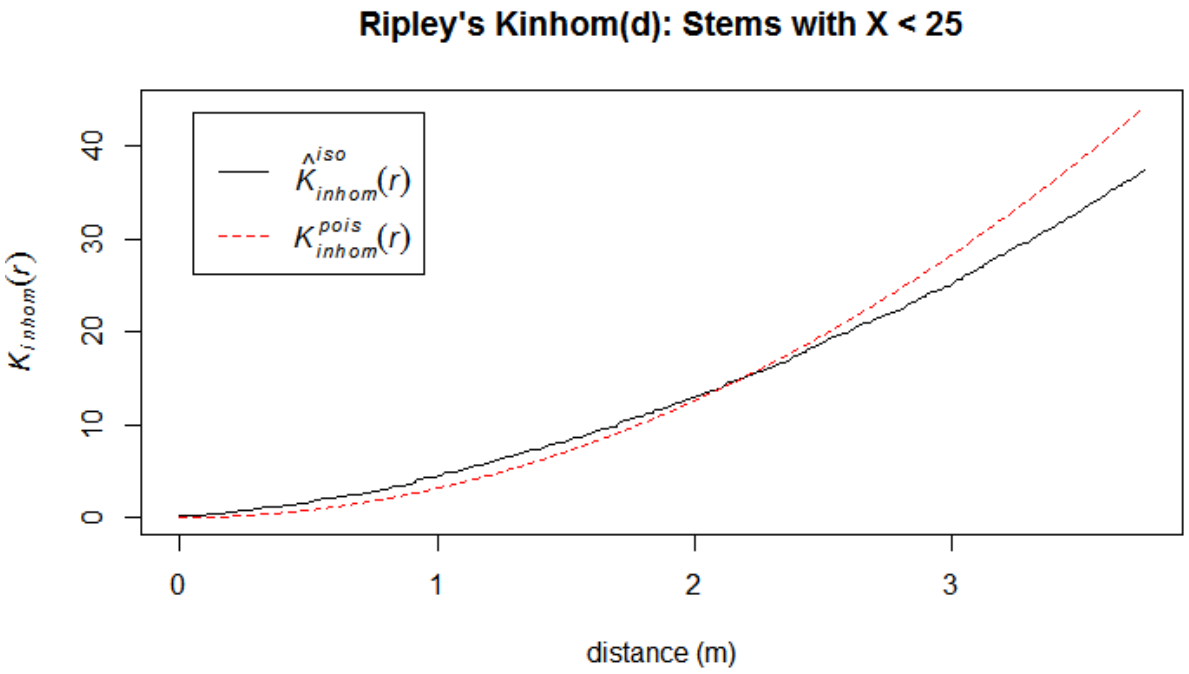


*Figure S 20.* Univariate Ripley's K for all stems x< 25m (n=507) indicates clustering at scales less than 2 meters and regular spatial pattern at scales greater than 2 meters. This plot is corrected for inhomogeneity and isotropy given that the spatial pattern is not consistent throughout the extent of the rectangular plot F.

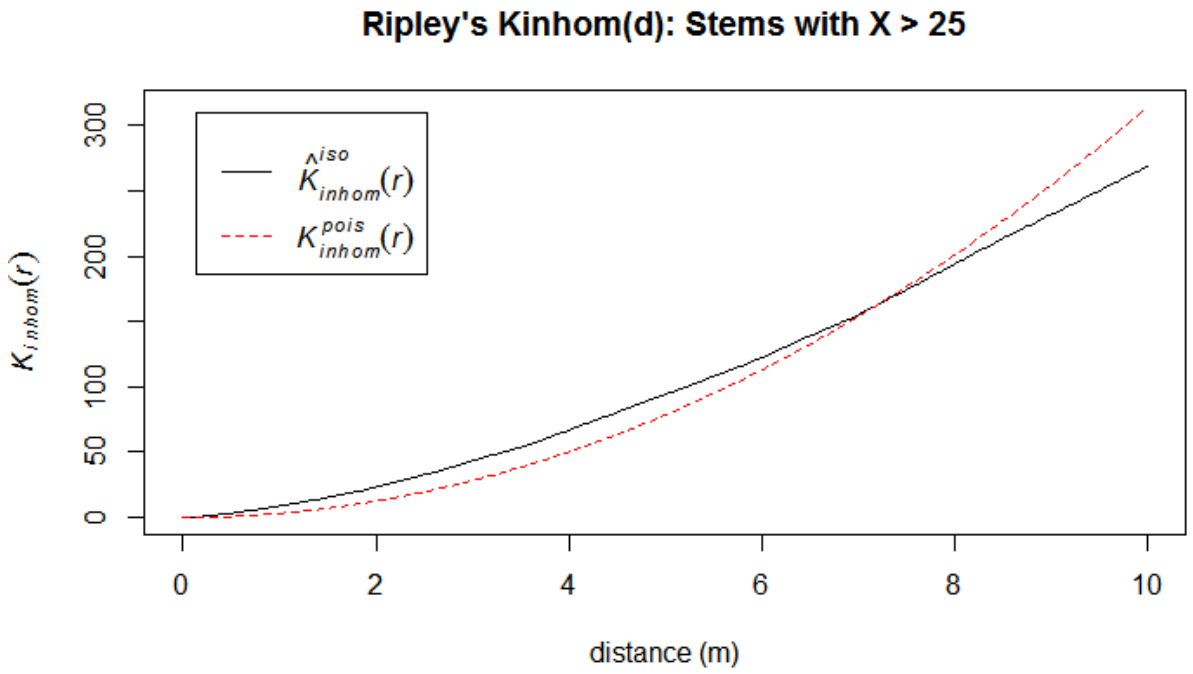


*Figure S 21.* Univariate Ripley's K for all stems x> 25m (n=480) indicates clustering at scales less than 6 meters and regular spatial pattern at scales greater than 6 meters. This plot is corrected for inhomogeneity and isotropy given that the spatial pattern is not consistent throughout the extent of the rectangular plot F.

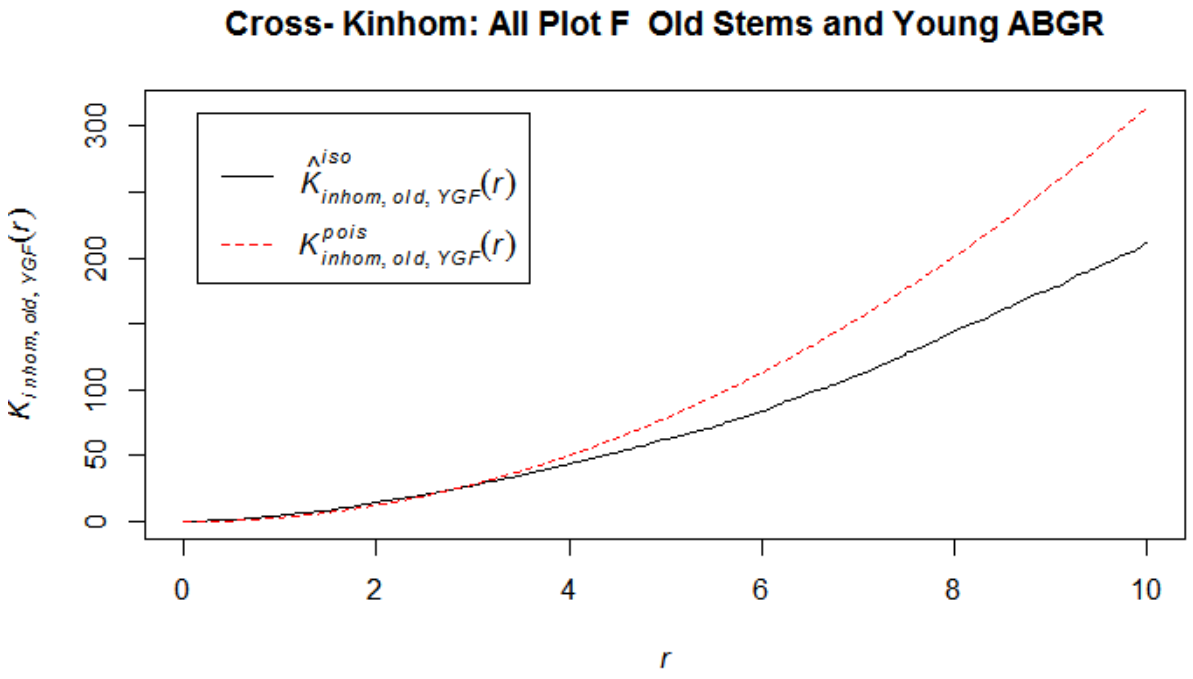


*Figure S 22.* Bivariate Ripley's K for old (n=130) and young ABGR (n=370) stems indicates no difference from random pattern at scales less than 4 meters and regular spatial pattern at scales greater than 4 meters. This plot is corrected for inhomogeneity and isotropy given that the spatial pattern is not consistent throughout the extent of the rectangular plot F.

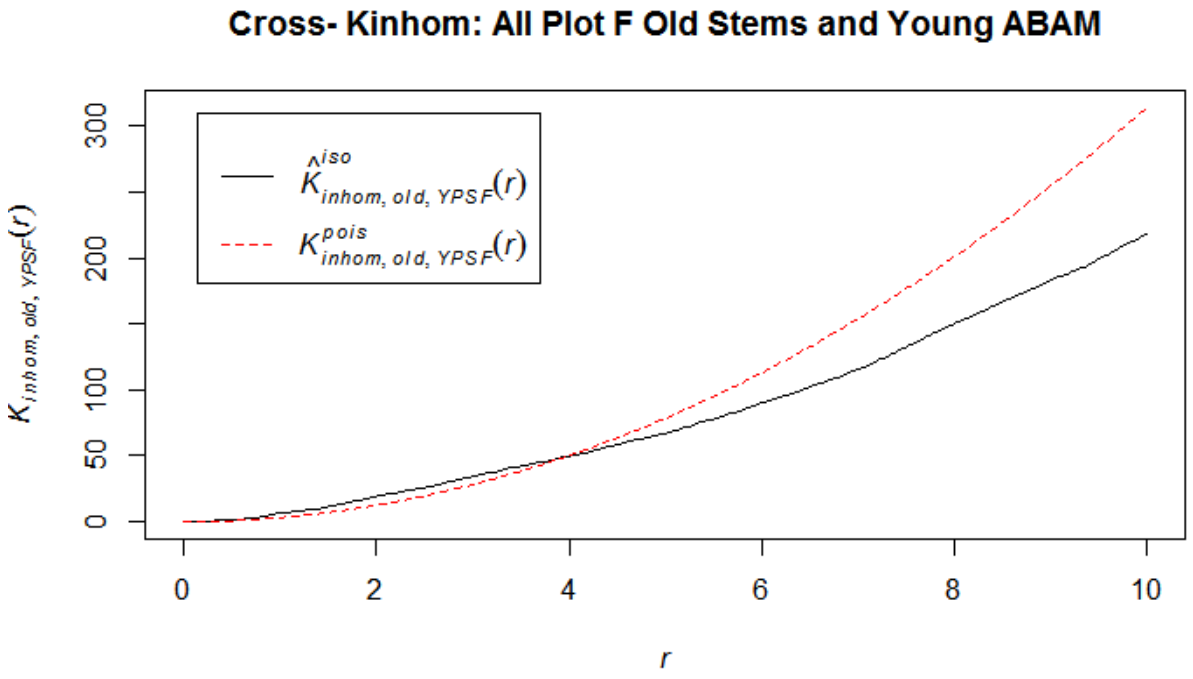


*Figure S 23.* Bivariate Ripley's K for old (n=130) and young ABAM (n=463) stems indicates clustering at scales less than 4 meters and regular spatial pattern at scales greater than 4 meters. This plot is corrected for inhomogeneity and isotropy given that the spatial pattern is not consistent throughout the extent of the rectangular plot F.

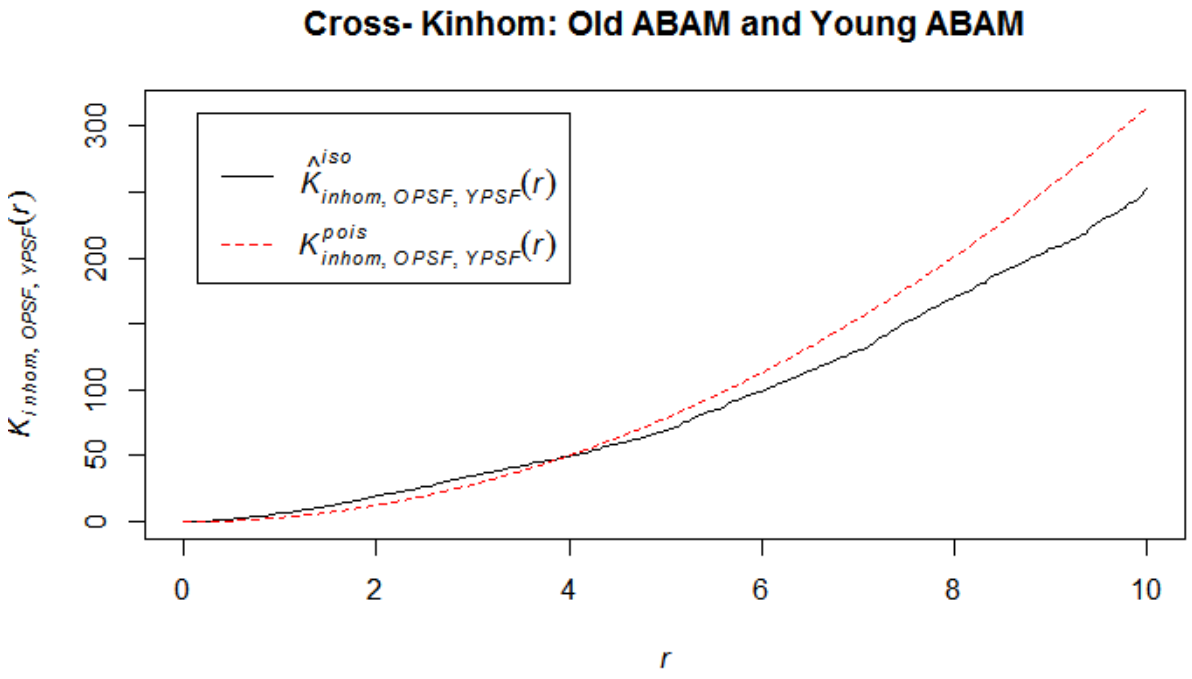


*Figure S 24.* Bivariate Ripley's K for old ABAM (n=72) and young ABAM (n=463) stems indicates clustering at scales less than 4 meters and regular spatial pattern at scales greater than 4 meters. This plot is corrected for inhomogeneity and isotropy given that the spatial pattern is not consistent throughout the extent of the rectangular plot F.

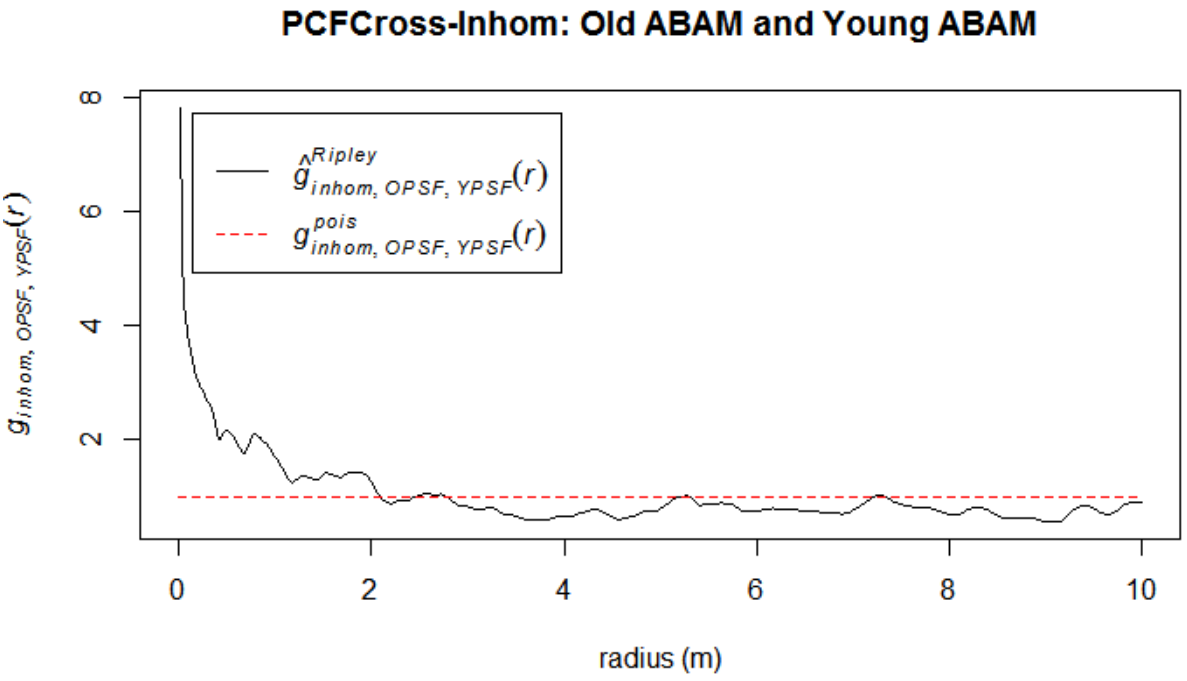


*Figure S 25.* Cross PCF for old ABAM (n=72) and young ABAM (n=463) stems indicates clustering at scales less than 2 meters and regular spatial pattern at scales greater than 2 meters. This plot is corrected for inhomogeneity and isotropy given that the spatial pattern is not consistent throughout the extent of the rectangular plot F.

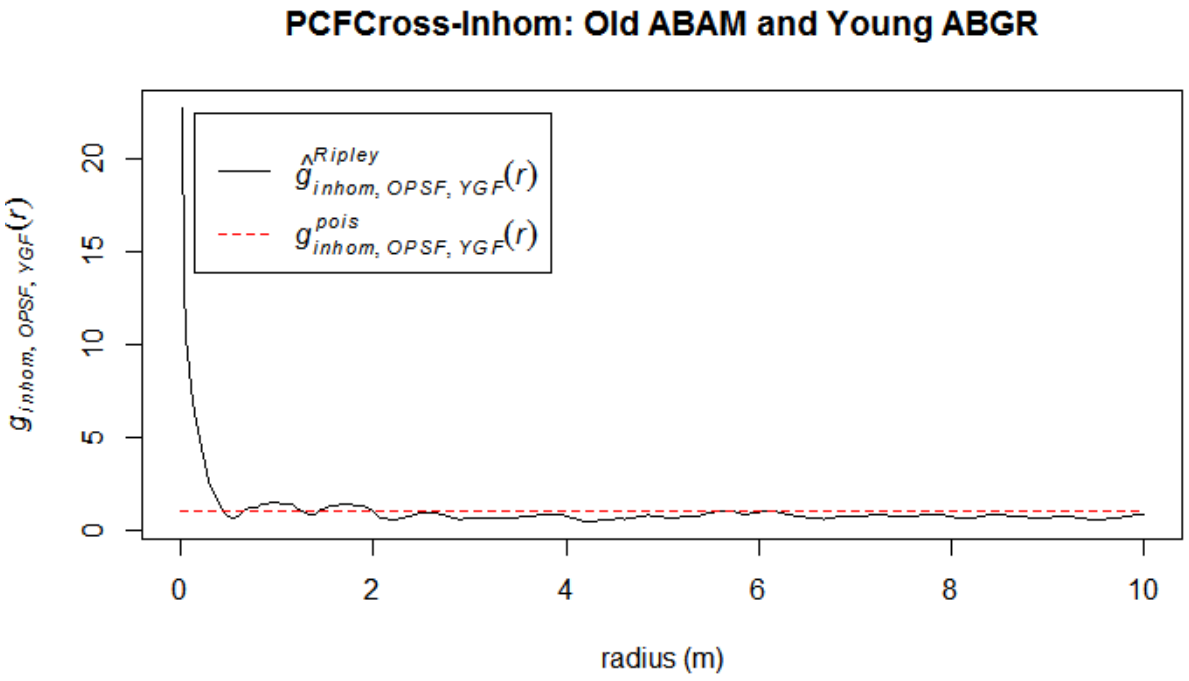


*Figure S 26.* Cross PCF for old ABAM (n=72) and young ABGR (n=370) stems indicates very weak clustering at scales less than 2 meters and regular spatial pattern at scales greater than 2 meters. This plot is corrected for inhomogeneity and isotropy given that the spatial pattern is not consistent throughout the extent of the rectangular plot F.

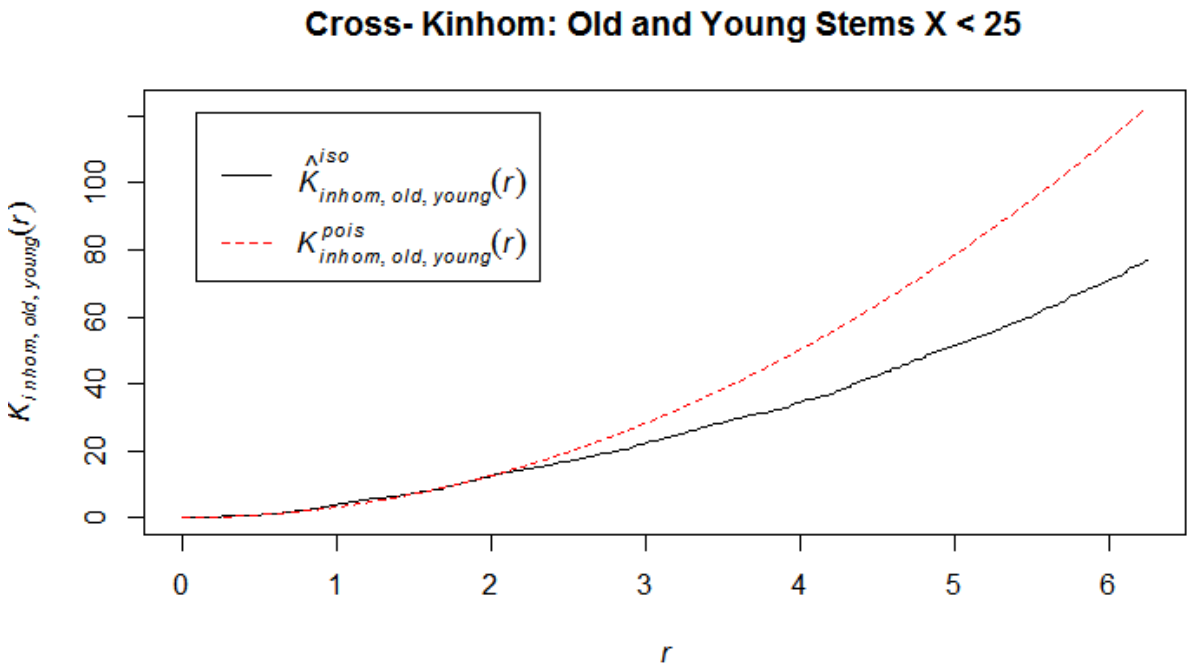


*Figure S 27.* Bivariate Ripley's K for all stems x< 25m (n=507) indicates random pattern up to 2 meters and regular spatial pattern at scales greater than 2 meters. This plot is corrected for inhomogeneity and isotropy given that the spatial pattern is not consistent throughout the extent of the rectangular plot F.

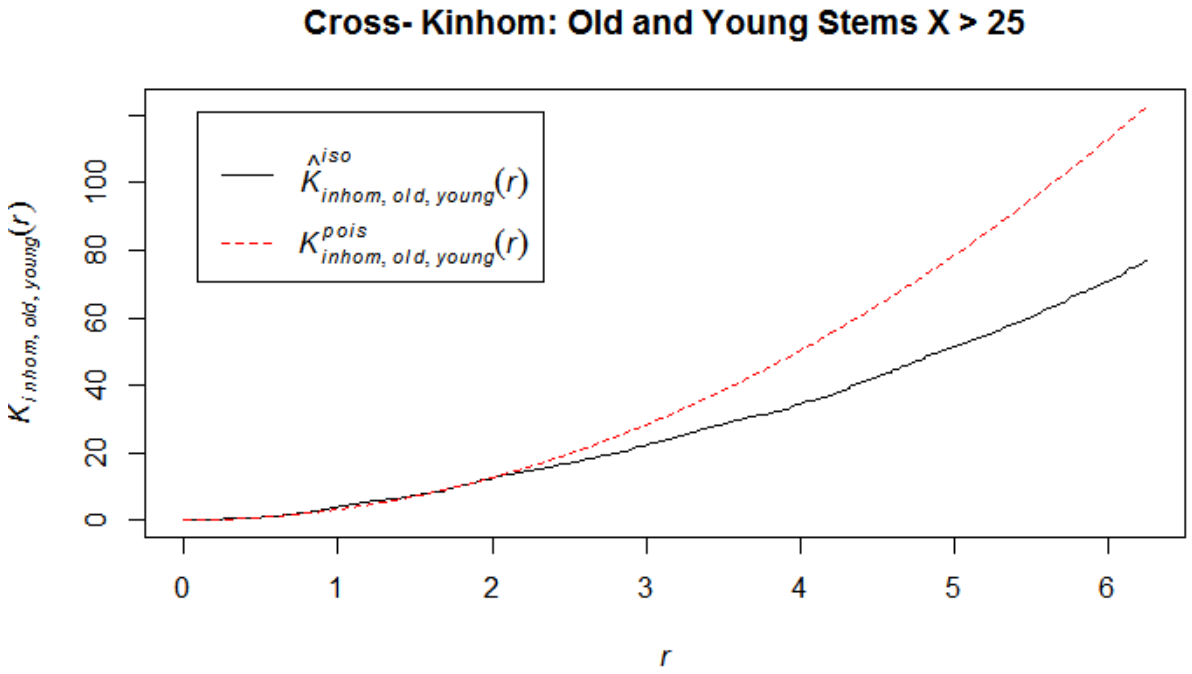


*Figure S 28.* Bivariate Ripley's K for all stems x>25m (n=480) indicates random pattern up to 2 meters and regular spatial pattern at scales greater than 2 meters. This plot is corrected for inhomogeneity and isotropy given that the spatial pattern is not consistent throughout the extent of the rectangular plot F.

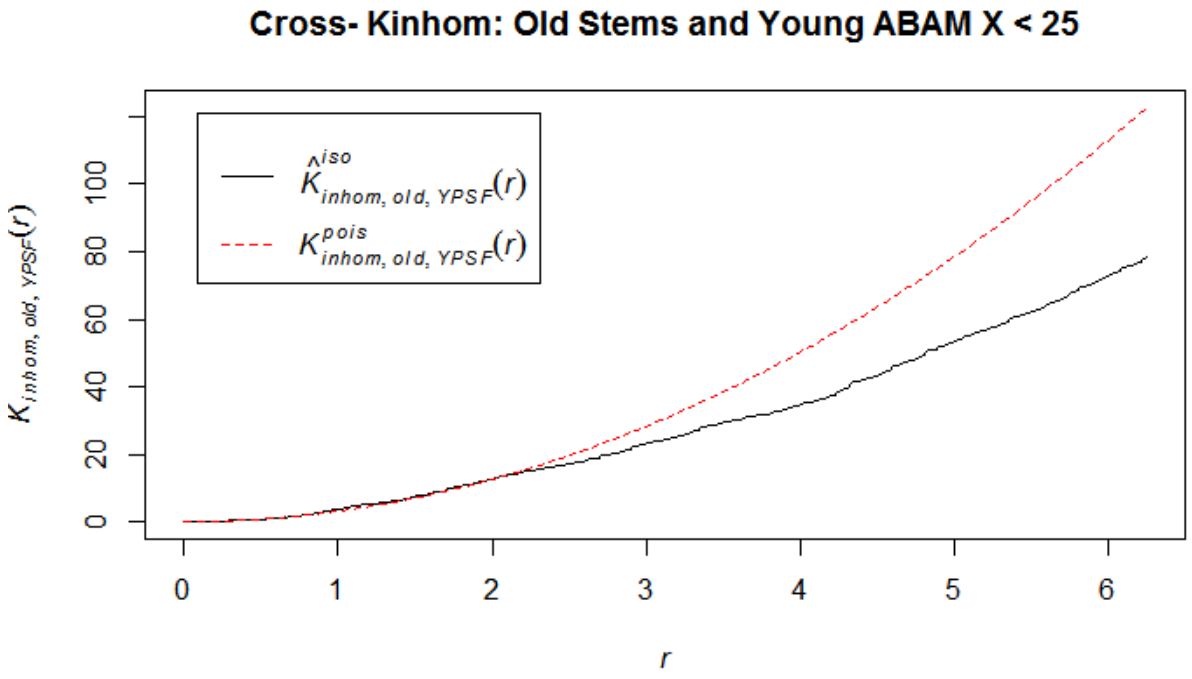


*Figure S 29.* Bivariate Ripley's K for old stems (n=83) and young ABAM (n=207) stems x<25m indicates random pattern up to 2 meters and regular spatial pattern at scales greater than 2 meters. This plot is corrected for inhomogeneity and isotropy given that the spatial pattern is not consistent throughout the extent of the rectangular plot F.

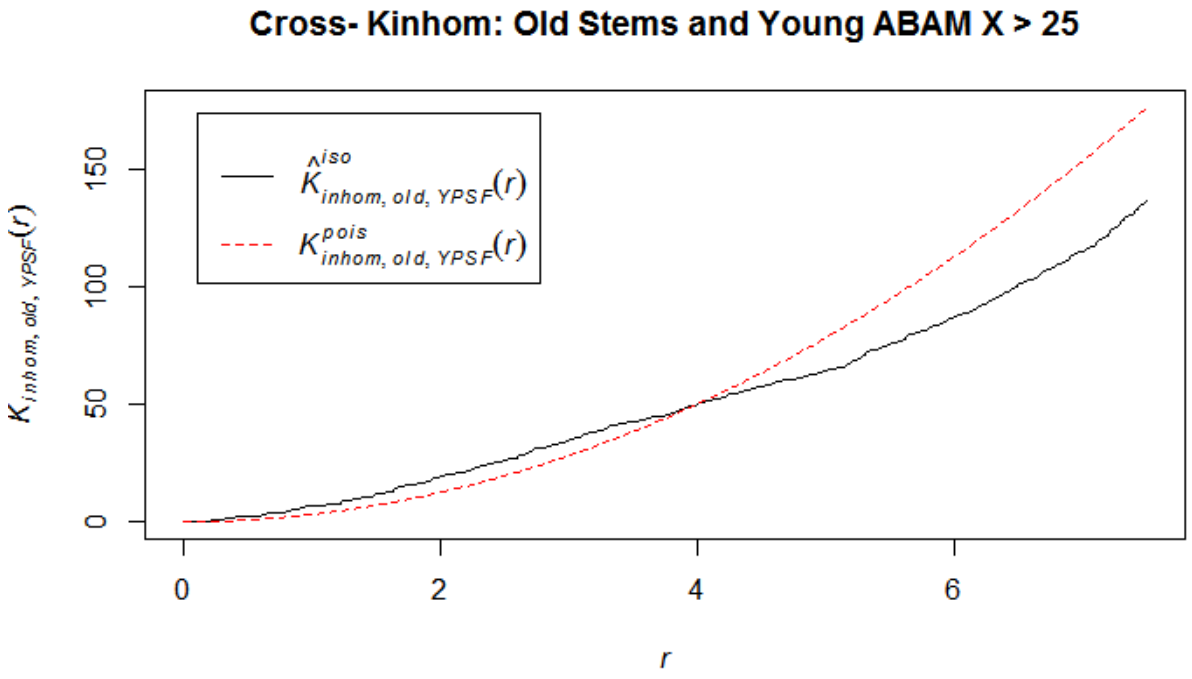


*Figure S 30.* Bivariate Ripley's K for old stems (n=40) and young ABAM (n=256) stems x>25m indicates clustering up to 4 meters and regular spatial pattern at scales greater than 4 meters. This plot is corrected for inhomogeneity and isotropy given that the spatial pattern is not consistent throughout the extent of the rectangular plot F.

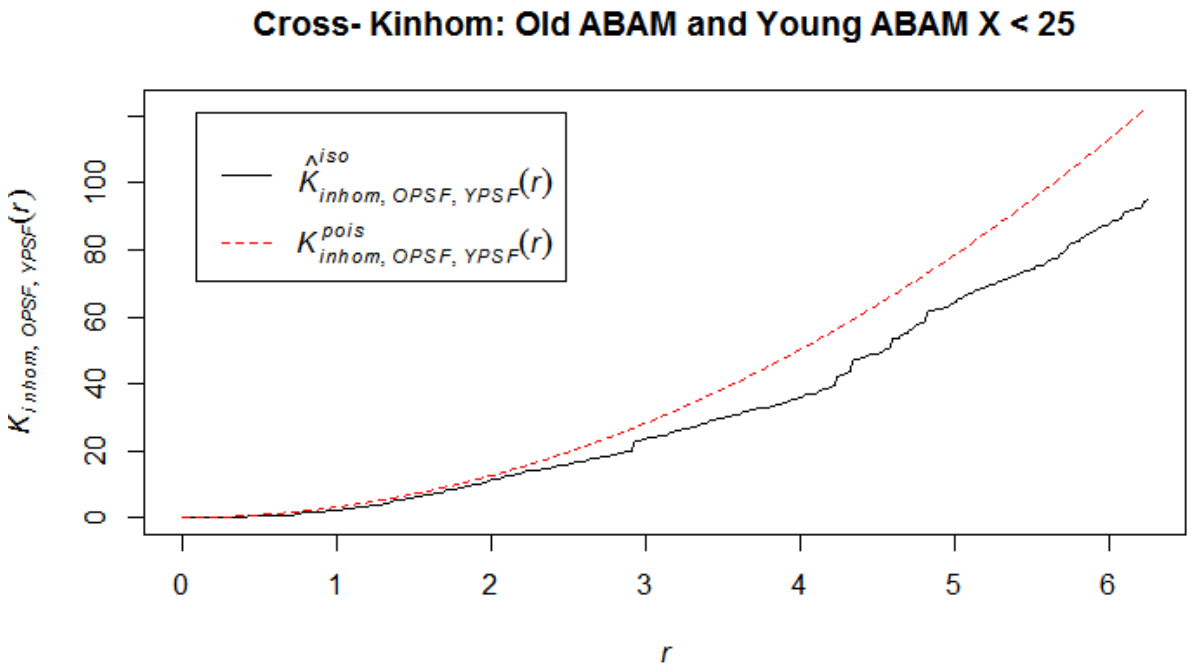


*Figure S 31.* Bivariate Ripley's K for old ABAM (n=55) and young ABAM (n=256) stems x<25m indicates dispersal at all scales. This plot is corrected for inhomogeneity and isotropy given that the spatial pattern is not consistent throughout the extent of the rectangular plot F.

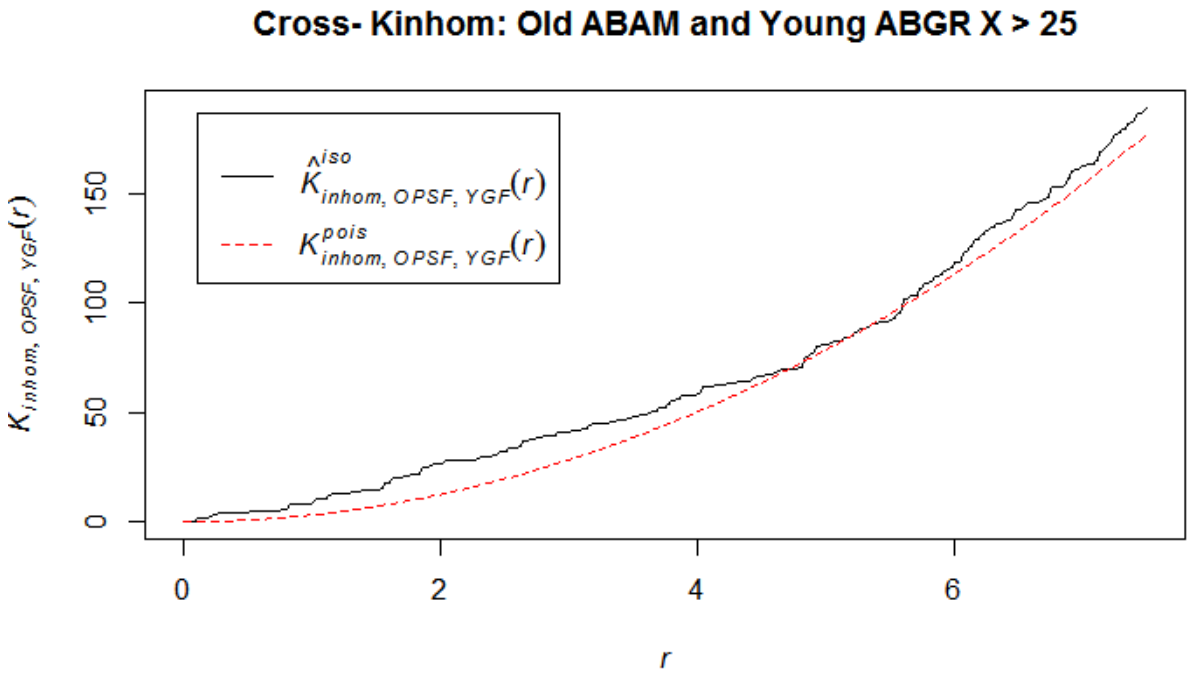


*Figure S 32.* Bivariate Ripley's K for old ABAM (n=14) and young ABGR (n=174) stems x>25m indicates clustering at scales less than 5 meters, random pattern from 5 to 6 meters, then further clustering at scales beyond 6 meters. This plot is corrected for inhomogeneity and isotropy given that the spatial pattern is not consistent throughout the extent of the rectangular plot F.

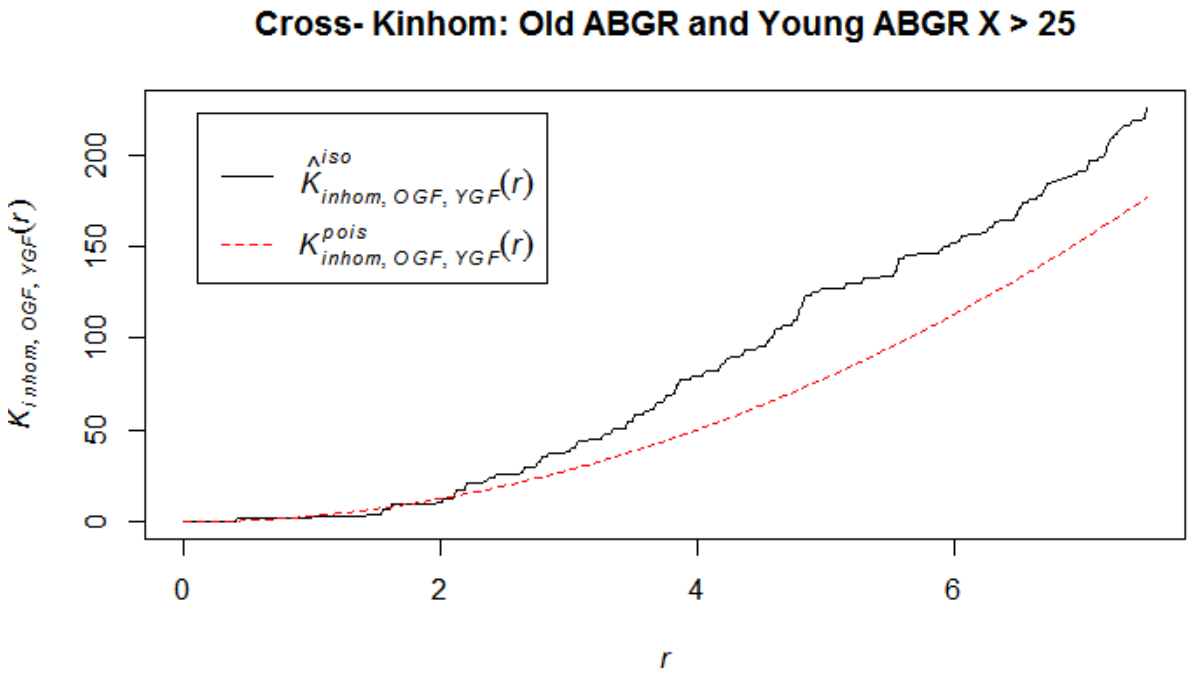


*Figure S 33.* Bivariate Ripley's K for old ABGR (n=11) and young ABGR (n=174) stems x>25m indicates dispersal or random pattern at scales less than 2 meters, then clustering at scales greater than 2 meters. This plot is corrected for inhomogeneity and isotropy given that the spatial pattern is not consistent throughout the extent of the rectangular plot F.

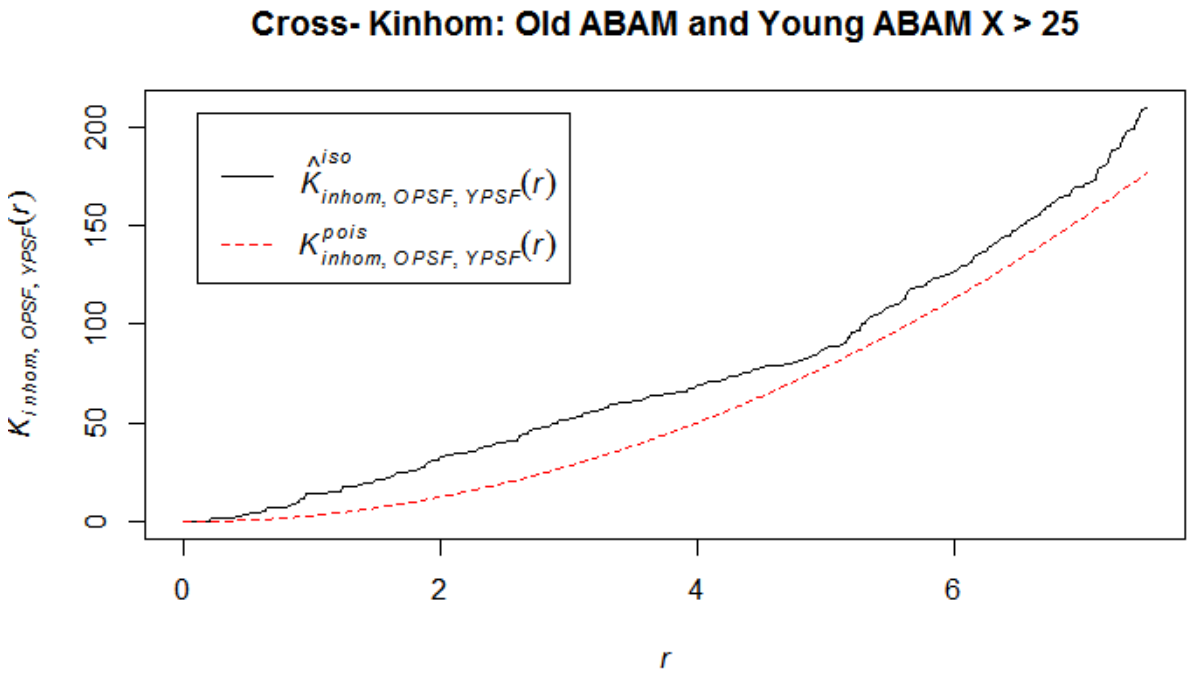


*Figure S 34.*. Bivariate Ripley's K for old ABGR (n=14) and young ABGR (n=256) stems x>25m indicates clustering at all scales. This plot is corrected for inhomogeneity and isotropy given that the spatial pattern is not consistent throughout the extent of the rectangular plot F.

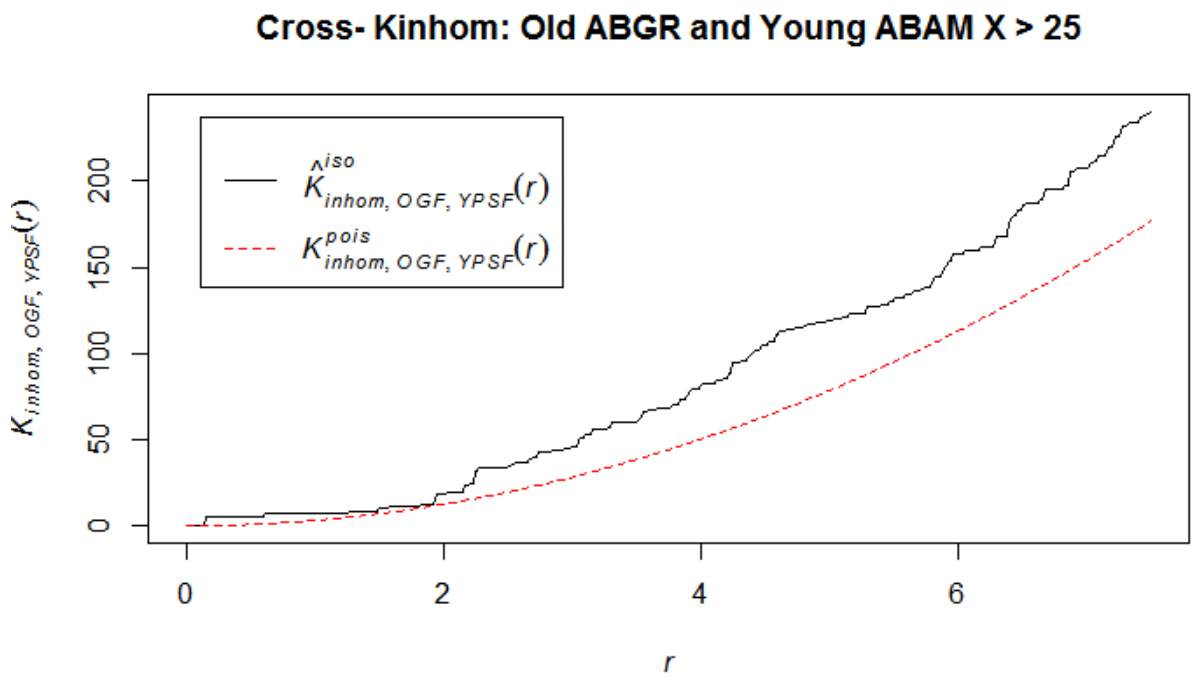


*Figure S 35.* Cross PCF for old ABGR (n=11) and young ABGR (n=174) stems x>25m indicates clustering at all scales. This plot is corrected for inhomogeneity and isotropy given that the spatial pattern is not consistent throughout the extent of the rectangular plot F

.

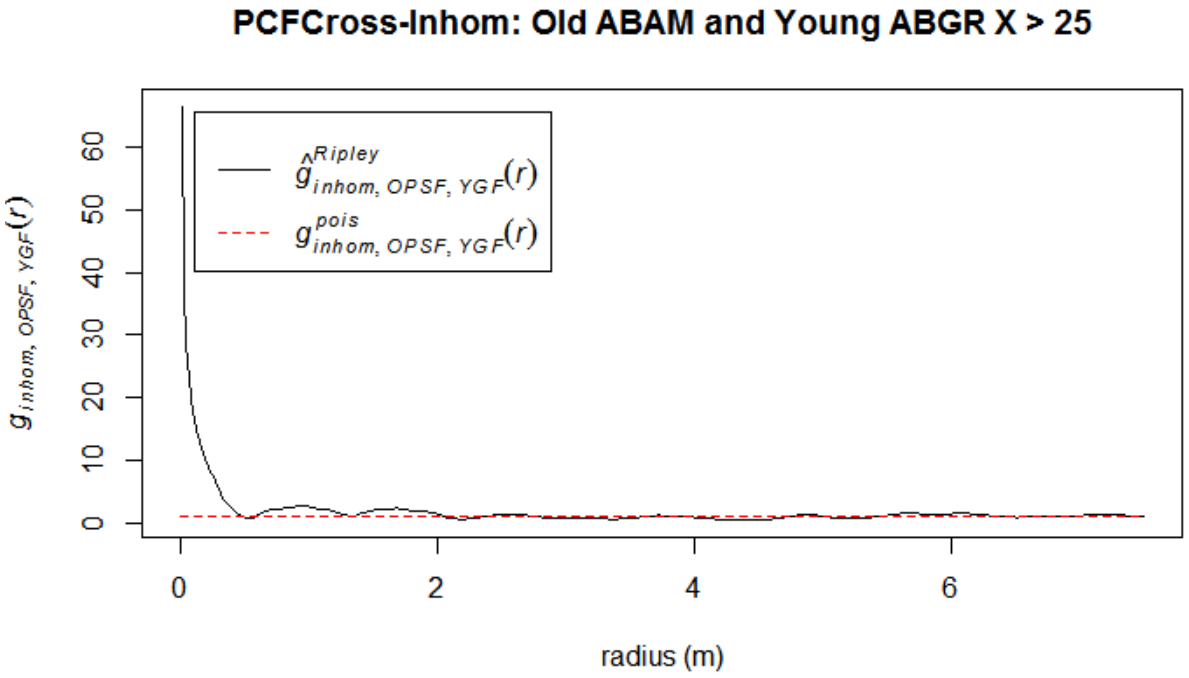


*Figure S 36.* Cross PCF for old ABAM (n=14) and young ABGR (n=174) stems x>25m indicates clustering at scales finer than 2 meters, then transitioning to random or dispersed pattern. This plot is corrected for inhomogeneity and isotropy given that the spatial pattern is not consistent throughout the extent of the rectangular plot F.

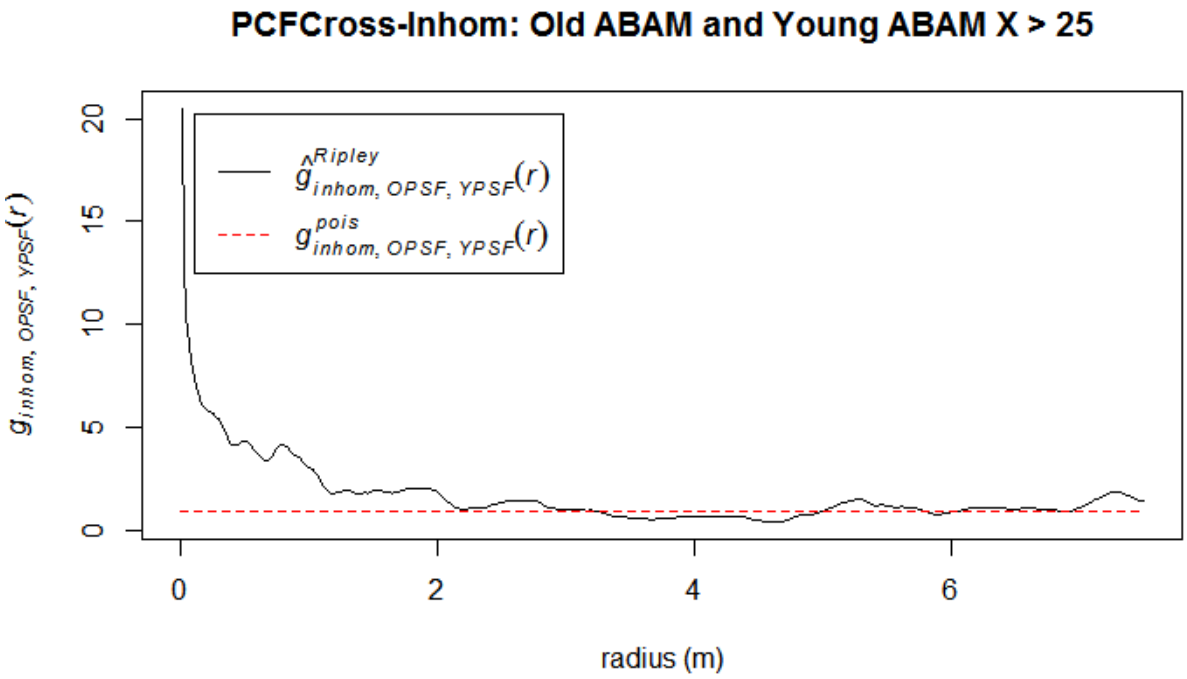


*Figure S 37.* Cross PCF for old ABAM (n=14) and young ABAM (n=256) stems x>25m indicates clustering at scales finer than 3 meters, then transitioning to random or dispersed pattern. This plot is corrected for inhomogeneity and isotropy given that the spatial pattern is not consistent throughout the extent of the rectangular plot F.

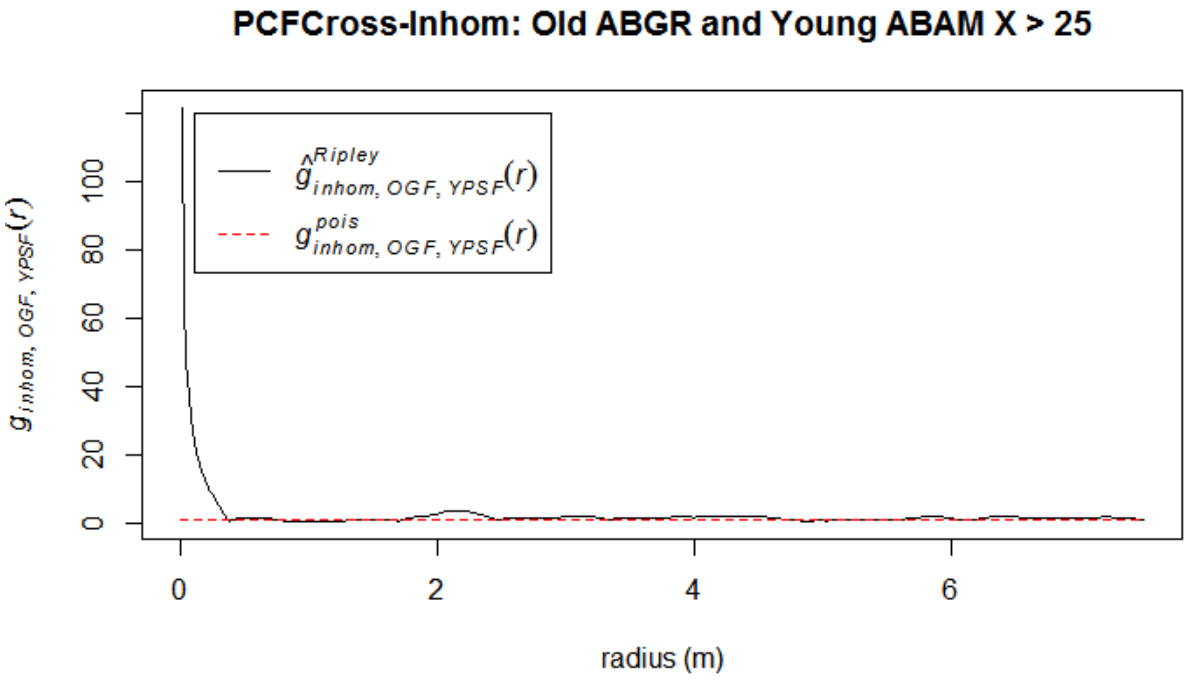


*Figure S 38.* Cross PCF for old ABAM (n=11) and young ABAM (n=174) stems x>25m indicates clustering right at 2 meters, then transitioning to random or dispersed pattern. This plot is corrected for inhomogeneity and isotropy given that the spatial pattern is not consistent throughout the extent of the rectangular plot F.